Bismuth based (nano)materials and platforms for (bio)sensing

Miquel Cadevall Riera

Tesis doctoral

Doctorat en Química

Directors:

Prof. Arben Merkoçi

ICREA & Nabioelectronics and Biosensors Group, Institut Catala de Nanociencia i Nanotecnologia (ICN2)

Prof. Josep Ros

Departament de Química, Univerisitat Autónoma de Barcelona

Departament de Química

Facultat de Ciències

2014

The present work entitled "*Bismuth based (nano)materials and platforms for (bio)sensing*", presented by **Miquel Cadevall** to obtain the degree of doctor by Universitat Autònoma de Barcelona, was performed at the Nanobioelectronics and Biosensors Group at the Institut Català de Nanociencia i Nanotecnologia (ICN2), under the supervision of Prof. Arben Merkoçi, ICREA Professor and Group Leader, and in Department of Chemistry, Universitat Autònoma de Barcelona, under the supervision of Prof. Josep Ros, Profesor and Group Leader.

Bellaterra, 16th September 2014

The supervisors

Prof. Arben Merkoçi Prof. Josep Ros

The present Thesis was performed also under the doctoral program studies **"Doctorat en Química**" at the Faculty of Sciences, Universitat Atunònoma de Barcelona.

Acknowledgements for the economic and logistic support:

The progects from Ministerio de Educación y Ciencia (Spain) MAT2011-25870, Spain-Japan International Bilateral Project, PIB2010JP-00278 and MAT2008-03079/NAN are acknowledged. The projects from European Union in the Seventh Framework Programme (FP7/2007–2013) under grant agreement n° NMP-LA-2012-280432 and n° NMP-LA-2012-280432 are also acknowledged.

I would make a special acknowledgement to the Universitat Autònoma de Barcelona for the predoctoral fellowship (PIF 2009).

INDEX

THESIS OVERVIEW

Thesis Overview

The thesis is focused on the fabrication of new sensing and biosensing platforms for pollutants detection. Although bismuth-based micro and nanomaterials seem to be the appropriated materials to achieve this objective nevertheless new platforms including for example those based on paper are also proposed.

In the **first chapter** the main objectives of this thesis are described in detail.

The introduction part (**chapter 2**) of this thesis is dedicated to the revision of the recent reports / achievements on bismuth-based nanomaterials in different application fields that include medicine, photodegradation of organic pollutants, cosmetics, pigments and alloys. An important section of this part is focused on the description of the effect of bismuth-based materials in heavy metals and biosensing applications.

Bismuth nanoparticles are found as an innovative material in heavy metals sensing and biosensing applications. A study on the effect of the modification of screen-printed electrodes with bismuth nanoparticles and its use for the heavy metal detection is shown (**chapter 3**). Different modifications of polyol based bismuth nanoparticles synthesis have been evaluated in aim to obtain the more efficient nanoparticles with interest in heavy metal sensing. In addition the results obtained for the detection of lead and cadmium is also shown in the same chapter.

In the **chapter 4** a new electrode modification strategy is presented. This new strategy is based on the use of magnetic core/shell bismuth nanoparticles. Taking advantages of the bismuth oxide presence onto the shell of these nanoparticles, heavy metal detection in different On-Off sensing platforms is shown. The modification of

electrodes is clearly demonstrated by doing cycles with both modification and cleaning of the electrodes obtaining a kind of digital (On-Off) response of heavy metals.

To solve sampling and sample pretreatment issues a heavy metal sensing platform that uses a paper-based lateral flow chip is also developed and described at **chapter 5.** Fabrication and the optimization of this new heavy metal sensor are shown; it takes advantage of the use of a filter paper substrate. This new platform is capable to detect lead and cadmium in different matrixes including mud.

In the last chapter **(chapter 6)**, the integration of bismuth nanoparticles into a phenol biosensing system is shown. It takes advantages of the use of tyrosinase enzyme which brings certain selectivity in phenolic compounds detection. Morphological and electrochemical characterizations of the developed biosensor also are shown in this chapter. The developed biosensor shows good performance in catechol detection.

Finally in the **chapter 7** the general conclusions and some future perspectives are given.

Resum de la tesi

La tesi està basada en la fabricació de nous sensors i biosensors per a la detecció de contaminants. Els micro i nanomateials basats en bismut semblen ser materials molt apropiats per aconseguir aquest objectiu, tanmateix també s'han proposat altres plataformes sensores. En **el primer capítol** es descriuen detalladament els principals objectius d'aquesta tesi.

La introducció d'aquesta tesi descriu les aplicacions més recents i rellevants basades en la utilització de nanomaterials de bismut, com ara en els camps de la medicina, la fotodegradació de contaminants orgànics, la cosmètica, els pigments o els aliatges. Aquesta part precedeix la descripció dels mètodes de síntesi més innovadors, dels sensors més eficients, bàsicament de metalls pesants, i de les aplicacions en el camp dels biosensors. Aquest recull es pot trobar **al capítol 2**.

Les nanopartícules de bismut són una bona plataforma per a sensors i biosensors. En aquest sentit s'ha estudiat la modificació d'elèctrodes serigrafiats amb nanopartícules de bismut. En **el capítol 3**, s'avaluen diferents mètodes de síntesi de nanopartícules de bismut amb l'objectiu d'obtenir les nanopartícules més eficients en la detecció de metalls pesants; en aquest cas centrat en la detecció de cadmi i plom.

Al capítol 4 es presenta una nova estratègia de modificació d'elèctrodes. Aquesta estratègia es basa en la utilització de nanopartícules *core-shell*. Tenint en compte l'avantatge que dóna el recobriment de bismut, aquestes nanopartícules s'han utilitzat en la detecció de metalls pesants en diferents plataformes sensores. La bona modificació d'aquests elèctrodes es demostra clarament fent cicles de modificat i neteja; el

comportament d'aquests elèctrodes modificat es podria considerar com a una resposta digital.

L'última plataforma sensora per a metalls pesants proposada es basa en xips de paper. **El capítol 5 descriu** la fabricació i optimització d'aquests dispositius. Aprofitant la capacitat de filtrar del substrat de paper de filtre, aquestes simples plataformes són capaces de detectar plom i cadmi en diferents matrius, com ara solució tampó, aigua de mar o fangs.

En aquest últim capítol es mostra la integració de les nanopartícules de bismut en un biosensor de fenol, basat en l'activitat enzimàtica de la tirosinasa. **El capítol 6** inclou la caracterització morfològica i electroquímica del sensor. Aquests elèctrodes modificats amb nanopartícules de bismut i tirosinasa tenen una molt bona resposta en la detecció de fenol i catecol i un baix efecte de les interferències.

Finalment al **capítol 7** hi ha les conclusions generals i les futures perspectives que obre aquest treball.

En els annexos s'hi pot trobar una descripció dels mètodes de fabricació de les diferents plataformes sensores, les abreviatures utilitzades i la producció científica derivada d'aquest treball.

CHAPTER 1: OBJECTIVES

The general objective of this PhD thesis is the development of new tools for sensing and biosensing platforms with interest in pollutants detection in real samples. These new tools should be able to simplify the existing configurations and improve their performance. The final purpose of this is to obtain robust, sensitive and more efficient (bio) sensing platforms for in/field applications, with high performance. In addition, the development of new sensing platforms with interest for lab/on/chip applications is also a focus of the thesis. Indeed the development of efficient analytical platforms for pollutants detection is of great concern nowadays both to address environmental and/or health, safety and security related issues.

More in details bismuth-based nanomaterials are proposed to achieve better analytical performance in heavy metals and phenol detections. For this reason, two different nanomaterials are proposed: bismuth nanoparticles and magnetic/bismuth oxide core-shell nanoparticles.

The detailed objectives of this thesis can be summarized as following:

I. The study of the best way to synthesize bismuth nanoparticles (BiNPs) with the aim of modifying electrodes for heavy metal and phenol sensing.

- The role of bismuth in electrode modification to be used for heavy metals detection is well known as an alternative to mercury. The use of bismuth nanoparticles is an interesting choice that is in a deeper way studied in this thesis following these objectives:
    - The optimization of the BiNP synthesis and characterization of the obtained product.
    - The modification of electrodes with the most reactive BiNPs and their use in heavy metals sensing.
    - Study of the use of the BiNPs in the detection of lead and cadmium in seawater samples.

- Evaluation of analytical parameters such as the reproducibility, sensibility, the limits of detection and quantification, range of response and the multidetection capability.

- The integration of the BiNPs into a biosensor system for phenol and catechol detection.
  - Design and study of the best biosensor configuration.
  - Evaluation of the sensibility, the limits of detection and quantification and the selectivity of the biosensor.
  - Study of the detection mechanism and proposing of a possible detection principle model.
  - Evaluation of the effect of BiNPs in terms of electrode conductivity.

II. The development of new On-Off detection strategies to be used as in-situ heavy metal sensing system.

- Sensors applied in heavy metals detection use to suffer from surface fouling after a certain period of use. To solve this problem the use of magnetic nanoparticles modified with bismuth is proposed following these objectives:
  - The synthesis, characterization and study of magnetic nanoparticles functionalized with bismuth.
  - The optimization of the best modification conditions in different sensing platforms.
  - Using of the obtained bismuth /magnetic nanoparticles in the detection of lead and cadmium in buffer samples.
  - Integrating the sensors in a microfluidic platform and demonstration of simple On-Off heavy metals detection.

III. The study and design of a new microfluidic platform using simple materials

- The detection of pollutants in environmental samples usually has problems in terms of sampling and sample pretreatment. For this reason a new sensing strategy for the analysis of heavy metals in turbid samples based on the use of paper-based platform is proposed following these objectives:
  - Design of a filter paper-based platform for heavy metals sensing
  - Optimizing all the sensing parameters for lead and cadmium detection
  - Performing the heavy metal detection in real samples, such as mud or seawater.

CHAPTER 2: BISMUTH BASED NANOMATERIALS AND PLATFORMS FOR (BIO)SENSING APPLICATIONS

A very brief introduction to the application of bismuth nanoparticles and other bismuth based materials in different fields is made, especially in their application to sensors and biosensors. The most relevant fabrication procedures are also described.

2.1 General properties and applications of bismuth

Bismuth has been known from ancient times, although until the 18th century it was often mistaken with lead and tin, which share some similar physical properties (1-3). Its name come from German and is related to its meaning of having the properties of antimony (*weisse masse* or *wismuth* which mean "white mass") that was translated in the mid 16th century to New Latin word bisemutum. It has a high electrical resistance and the thermal conductivity is lower than any other metal, except mercury; considering that, bismuth sometimes is called as a semi-metal (4). This semi-metallic properties are particularly interesting for its use as a thermoelectric material because of its low effective mass, highly anisotropic Fermi surface and its potential to induce a semi-metal/semi-conductor transition with decreasing crystallite size that is typical for soft metals (5). Among the soft metals, Bi and Pb are the most widely studied due to their thermoelectric and corrosion resistance properties, respectively.

Similar to the noble metals, a typical synthesis of bismuth nanoparticles begins with the decomposition or reduction of a precursor compound, forming nuclei which then grow into nanocrystals (6). For those nanocrystals prepared by a thermal decomposition method, often the reaction temperature has to be kept above the melting point of the metal (7). Consequently, the “nanocrystals” remain in a liquid state throughout the entire synthesis and assume a spherical shape so as to minimize their surface area and thus the total interfacial free energy. When the reaction is quenched (typically by cooling down the solution), the liquid “nanocrystals” solidify into nanospheres with smooth surfaces.

Bismuth nanomaterials are being used for various applications, see Figure 2.1. Thanks to the low toxicity in comparison to heavy metals, the use of bismuth in fields, such as medicine, photodegradation of organic pollutants, cosmetics, pigments and alloys, where replaces lead in free-machining brasses for plumbing applications is reported (8). Historically, several bismuth salts were used in medicine; as examples of that, bismuth tartarate was used to treat syphilis, while bismuth sodium triglycollamate has been used to treat warts, stomatitis and upper respiratory tract infections (9-11). Two compounds have been extensively used for gastrointestinal medication for decades. Pepto-Bismol contains bismuth subsalicylate (BSS), and De-Nol contains colloidal bismuth subcitrate (CBS). Other bismuth compounds are used as X-Ray and NMR contrast agents.

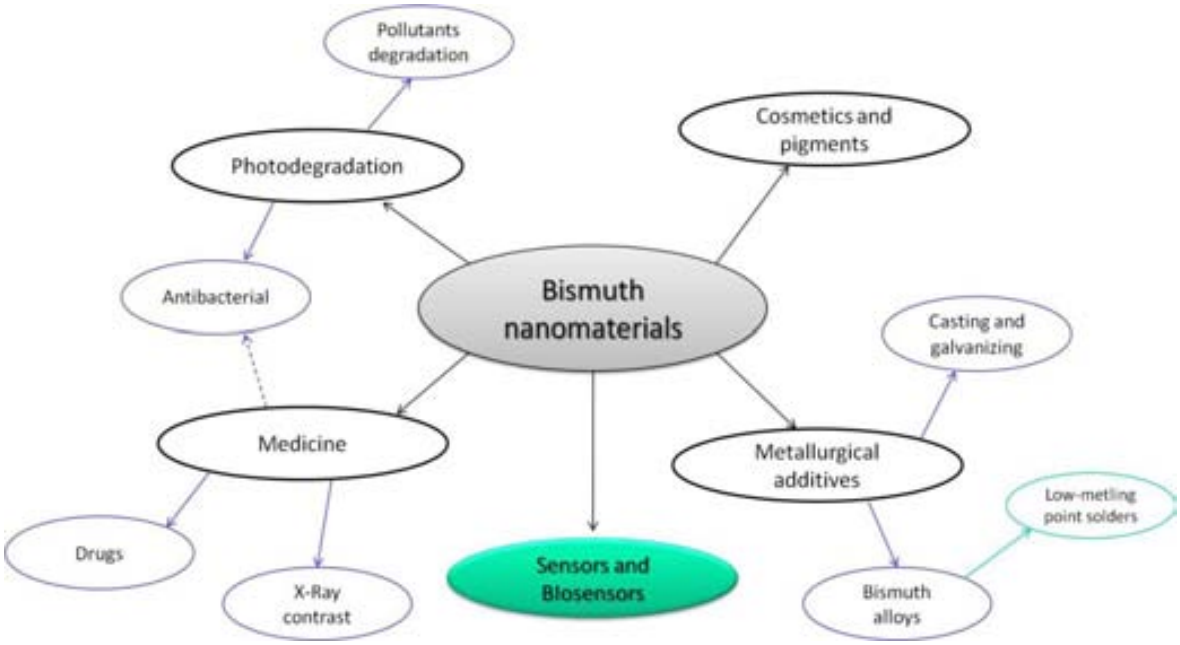

Figure 2.1 Summary of the various application fields of bismuth nanomaterials.

Recently, there has been intensive research in fabrication of structured photocatalytic materials for both energetic and environmental applications, such as photocatalytic hydrogen evolution (12), degradation of organic contaminants (13), disinfection of water (14), and conversion of carbon dioxide into hydrocarbon fuels. Different bismuth based photocatalytic materials, which exhibited superior photocatalytic performance in pollutants degradation due to their special morphological structure with respect to specific surface areas have been fabricated by various approaches. As an example, synthetic $(BiO)_2CO_3$ is found to display interesting activity in antibacterial and environmental applications (15, 16).

Beside the various applications, the use of bismuth in the fabrication of sensing and biosensing platforms show a great interest. Its use in relation to electrochemical stripping analysis with interest for heavy metals analysis is one of the most important. Electrochemical stripping techniques are particularly suitable for the determination of trace metals in samples of environmental and biological origin, due to their excellent detection limits, their sensitivity to the presence of different metal species, their capacity to perform multielement determination, and their relatively low cost. Bismuth based nanomaterials, as shown below, play an important role in this field being the principal function its use for the surface modification of working electrodes.

2.2 Bismuth nanoparticles synthesis

Various strategies for the synthesis of bismuth nanoparticles (BiNP) have been reported from the middle of 1990th. As demonstrated for other metallic nanoparticles (17, 18), BiNPs are able to be synthesized by laser ablation, electro-hydrodynamic techniques, high energy ball milling, vapour flow condensation, inverse micelles technique, high temperature/ low temperature chemical reduction, etc.

BiNPs can be easily obtained from bulk metallic bismuth (19) by using thermal decomposition, although this method usually is not efficient enough in terms of production yield. On the other hand reductive methods to synthesize BiNPs also have been reported. Various reducing agents and bismuth precursors have been used to prepare Bi crystals. In fact, the use of an organometallic complex of bismuth as a precursor for the decomposition is the most used. In addition to the decomposition of a compound or reduction of a salt precursor, nanocrystals of low-melting metals as in the case of bismuth, can be prepared by directly breaking large droplets of the molten metals under a shear force. BiNP synthesis strategies reported so far are grouped in chemical and physical methods and described in the next sections.

2.2.1 Chemical methods

Chemical methods employed for BiNPs synthesis are based on the use of reducing agents able to reduce the bismuth precursor. The distribution of the reducing agent into the synthesis medium directly affects the local variations in the rates of nucleation and growth that are directly related with the formation of polydisperse particles. To address this problem, different strategies such as the use of strong

reducing agents with slow kinetics that enable homogeneous nucleation and growth have been used. Reducing agents such us ethylene-glycol (20), sodium borohydride (21), aqueous hydrazine solution (22), ethylene diamine and, recently, sodium hyposphite (23) have been used to prepare Bi nanocrystals. The use of an organometallic complex of bismuth as a precursor has been recently reported (24, 25). In addition, photochemical activation has been used to synthesize bismuth nanoparticles (26, 27). In the following parts these strategies are described in more details.

Polyol process is found as one of the most used methodologies in the synthesis of bismuth and other metallic nanoparticles. This method of synthesis have been useful to prepare platinum (28), silver (29), gold (30), copper (31) and nickel (32) nanoparticles with the idea to achieve nanoparticles of different shapes and sizes (33). The simple reagents and materials used in this technique are the main advantages. More advantages are the low cost of the reagent and the relative large productivity; nevertheless anaerobic atmosphere and stabilizing agents are required during the synthesis. Different strategies that try to solve these drawbacks and achieve an appropriate control of the obtained nanostructure have been reported.

In 2004, Y. Xia, et al. reported two different solution-based approaches that allowed them to process metals with melting points below 400 °C. Using both approaches, monodispersed spherical bismuth colloids, in high quantities and with controlled diameters in the range of 100 to 600 nm can be obtained, depending on the synthesis conditions (34). The versatility of polyol process is clearly demonstrated by the authors with bismuth as an example. The production of monodispersed BiNPs was

performed by either thermal decomposition of bismuth acetate in boiling ethylene glycol (the bottom-up approach) or by emulsifying molten drops of bismuth in boiling diethylene glycol (the top-down approach),; this procedure was schematically resumed in the figure 2. Depending on the concentration of Bi precursor and the stirring rate, the diameters of these uniform spherical colloids could be readily varied from 100 to 600 nm. The synthetic protocols have also been extended to prepare uniform spherical colloids from other metals with relatively low melting points, and typical examples include Pb, In, Sn, Cd, and their alloys.

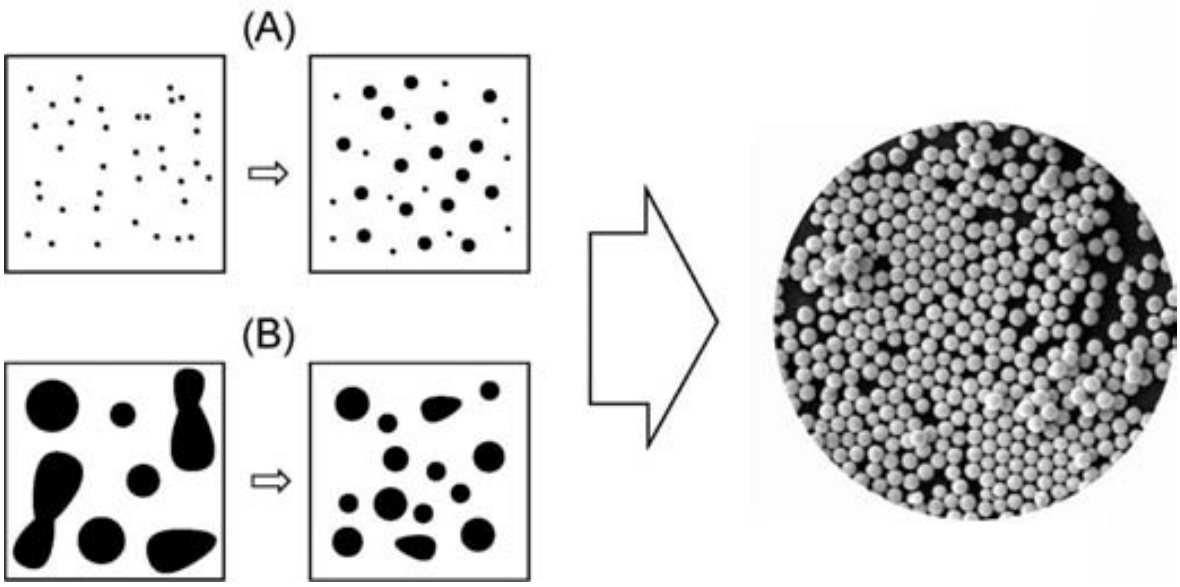

Figure 2.2 Schematic illustrations of two different approaches to obtain monodispersed spherical colloids of metals with relatively low melting points. (A) The bottom-up approach, where a molecular precursor is decomposed to generate metal atoms that nucleate and grow into monodispersed colloids. (B) The top-down approach, where large drops of a metal are broken into smaller pieces and then transformed into uniform droplets by shear forces through a mechanism similar to conventional emulsification. "Reprinted with permission from reference 34. Copyright 2004, American Chemical Society.

This methodology was improved by the addition of polymeric materials, which are usually used as stabilizers to prevent the agglomeration and precipitation. The most used polymer in this type of synthesis was polyvinyl pyrrolidone (PVP); in fact PVP has been used from years as a capping agent in the synthesis of nanoparticles of silver (35-37), gold (38), nickel (39, 40), copper (41) and different metal and semi-metal oxide nanoparticles (42-44). The chain length of PVP in the synthesis can affect dramatically the prepared particles (45).

In the case of bismuth nanoparticles, PVP was found to be the most critical element in the control of the shape. W. S. Wang, et al. demonstrated this phenomenon while synthesizing BiNPs from sodium bismuthate (V) using different amounts of PVP (46). Bismuth nanoparticles with different shapes such as sphere, triangles and cubes were found.

Later, the synthesis of BiNPs was focused on the obtaining of spherical nanoparticles using a simple refluxing method being PVP one of the most important ingredients. Although the use of less oxidized states of bismuth was also studied (47). Nevertheless, the use of anionic species of bismuth (III) was found to improve the synthesis. The examples include the addition of NaOH to bismuth trichloride solution (48) or the use of Bi^{3+} complex with mannitol as a precursor (49).

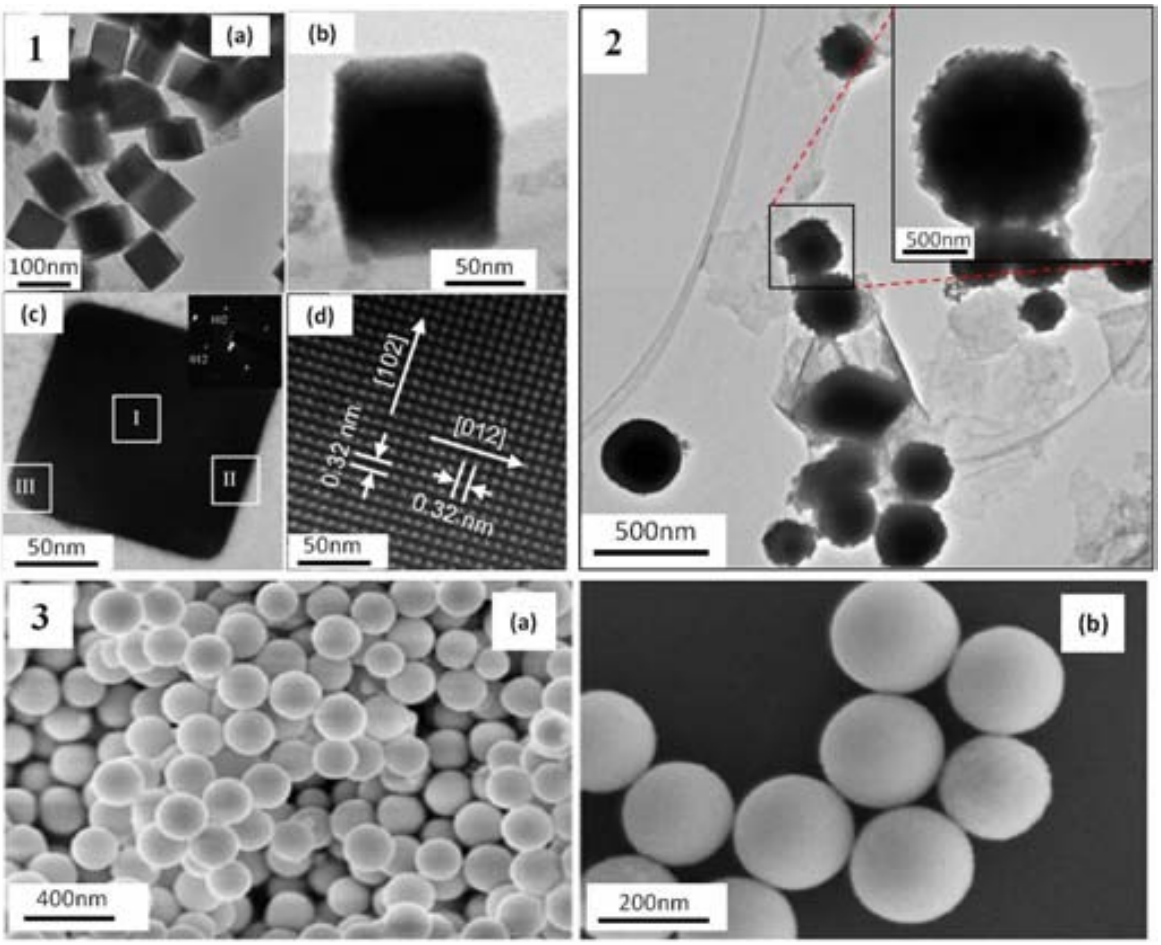

Figure 2.3 TEM images from different examples of bismuth nanostructures generated through polyol reduction in presence of different amounts of PVP: 1) cubic, 2) and 3) spherical nanoparticles. Adapted by permission of American Chemical Society (Copyright 2006), Elsevier (Copyright 2013) and Sppringer (Copyright 2011) from references: 1) 46, 2) 47 and 3) 49).

Although PVP was found necessary as a protective agent to promote nucleation and prevent nanoparticles aggregation, the use of other polymers or surfactant offers other interesting properties. Polyethylene glycol (PEG) and cetyltrimethylammonium bromide (CTAB) are also used in the synthesis of bismuth micro- and nanospheres in ethylene glycol by a simple refluxing method (50). As a variation of the polyol process, the use of reducing agents such as hydrazine (22), sodium borhydride (51), sodium hydride (52) or potassium hydrogen phosphite was also reported (23). The change of

the reducing agent, as well as of the capping agents, plays crucial roles in the size and the stability of the particles.

Synthesis of metallic nanoparticles by using an organometallic complex as precursor is another interesting strategy. The conditions of the decomposition of the complex and the stability of the ligand are crucial in the resultant nanoparticles. Due to their affinity with sulphur compounds, thiol ligands are commonly used in the synthesis, in example dodecanothiol ligand are used to synthesize disc-shaped bismuth nanoparticles (53). However, tris[bis(trimethylsilyl)amide] (54), 2-ethylhexanoate (55) and ethyl (56) ligands can also be used to functionalize the surface of bismuth nanoparticles.

Bismuth nanoclusters can be prepared through reduction of an aqueous bismuth salt inside of AOT (dioctyl sulfosuccinate, sodium salt) reverse micelles (57). J. Lin, et al. reported for the first time a self-assembly of bismuth nanoparticles, formed by reducing an organometallic bismuth complex (bismuth 2-ethylhexanoate) with hard reducing agent (lithium triethylborohydride) at high temperature. The synthesis of bismuth nanocrystallites was carried out in dioctyl ether ($[CH_3(CH_2)_7]_2O$, a non-polar solvent with high boiling point), using standard organometallic reaction procedures with anaerobic atmosphere and commercially available reagents (55).

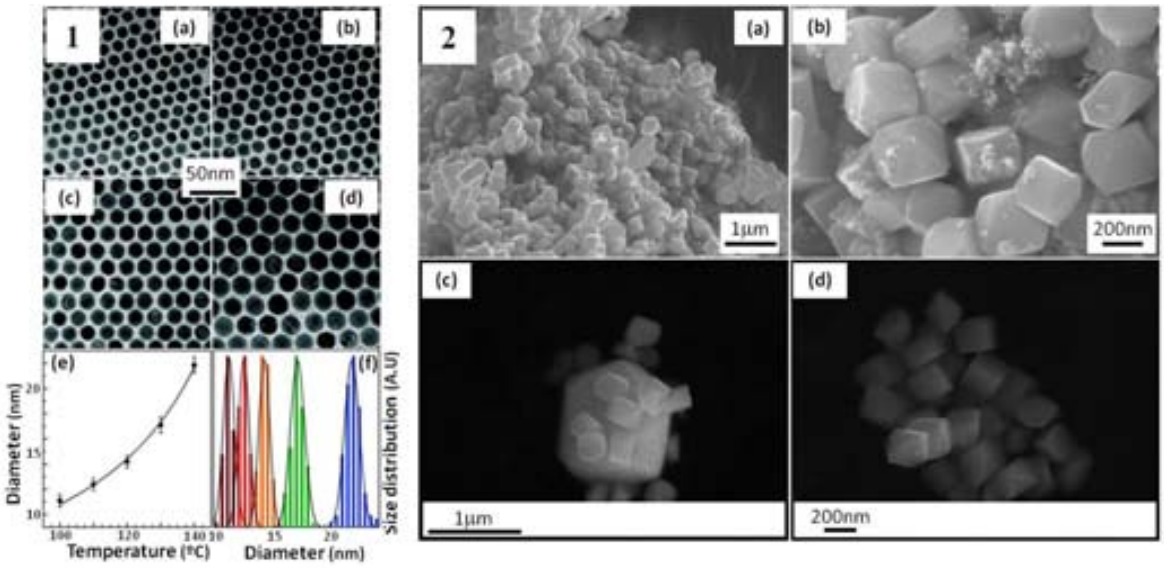

Figure 2.4 Examples of bismuth nanostructures generated by: 1) a decomposition of a bismuth $Bi[N(SiMe_3)_2]_3$ compound and 2) by thermal decomposition of the novel subvalent metal organic precursor tetraethyldibismuthine Bi_2Et_4 under kinetic control at low temperatures. Adapted by permission of American Chemical Society, Copyright 2010 and 2012, from references: 1) 54 and 2) 56).

Smaller and more homogenous nanoparticles can be obtained from the descomposition of $Bi[N(SiMe_3)_2]_3$ (27), as shown in figure 4. An example of that is the development of a simple and large-scale synthetic route for uniform-sized Bi nanocrystals with controlled particle sizes ranging from 6 to 27 nm (54). To achieve it, the reduction of bismuth thiolate with TOP is needed. The electrical and thermal conductivities of the pressed bismuth nanocrystals were strongly size-dependent. Another recent synthesis is based on the thermal decomposition of ethyl-bismuth, in presence of $Na[N(SiMe_3)_2]$, a novel low-valent precursor and PVP obtaining highly crystalline cubic nanoparticles (56).

1.2.2 Physical methods

Another different way to synthetize BiNPs is focused on the physical attack to different bismuth species to obtain nanopowders. One of the first attempts was based upon solution dispersion of melted bismuth, taking advantage of their low melting point. On one hand, Y. Zhao et al. introduced a method using paraffin oil as a solvent and capping agent (19) and on the other hand, Y. Wang et al. presented a top-down approach synthesis using diethylene glycol as a solvent and PVP as a capping agent (34).

Another route to obtain bismuth nanostructures is by using electrochemical methods (58). The electrochemical reduction of Bi^{3+} solutions has resulted in a plethora of interesting shapes of metal nanoparticles such as spheres, cubes, prisms, dendrites, stars, spikes, rods and flowers to name just a few, some of them are shown in figure 5. The electrodeposition of nanostructured metals is an intense area of research interest with various important analytical applications (61). This kind of synthesis process can be controlled by a number of electrodeposition techniques, such as cyclic voltammetry (CV), step methods such as chronoamperometry (CA), chronopotentiometry (CP) and chronocoulometry (CC), pulsed plating at a fixed or varying potential or using AC methods.

A good way to improve the properties of bismuth nanostructures obtained during electrochemical methods is the use of different template techniques: the use of chemical or physical templates. The aim of chemical templating is to include in the deposition bath a ligand that is capable of directing the growth of the material and therefore its properties such as shape and/or crystallography, in the same way as in chemical synthesis. The surfactants are often the same as used in chemical syntheses

and are able to alter the growth kinetics at particular facets of the electrodeposited material due to their preferential adsorption at these sites. A good example of that is the use of Nafion, which was carried out by ion-exchange in Nafion film coated on the electrode surface and subsequent on-site electrochemical reduction of Bi^{3+} ions to BiNPs (62).

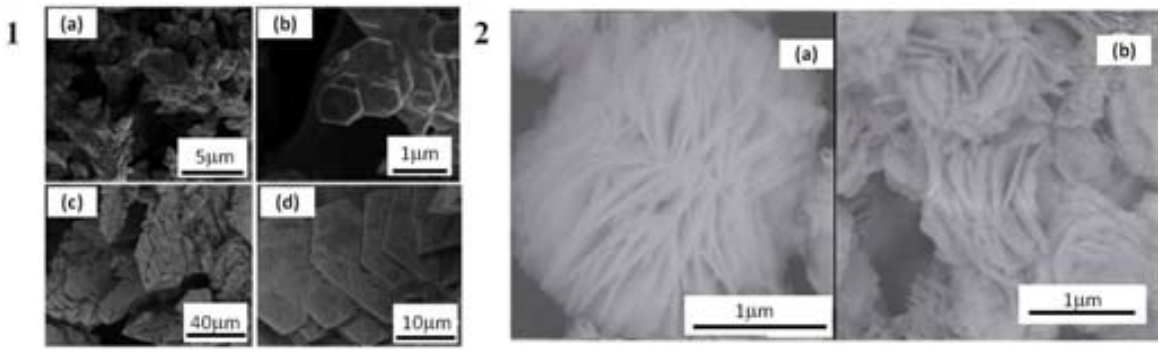

Figure 2.5 Examples of bismuth nanostructures generated by electrodeposition. 1) hexagonal discs and 2) nanoflowers. Adapted by permission of Willey and American Chemical Society (Copyright 2012) and Chemical Society of Japan from references: 1) 59, 2) 60 and 3) 58)

2.3 Chemical sensing

The use of bismuth in sensing field started on 2000 by J. Wang et al. by using bismuth film electrodes (76). Bismuth-coated carbon electrodes display an attractive stripping voltammetric performance which compares favourably with that of common mercury-film electrodes. These bismuth-film electrodes were prepared by adding 400 µg/L (ppb) Bi^{3+} directly to the sample solution and simultaneously depositing bismuth and target metals (i.e. cadmium, lead, thallium, and zinc) on the glassy-carbon or, also, carbon-fiber substrate (68, 77-80). The use of bismuth was focused on bismuth film based sensors and the use of different techniques such as electrochemical stripping analysis (77, 81), electrochemical impedance spectroscopy (82), and amperometry (83). Bismuth films have been normally generated by its electroplating onto electrode surfaces such as glassy carbon electrodes (84), carbon paste electrodes (85), boron doped diamond electrodes (86, 87), gold microelectrodes (88, 89) and screen-printed electrodes (90, 91).

Beside the use of Bi-film electrodes synthetic bismuth nanoparticles (92) and bismuth nanopowders (93-95) were also considered as modifiers of electrodes. Chang-Kyu Rhee (96, 97) reported a sensitive and conveniently usable electrode sensor for a trace analysis of heavy metal developed by using Bi nanopowder synthesized by levitational gas condensation (LGC) method. This electrode has been proven to be highly sensitive and reliable for trace analysis of heavy metals in conjunction with an anodic stripping voltammetry. The detection limits of 0.15 µg/l for Cd and 0.07 µg/l for Pb confirm the good performance of this sensor.

Another way to improve heavy metal sensing is the combination of bismuth films or nanostructures with other nanomaterials, such as carbon nanotubes (98), grapheme (99) or carbon nanofibres (100). G. H. Hwang et al. describes the possibility of the Bi-CNT electrode for the determination of cadmium, lead and zinc (78). This Bi-CNT electrode was successfully applicable to analysis of trace metals in real environments.

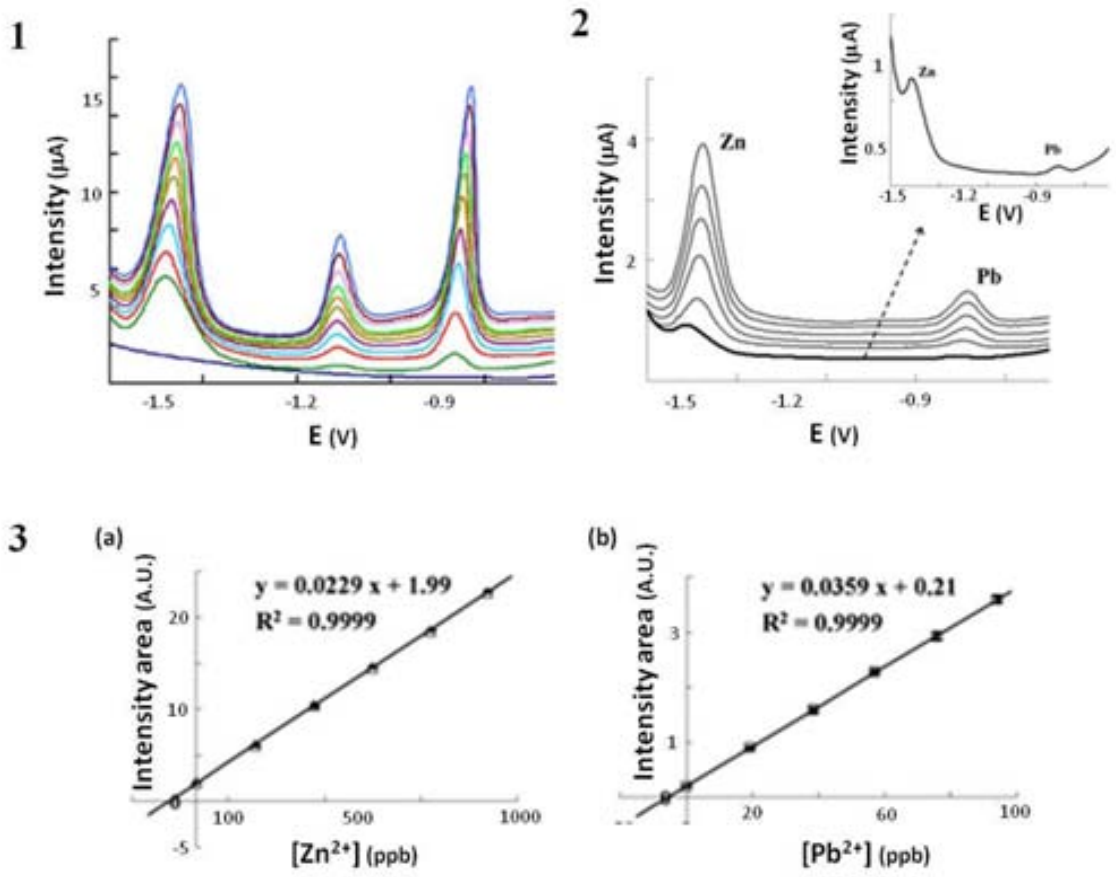

Figure 2.6 1) Example of multielemental analysis using *ex-situ* deposited bismuth film onto SPCE and (2a) DPASV measurements in tap water samples on BiSPCE at pH 6 in 0.01 mol l^{-1} maleic–maleate buffer using an E_d of −1.50 V during 120 s and t_r of 5 s; (2b) and (2c) standard addition plots for the determination of Zn^{2+} and Pb^{2+}, respectively (2). Experimental data from reference 91 by permission of Springer (Copyright 2011).

Most of papers in the literature show the capacity of bismuth electrodes for cadmium, lead and zinc sensing. However, arsenic (107, 108), antimony (109), chromium (110), mercury, thallium (111), vanadium (112), cobalt (113), nickel (114), selenium (115) and uranium (116) have also been reported as targeted analyte to be detected using bismuth based electrodes. The most commonly used electrochemical stripping analysis techniques depending on the sample and the target analyte are square-wave anodic stripping voltammetry (SWASV) (102), Osteryang square-wave cathodic stripping voltammetry (OSWCSV) (108, 117), differential pulse anodic stripping voltammetry (DPASV) (78) and square wave adsorptive stripping voltammetry (SWAdSV) (118). Probably the most frequently reported parameter by which authors evaluate the electroanalytical performance of newly developed methods is the quoted limit of detection (LOD). Table 1 summarizes LOD values reported by using different Bi based electrodes while detecting various metals in different kind of samples.

Another way to generate bismuth electrodes is by using bismuth oxide as a precursor. In 2002, Pauliukaite et al. prepared a carbon paste electrode bulk-modified with Bi_2O_3 for the determination of Cd^{2+} and Pb^{2+}; this sensor was evaluated in synthetic solutions and real samples of river water (122).

In the field of environmental control and public health, the investigations are focused on the study of the evolution of heavy metals and other pollutants in seawater, river and lake water, drinking water and waste water. Examples of that are the on-line lead detection (123) in tap water samples and the detection of lead and cadmium in seawater samples using SPCE modified with bismuth nanoparticles.

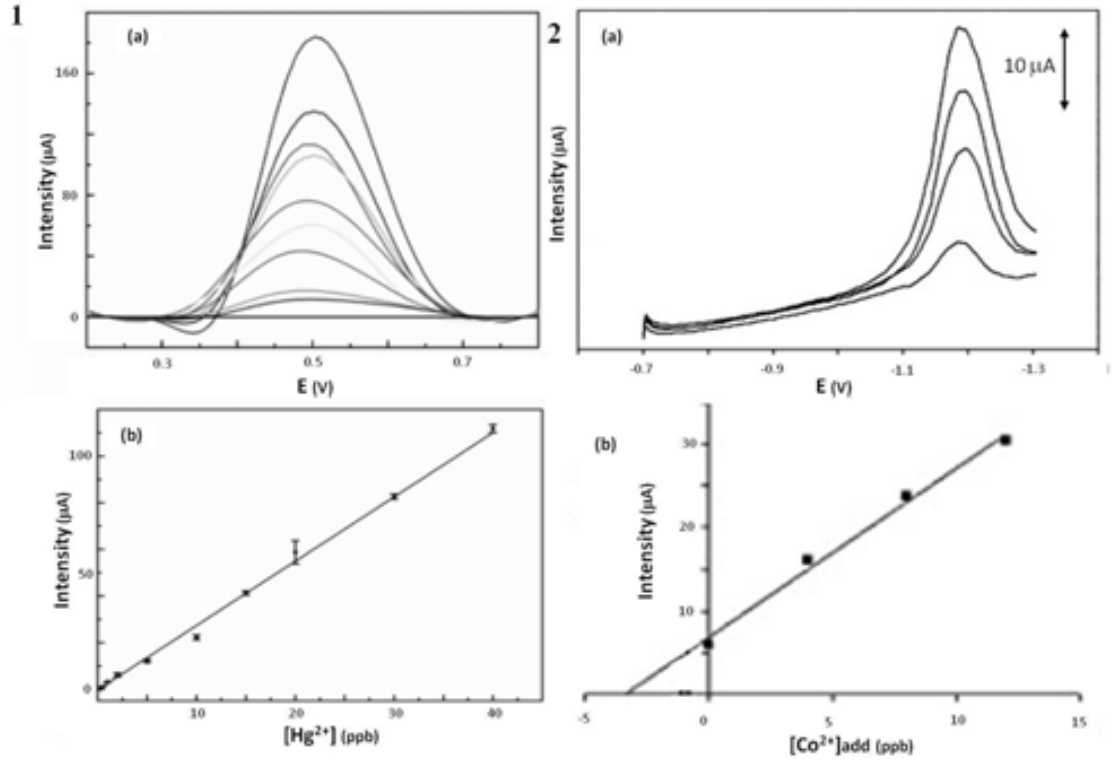

Figure 2.7 SW anodic stripping voltammograms (a) and calibration curve (b) for different concentrations of Hg obtained with MWCNT-modified SPBE (1) and SW voltammograms and standard addition curve for the determination of Co(II) in a certified river water sample after preconcentration for 60 s on a sputtered BiFE (2) Adapted by permission of Elsevier (Copyright 2009) and The Japan Soceity for Analytical Chemistry from references: 121 and 120 respectively).

Additionally, these applications in environmental control field the use of electrochemical methods in food and health applications are also achieved. Some examples are the analysis of chinese herbal remedies samples which contains germanium contaminations (115) or propolis a honeybee product which contains lead as one of the main contaminants (124, 125). In the second case, a bismuth film electrode plated on a modified glassy carbon electrode was prepared to determine lead and copper in raw propolis samples being a good alternative to the quality control of this kind of products (126).

Electrochemical platform	Technique	Analyte	LOD	Sample matrix	Ref.
BiNPs/Nafion/GCE	DNPASV	Pb	0.3nM	Tap and lake water	62
BiFE	SWASV	Zn	6µM	Human serum	101
BiNPs/SPCE	SWASV	Pb, Cd, Zn	0.9, 1.3, 2.6 ppb	Acetate buffer	92
Bi nanowires	SWASV	Pb, Cd, Cu, Hg	2.5-50 ppb	Acetate buffer	102
Nafion-Graphene/BFE	SWASV	Pb, Cd	0.1, 0.1 ppb	Lake water	103
MWCNTs-Nafion/BFE	DPASV	Pb, Cd	25, 40 ppt	Acetate buffer	79
MWCNT/BFE	SWASV	Pb, Cd, Zn	1.3, 0.7, 12 ppb	Acetate buffer	78
rGO/BFE	DPASV	Pb, Cd, Zn, Cu	0.55, 28, 17, 26 ppb	Acetate buffer	99
BiOx/SPE	CCSC	Pb, Cd	8, 16 ppb	Soil samples	104
BiF/SPE	SWASV	Pb, Cd, Zn	0.5, 3.9, 3.5 ppb	Tap water	91
BiBE	SWASV	Pb, Cd, Zn	3.2 ppb (Pb)	Acetate buffer	105
Bi-GECE	DPASV	Pb, Cd, Zn	23.1, 2.2, 600	Tap water, soil samples	106
BiFE	OSWCSV	As	0.7 ppt	Chlorhydric saline solution	108
BiFE	OSWCSV	Sb (III), Sb (V)	2, 2 ppt	Chlorhydric saline solution	117
BiFE	SWCadSV	Ge (IV)	5 ppb	Chinese herbal remedies samples	114
BiFE	SWAdSV	Cr (VI)	15 ppt	Acetate buffer	119
BiFµE	SWAdCSV	Ni (II), Co (II)	0.06 ppb, 0,07ppb	Ammonium buffer	100
BiFE	SWAdSV	Co (II)	0.09 ppb	Tap water	120
Bi/MWCNT/SPCE	SWASV	Hg (II)	0,09 ppb	Nitric acid solution	121

Table 2.1 Different bismuth based platforms used for detection of heavy metals. GCE: Glassy carbon electrode, BiFE: Bismuth film electrode; BiNP/SPCE: screen-printed carbon electrode modified with bismuth nanoparticles; MWCNT: multiwalled carbon nanotubes; rGO: reduced graphene oxide; BiOX: bismuth oxide; BiBE: Bismuth bare electrode, BiFµE: Bismuth film microelectrode, DNPASV: Diferencial normal pulse anodic stripping voltammetry, SWASV: Square-wave anodic striping voltammetry, DPASV: Diferencial pulse anodic stripping voltammetry, OSWCSV: Osteryang square-wave cathodic stripping voltammetry, SWCadSV: Square-wave cathodic adsotive stripping voltammetry,

Additionally, these applications in environmental control field the use of electrochemical methods in food and health applications are also achieved. Some examples are the analysis of chinese herbal remedies samples which contains germanium contaminations (115) or propolis a honeybee product which contains lead as one of the main contaminants (124, 125). In the second case, a bismuth film electrode plated on a modified glassy carbon electrode was prepared to determine lead and copper in raw propolis samples being a good alternative to the quality control of this kind of products (126).

Beside applications in heavy metal analysis bismuth based sensors have been seen with interest for sulphide detection. Using BiEFs as working electrode, an indirect determination method for sulphide in water samples, based on the determination of residual Cd^{2+} after reacting with S^{2-} is reported (127).

2.4 Biosensig applications

Although the analysis of organic compounds does not represent the most important part of the research activity of bismuth based electrodes in recent years it has been gaining presence in the literature (83). Bismuth based electrodes have been reported for the analysis of model organic compounds, pharmaceutical substances (128, 129), pesticides (130-132) as well as other compounds of biological relevance (133, 134).

Electrocatalysis for the oxidation of carbohydrates is important in various fields, including biological fuel cells, waste water treatments and sensors for medical and food industry applications. In particular, the electro-oxidation process of glucose at various types of platinum electrodes has been the subject of research interests for many years. In this way, a second generation glucose biosensor was developed by using neutral red (NR) as a mediator and bismuth film electrode (BiFE) as a transducer along with immobilized glucose oxidase (135). In this work, U. Anik et al. found a very low limit of detection, 40.56 □M, showing the possibility of future applications of bismuth based platforms in other samples.

The rapid *in situ* determination of phenolic compounds and their derivatives is an important environmental challenge because of the easy penetration of such species through membranes or skins of plants, animals and humans, with toxic side effects (136). The development of a novel immobilization procedure including electrodeposition of mushroom tissue onto the surface of a screen printed electrode (SPCE) with the aid of Bi^{3+} precursor that interacts with the tissue and gets reduced

onto the transducer surface was reported (137). The immobilization procedure represents an *in situ* bismuth and tissue deposition/entrapment without using any crosslinking agent. By this way, a disposable biosensor that gives promising results for phenol detection was obtained. This study demonstrates that this system can be with interest as a novel platform for biosensing studies and may open the door to other new configurations.

The use of bismuth nanoparticles in an amperometric BiNP/Tyr-based biosensor has been also demonstrated (47). Figure 8 shows the whole detection mechanism of this platform. This is achieved through BiNP/Tyr integration onto the working electrode of a screen printed carbon electrode (SPCE) by using glutaraldehyde as a crosslinking agent. The resulting BiNP/Tyr-based biosensor exhibited high sensitive response toward phenol and catechol detection with very low detection limits (26 nM for catechol and 62 nM for phenol) showing a linear response up to 100 µM and 71 µM for catechol and phenol, respectively.

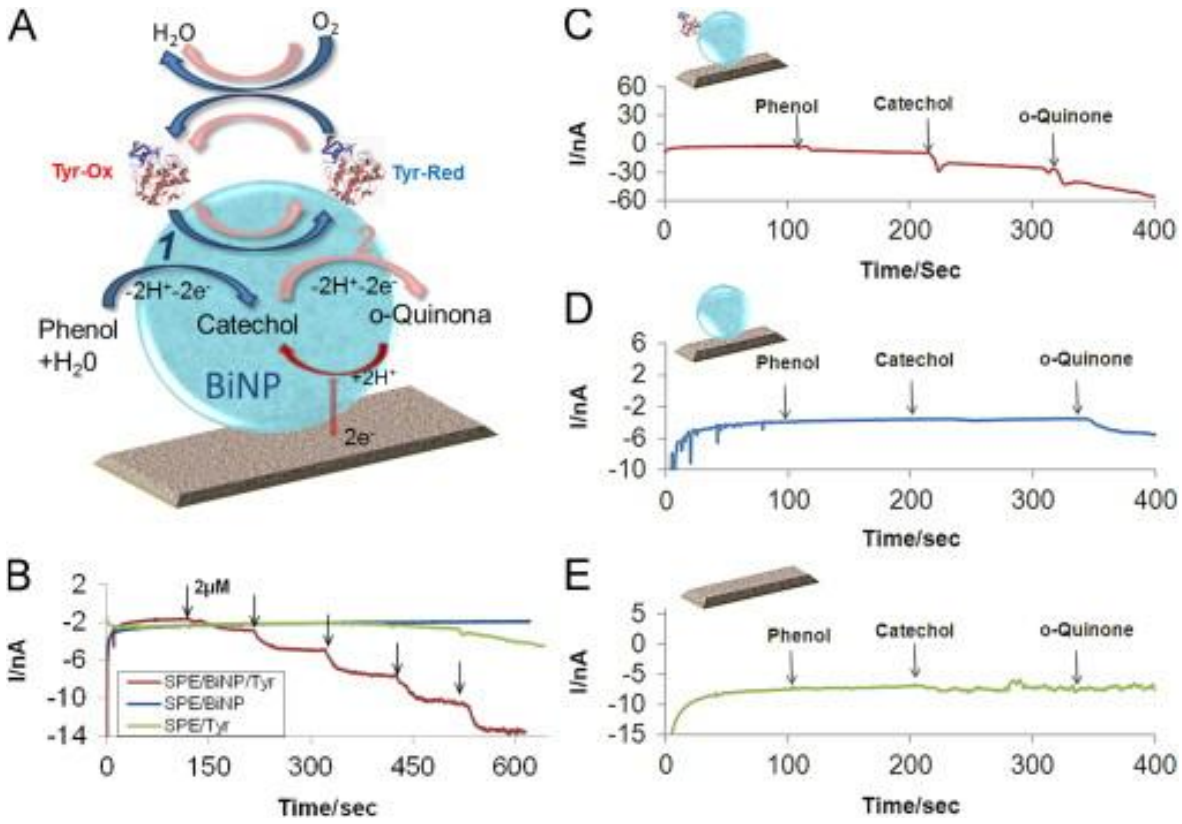

Figure 2.8 Proposed mechanism for the phenol and catechol electrocatalytic detection by using BiNP based biosensor (A). Current–time response curves of bare SPE, SPE/BiNP and SPE/BiNP/Tyr modified electrodes upon successive additions of 2 µM phenol (B). Chronoamperometric responses of SPE/BiNP/Tyr (C), SPE/BiNP (D), SPE (E) biosensors upon successive additions of 10 µM Phenol, catechol and o-quinone. All the experiments were carried at −200 mV, without nitrogen saturation. Experimental data from reference 47 by permission of Elsevier, Copyright 2013.

Another nanomaterial used is polycrystalline bismuth oxide films in combination, for the first time, with polyphenol oxidase (PPO) for the development of a biosensor for determination of phenolic compounds in environmental water samples (138). The use of Bi film is also extended in biosensing systems that involve immunoreaction assay such as interactions between IgE and anti-IgE molecules (139). The immobilized reagents and their interaction with anti-IgE were monitored by using atomic force microscopy technique and electrochemical impedance spectroscopy.

2.5 Conclusions

The most advanced methodologies for synthesis of bismuth nanostructures of different shapes and sizes based on the use of different reducing and stabilizing agents are shown. The most interesting approach is the one based on the use of ethylene glycol as both solvent and reducing agent and of the PVP as a nanoparticle protector. This versatile methodology is a good alternative for interesting applications due to the large variety of the obtained nanoparticles. In addition the use of electrochemical deposition methods opens up a range of new size and shape bismuth nanostructures.

Recent advances in bismuth-based platforms for sensing and biosensing applications are also shown. Bismuth started as a promising material, basically as an alternative to mercury. During the lasts 15 years the scientist focused their efforts in development of new mercury-free platforms. Nowadays, bismuth can be considered as an important candidate to develop reliable non-mercury electrode. Most of the bismuth-based nanostructures are used in heavy metal analysis. By using Bi-based platforms the detection of lead, cadmium, zing, nickel, cobalt, mercury, germanium, arsenic, chromium and copper has been successfully achieved. Besides the good performance in heavy metals detection bismuth is also reported to be with interest for application in biosensors systems. The biocompatibility of bismuth makes possible the conjugation of bismuth nanostructures with enzymes and antibodies. The analysis of organic compounds, pharmaceutical substances, and pesticides as well as other compounds of biological relevance are also achieved for bismuth-based biosensors.

It's important to highlight that overall in sensing applications and especially *in-situ* ones, the current electrochemical stripping technology would particularly benefit from the elimination of mercury electrodes by using bismuth nanostructures.

2.6 References

1. G. Rayner, TO. Canham. *Descriptive inorganic chemistry*. 5th Ed. ed. W. H. Freeman, New York, 2009.

2. J. Barrett, *Inorganic Chemistry in Aqueous Solution*. The Royal Society of Chemistry, Cambridge, 2003.

3. N. N. Greenwood. *Chemistry of the Elements,* 2nd Ed, Elsevier Butterworth-Heinemann, Oxford, 1997.

4. D. F. Shriver . *Inorganic Chemistry*, Oxford University Press; Oxford, 1999

5. P. Atkins TO, J. Rourke, M. Weller, F. Armstrong, *Inorganic Chemistry,* 5th Ed, OXFORD, Oxford, 2009.

6. J. Krüger, P. Winkler, E. Lüderitz, M. Lück, HU. Wolf, *Bismuth, Bismuth Alloys, and Bismuth Compounds*, Ullmann's Encyclopedia of Industrial Chemistry: Wiley-VCH Verlag GmbH & Co. KGaA, 2000.

7. A. Geoffrey, A. Ozin, *Nanochemistry: a chemical approach to nanomaterials,* 2nd Ed, Royal Society of Chemistry, Cambridge, 2009.

8. YN. Shevtsov, NF. Beizel, Pb distribution in multistep bismuth refining products *Inorganic Materials*, **1** (2), 47-51 (2011).

9. H. Li, H. Sun, Recent advances in bioinorganic chemistry of bismuth, *Current Opinion in Chemical Biology*, **16** (1-2),74-83 (2012).

10. TA. Udalova, OA. Logutenko, E. Timakova, LI. Afonina, ES. Naydenko, YM. Yukhin, *Bismuth compounds in medicine. Strategic Technologies*, Third International Forum, 2008.

11. GG. Briand, N. Burford, Bismuth Compounds and Preparations with Biological or Medicinal Relevance. *Chemical Reviews,* **99** (9), 2601-2658 (1999).

12. L. Wang, W. Wang, Photocatalytic hydrogen production from aqueous solutions over novel Bi0.5Na0.5TiO3 microspheres, *International Journal of Hydrogen Energy*, **37** (4), 3041-3047 (2012).

13. J. Cao, C. Zhou, H. Lin, B. Xu, S. Chen, Surface modification of *m*-$BiVO_4$ with wide band-gap semiconductor BiOCl to largely improve the visible light induced photocatalytic activity. *Applied Surface Science*, **284**, 263-269 (2013).

14. T. Soltani, MH. Entesari, Solar photocatalytic degradation of RB5 by ferrite bismuth nanoparticles synthesized via ultrasound, *Ultrasonis sonochemistry*, **20** (5), 1245-1253 (2013).

15. Y. Liu, Z. Wang, B. Huang, K. Yang, X. Zhang X, X. Qin, *et al*. Preparation, electronic structure, and photocatalytic properties of $Bi_2O_2CO_3$ nanosheet, *Applied Surface Science,* **257** (1), 172-175 (2010).

16. F. Dong, WK. Ho, SC Lee, Z. Wu, M. Fu, S. Zou, *et al*. Template-free fabrication and growth mechanism of uniform $(BiO)_2CO_3$ hierarchical hollow microspheres with outstanding photocatalytic activities under both UV and visible light irradiation. *Journal of Materials Chemistry*, **21** (33), 12428-124236 (2011)

17. Y. Xia, Y. Xiong, B. Lim, SE. Skrabalak. Shape-Controlled Synthesis of Metal Nanocrystals, Simple Chemistry Meets Complex Physics? *Angewandte Chemie International Edition,* **48** (1), 60-103 (2009).

18. DV. Goia, Preparation and formation mechanisms of uniform metallic particles in homogeneous solutions. *Journal of Materials Chemistry,* **14** (4), 451-458 (2004).

19. YB. Zhao, KJ. Zhang, HX Dang. A simple way to prepare bismuth nanoparticles. *Materials Letters*.**58** (5), 790-793 (2004).

20. J. Li, H. Fan, J. Chen, L. Liu, Synthesis and characterization of poly(vinyl pyrrolidone)-capped bismuth nanospheres. *Colloids and Surfaces A:Physicochemical and Engineering Aspects*, **340** (1-3):66-69 (2009).

21. Y. Wang, J. Chen, L. Chen, YB. Chen, LM. Wu, Shape-Controlled Solventless Syntheses of Nano Bi Disks and Spheres. *Crystal Growth & Design*, **10** (4), 1578-1584 (2010).

22. D. Ma, J. Zhao, Y. Li, X. Su, S. Hou, Y. Zhao, *et al*. Organic molecule directed synthesis of bismuth nanostructures with varied shapes in aqueous solution and their optical characterization. *Colloids and Surfaces a-Physicochemical and Engineering Aspects*, **368** (1-3), 105-111 (2010).

23. D. Ma, J. Zhao, R. Chu, S. Yang, Y. Zhao, X. Hao, *et al*. Novel synthesis and characterization of bismuth nano/microcrystals with sodium hypophosphite as reductant. *Advanced Powder Technology*. **24** (1):79-85 (2013).

24. G. Carotenuto, CL. Hison, F. Capezzuto, M. Palomba, P. Perlo, P. Conte. Synthesis and thermoelectric characterisation of bismuth nanoparticles. *Journal of Nanoparticle Research,* **11** (7), 1729-38 (2009).

25. JS. Son, K. Park, MK. Han, C. Kang, SG. Park, JH. Kim, *et al*. Large-Scale Synthesis and Characterization of the Size-Dependent Thermoelectric Properties of Uniformly Sized Bismuth Nanocrystals. *Angewandte Chemie-International Edition*, **50** (6), 1363-1366 (2011).

26. A. Luz, C Feldmann, Reversible photochromic effect and electrochemical voltage driven by light-induced Bi-0 formation, *Journal of Materials Chemistry,* **19** (43), 8107-8111 (2009).

27. SC. Warren, AC. Jackson, ZD. Cater-Cyker, FJ. Di Salvo, U. Wiesner. Nanoparticle synthesis via the photochemical polythiol process, *Journal of the American Chemical Society*, **129** (33), 10072 (2007)

28. J. Chen, T. Herricks, M.Geissler, Y. Xia, Single-Crystal Nanowires of Platinum Can Be Synthesized by Controlling the Reaction Rate of a Polyol Process. *Journal of the American Chemical Society*, **126** (35), 10854-10855 (2004).

29. T. Yao, H. Wei, Z. Guoyun, W. Shouxu, YT. Xiaojian, T. Zhihua, *et al*. A new approach causing the patterns fabricated by silver nanoparticles to be conductive without sintering. *Nanotechnology*, **23** (35), 355304 (2012).

30. YH. Lee, DW. Kim, SI. Shini, SG. Oh, Preparation of Au colloids by polyol process using NaHCO3 as a buffering agent. *Materials Chemistry and Physics*, **100** (1), 85-91 (2006).

31. J. Sun, Y. Jing, Y. Jia, M. Tillard, C. Belin. Mechanism of preparing ultrafine copper powder by polyol process. *Materials Letters*, **59** (29–30), 3933-3936 (2005).

32. K. Yu, DJ. Kim, HS. Chung, H. Liang. Dispersed rodlike nickel powder synthesized by modified polyol process. *Materials Letters*, **57** (24–25), 3992-3997 (2003).

33. MB. Cortie, AM. McDonagh, Synthesis and Optical Properties of Hybrid and Alloy Plasmonic Nanoparticles. *Chemical Reviews*, **111** (6):3713-3735 (2011).

34. Y. Wang, Y. Xia. Bottom-Up and Top-Down Approaches to the Synthesis of Monodispersed Spherical Colloids of Low Melting-Point Metals. *Nano Letters*, **4** (10), 2047-5200 (2004).

35. WT. Cheng, YW. Chih Manipulation of silver nanostructures using supercritical fluids in the presence of polyvinylpyrrolidone and ethylene glycol. *Journal Supercrit Fluids*, **54** (2), 272-280 (2010).

36. HS. Shin, HJ. Yang, SB. Kim, MS. Lee. Mechanism of growth of colloidal silver nanoparticles stabilized by polyvinyl pyrrolidone in gamma-irradiated silver nitrate solution. *Journal of Colloid Interface Science*, **274** (1), 89-94 (2004).

37. YZ. Wang,YX. L, ST. Yang, GL. Zhang, DM. An, C. Wang C, *et al*. A convenient route to polyvinyl pyrrolidone/silver nanocomposite by electrospinning. *Nanotechnology*, **17** (13), 3304-3307 (2006).

38. N. Misra, J. Biswal, A. Gupta, JK. Sainis, S. Sabharwal. Gamma radiation induced synthesis of gold nanoparticles in aqueous polyvinyl pyrrolidone solution and its application for hydrogen peroxide estimation. *Radiat Phys Chem*, **81** (2), 195-200 (2012).

39. JM. Khurana, K. Vij. Nickel Nanoparticles Catalyzed Knoevenagel Condensation of Aromatic Aldehydes with Barbituric Acids and 2-Thiobarbituric Acids. *Catal Lett*, **138** (1-2), 104-110 (2010).

40. D. Li, S. Komarneni. Microwave-Assisted Polyol Process for Synthesis of Ni Nanoparticles. *Journal of the American Ceramic Society*, **89** (5), 1510-1517 (2006).

41. W. Yu, H. Xie, L. Chen, Y. Li. Investigation on the thermal transport properties of ethylene glycol-based nanofluids containing copper nanoparticles. *Powder Technology*, **197** (3), 218-21 (2010).

42. S. Horiuchi, T. Hanada, N. Izu, I. Matsubara. Electron microscopy investigations of the organization of cerium oxide nanocrystallites and polymers developed in polyvinylpyrrolidone-assisted polyol synthesis process. *Journal of Nanoparticle Research*, **14** (3) (2012).

43. H. Huang, QP. Xie, MX. Kang, B. Zhang, H. Zhang, J. Chen, *et al*. Labeling transplanted mice islet with polyvinylpyrrolidone coated superparamagnetic iron oxide nanoparticles for in vivo detection by magnetic resonance imaging. *Nanotechnology,* **20** (36) (2009).

44. TT. Tseng, WJ. Tseng. Effect of polyvinylpyrrolidone on morphology and structure of In_2O_3 nanorods by hydrothermal synthesis. *Ceram Int,* **35** (7), 2837-2844 (2009).

45. M. Tsuji, Y. Nishizawa, K. Matsumoto, M. Kubokawa, N. Miyamae, T. Tsuji. Effects of chain length of polyvinylpyrrolidone for the synthesis of silver nanostructures by a microwave-polyol method. *Materials Letters*, **60** (6), 834-838 (2006).

46. WZ. Wang, B. Poudel, Y. Ma, ZF. Ren. Shape Control of Single Crystalline Bismuth Nanostructures. *The Journal of Physical Chemistry B*, **110** (51), 25702-25706 (2006).

47. CC. Mayorga-Martinez, M. Cadevall, M. Guix, J. Ros, A. Merkoci A. Bismuth nanoparticles for phenolic compounds biosensing application. *Biosens Bioelectron*, **40** (1), 57-62 (2013).

48. YW. Wang, KS. Kim. Large-scale polyol synthesis of single-crystal bismuth nanowires and the role of NaOH in the synthesis process. *Nanotechnology*, **19** (26) (2008).

49. J. Wu, F. Qin, Z. Lu, HJ. Yang, R. Chen, Solvothermal synthesis of uniform bismuth nanospheres using poly(N-vinyl-2-pyrrolidone) as a reducing agent. *Nanoscale Research Letters*, **6,** 66 (2011).

50. G. Cheng, J. Wu, F. Xiao, H. Yu, Z. Lu, X. Yu, *et al*. Synthesis of bismuth micro- and nanospheres by a simple refluxing method. *Materials Letters*, **63** (26), 2239-2242 (2009).

51. YW. Wang, BH. Hong, KS. Kim. Size control of semimetal bismuth nanoparticles and the UV-visible and IR absorption spectra. *Journal of Physical Chemistry B*, **109** (15), 7067-7072 (2005).

L. Balan, R. Schneider, D. Billaud, Y. Fort, J. Ghanbaja. A new synthesis of ultrafine nanometre-sized bismuth particles. *Nanotechnology*, **15** (8), 940 (2004).

Y. Wang, J. Chen, L. Chen, YB. Chen, LM. Wu, Shape-Controlled Solventless Syntheses of Nano Bi Disks and Spheres, *Crystal Growth & Design*, **10** (4), 1578-1584 (2010).

54 M. Yarema, MV. Kovalenko, G. Hesser, DV. Talapin, W. Heiss. Highly Monodisperse Bismuth Nanoparticles and Their Three-Dimensional Superlattices. *Journal of the American Chemical Society*, **132** (43), 15158-15159 (2010).

55. J. Fang, KL. Stokes, WL. Zhou, W. Wang, J. Lin. Self-assembled bismuth nanocrystallites. *Chemical Communications*, **0** (18), 1872-1873 (2001).

56. S. Schulz, S. Heimann, C. Woelpe, W. Assenmacher. Synthesis of Bismuth Pseudocubes by Thermal Decomposition of Bi_2Et_4. *Chemistry of Materials*, **24** (11), 2032-2039 (2012).

57. EE. Foos, RM. Stroud, AD. Berry, AW. Snow, JP. Armistead. Synthesis of Nanocrystalline Bismuth in Reverse Micelles. *Journal of the American Chemical Society*, **122** (29), 7114-7115 (2000).

58. HF. Yang, Y. Yan, JF. Li, XJ. Lu, GC. Xi, Q. Zhang, *et al*. Low-temperature Hydrothermal Synthesis of Bismuth Nanoflowers and Their Application for Heavy Metal Detection. *Chemistry Letters*, **42** (2), 150-152 (2013).

59. T. Som, A. Simo, R. Fenger, *et al* Bismuth Hexagons: Facile Mass Synthesis, Stability and Applications, *ChemPhysChem*, **13** (8), 2162-2169 (2012).

60. Y. Ni, Y. Zhang, L. Zhang, J. Hong, Mass synthesis of dendritic Bi nanostructures by a facile electrodeposition route and influencing factors, *CrystEngComm*, **13**, 794-799 (2011).

61. BJ. Plowman, SK. Bhargava, AP. O'Mullane. Electrochemical fabrication of metallic nanostructured electrodes for electroanalytical applications. *Analyst*, **136** (24), 5107-5119 (2012).

62. W. Shijie, L. Wenjing, K. Qi, S. Dazhong, P. Dawei P. Site synthesis of bismuth nanoparticles for electrochemical determination of lead. *Micro & Nano Letters, IET*, **7** (12), 1260-1263 (2012).

63. V. Beni, DWM. Arrigan. Microelectrode arrays and microfabricated devices in electrochemical stripping analysis. *Current Analytical Chemistry*, **4** (3):229-241 (2008).

64. G. Aragay, A. Puig-Font, M. Cadevall, A. Merkoci A. Surface Characterizations of Mercury-Based Electrodes with the Resulting Micro and Nano Amalgam Wires and Spheres Formations May Reveal Both Gained Sensitivity and Faced Nonstability in Heavy Metal Detection. *J Phys Chem C*, **114** (19), 9049-9055 (2010).

65. I. Svancara, C. Prior, SB. Hocevar, J. Wang. A Decade with Bismuth-Based Electrodes in Electroanalysis. *Electroanalysis*, **22** (13), 1405-1420 (2010).

66. J. Wang, *Electroanalysis*, **17**, 1341 (2005).

67. N. Serrano, A. Alberich, JM. Díaz-Cruz, C. Ariño, M. Esteban. Coating methods, modifiers and applications of bismuth screen-printed electrodes. *Trends in Analytical Chemistry*, **46** (0), 15-29 (2013).

68. O. Domínguez-Renedo, MJ Gómez González, MJ Arcos-Martínez, Determination of Antimony (III) in Real Samples by Anodic Stripping Voltammetry Using a Mercury Film Screen-Printed Electrode. *Sensors*, **9** (1), 219-231 (2009).

69. I. Palchetti, S. Laschi, M. Mascini, Miniaturised stripping-based carbon modified sensor for in field analysis of heavy metals. *Analytica Chimica Acta*, **530** (1), 61-67 (2005).

70. R. Güell, G. Aragay, C. Fontàs, E. Anticó, A. Merkoçi. Sensitive and stable monitoring of lead and cadmium in seawater using screen-printed electrode and electrochemical stripping analysis. *Analytica Chimica Acta*, **627** (2), 219-224 (2008).

71. G. Aragay, J. Pons, A. Merkoçi. Recent Trends in Macro-, Micro-, and Nanomaterial-Based Tools and Strategies for Heavy-Metal Detection. *Chemical Reviews*, **111** (5), 3433-3458 (2011).

72. G. Aragay, A. Merkoçi, Nanomaterials application in electrochemical detection of heavy metals. *Electrochimica Acta*, **84** (0), 49-61 (2012).

73. A. Merkoçi. Electrochemical biosensing with nanoparticles. *FEBS Journal*, **274** (2), 310-316 (2007).

74. F. Arduini, JQ. Calvo, A. Amine, G. Palleschi, D. Moscone. Bismuth-modified electrodes for lead detection. *Trends in Analytical Chemistry*, **29** (11), 1295-1304 (2010).

75. MT. Castaneda, B. Perez B, M. Pumera, M. del Valle, A. Merkoci, S. Alegret, Sensitive stripping voltammetry of heavy metals by using a composite sensor based on a built-in bismuth precursor. *Analyst*, **130** (6), 971-976 (2005).

76. J. Wang, J. Lu, SB. Hocevar, PAM Farias, B. Ogorevc, Bismuth-Coated Carbon Electrodes for Anodic Stripping Voltammetry. *Analytical Chemistry*, **72** (14), 3218-3222 (2000).

77. MÁ. Granado-Rico, M. Olivares-Marín, E. Pinilla-Gil. A Novel Cell Design for the Improved Stripping Voltammetric Detection of Zn(II), Cd(II), and Pb(II) on Commercial Screen-Printed Strips by Bismuth Codeposition in Stirred Solutions. *Electroanalysis*, **20** (24), 2608-2613 (2008).

78. GH. Hwang, WK. Han, JS. Park, SG. Kang, Determination of trace metals by anodic stripping voltammetry using a bismuth-modified carbon nanotube electrode. *Talanta*, **76** (2), 301-308 (2008).

79. H. Xu, L. Zeng, S. Xing, Y. Xian, G. Shi, L. Jin. Ultrasensitive Voltammetric Detection of Trace Lead(II) and Cadmium(II) Using MWCNTs-Nafion/Bismuth Composite Electrodes. *Electroanalysis*, **20** (24):2655-2662 (2008).

80. J. Wang, J. Lu, Ü. Anik, SB. Hocevar, B. Ogorevc. Insights into the anodic stripping voltammetric behavior of bismuth film electrodes. *Analytica Chimica Acta*, **434** (1), 29-34 (2001).

80. SB. Hocevar, J. Wang, RP. Deo, B. Ogorevc. Potentiometric Stripping Analysis at Bismuth-Film Electrode. *Electroanalysis*, **14** (2), 112-115 (2002).

82. R. Pauliukaitė, CMA. Brett. Characterization and Application of Bismuth-Film Modified Carbon Film Electrodes. *Electroanalysis*, **17** (15-16), 1354-1359 (2005).

83. EA. Hutton, B. Ogorevc, MR. Smyth. Cathodic Electrochemical Detection of Nitrophenols at a Bismuth Film Electrode for Use in Flow Analysis. *Electroanalysis*, **16** (19), 1616-1621 (2004).

84. G. Kefala, A. Economou, A. Voulgaropoulos, M. Sofoniou, A study of bismuth-film electrodes for the detection of trace metals by anodic stripping voltammetry and their application to the determination of Pb and Zn in tapwater and human hair. *Talanta*, **61** (5), 603-610 (2003).

85. GU. Flechsig, O. Korbout, SB. Hocevar, S. Thongngamdee B. Ogorevc, P. Gründler, *et al*. Electrically Heated Bismuth-Film Electrode for Voltammetric Stripping Measurements of Trace Metals. *Electroanalysis*, **14** (3), 192-196 (2002).

86. KE. Toghill, L. Xiao, GG. Wildgoose, RG. Compton, Electroanalytical Determination of Cadmium(II) and Lead(II) Using an Antimony Nanoparticle Modified Boron-Doped Diamond Electrode. *Electroanalysis*, **21** (10), 1113-1138 (2009).

87. KE. Toghill, GG. Wildgoose, A. Moshar, C. Mulcahy, RG. Compton. The Fabrication and Characterization of a Bismuth Nanoparticle Modified Boron Doped Diamond Electrode and Its Application to the Simultaneous Determination of Cadmium(II) And Lead(II). *Electroanalysis*, **20** (16), 1731-1737 (2008).

88. Z. Zou, A. Jang, E. MacKnight, PM. Wu, J. Do, PL. Bishop, *et al*. Environmentally friendly disposable sensors with microfabricated on-chip planar bismuth electrode for in situ heavy metal ions measurement. *Sensors and Actuators B-Chemical*, **134** (1), 18-24 (2008).

89. C. Kokkinos, A. Economou, I. Raptis. Microfabricated disposable lab-on-a-chip sensors with integrated bismuth microelectrode arrays for voltammetric determination of trace metals. *Analytica Chimica Acta*, **710** (0), 1-8 (2012).

90. N. Lezi, A. Economou, PA. Dimovasilis, PN. Trikalitis, MI. Prodromidis. Disposable screen-printed sensors modified with bismuth precursor compounds for the rapid voltammetric screening of trace Pb(II) and Cd(II). *Analytica Chimica Acta,* **728** (0), 1-8 (2012).

91. N. Serrano, J. Díaz-Cruz, C. Ariño, M. Esteban. Stripping analysis of heavy metals in tap water using the bismuth film electrode. *Anal Bioanal Chem*, **396** (3), 1365-1369 (2010).

92. MÁ. Granado-Rico, M. Olivares-Marín, E. Pinilla-Gil. Modification of carbon screen-printed electrodes by adsorption of chemically synthesized Bi nanoparticles for the voltammetric stripping detection of Zn(II), Cd(II) and Pb(II). *Talanta*, **80** (2), 631-635 (2009).

93. I. Švancara, L. Baldrianová, E. Tesařová, SB. Hočevar, SAA. Elsuccary, A. Economou, *et al*. Recent Advances in Anodic Stripping Voltammetry with Bismuth-Modified Carbon Paste Electrodes. *Electroanalysis*, **18** (2), 177-185 (2006).

94. NA. Malakhova, AA. Mysik, SY. Saraeva, NY. Stozhko, MA. Uimin, AE. Ermakov, *et al*. A voltammetric sensor on the basis of bismuth nanoparticles prepared by the method of gas condensation. *J Anal Chem*, **65** (6), 640-647 (2010).

95. SB. Hočevar, I. Švancara, K. Vytřas, B. Ogorevc. Novel electrode for electrochemical stripping analysis based on carbon paste modified with bismuth powder. *Electrochimica Acta*, **51** (4), 706-710 (2005).

96. GJ. Lee, HM. Lee, CK. Rhee, Bismuth nano-powder electrode for trace analysis of heavy metals using anodic stripping voltammetry. *Electrochemistry Communications*, **9** (10), 2514-2518 (2007).

97. GJ. Lee, HM. Lee, CK. Rhee, Effect of phase stability degradation of bismuth on sensor characteristics of nano-bismuth fixed electrode. *Talanta*, **83** (2), 682-685 (2010).

98. G. Liu, Y. Lin, Y. Tu, Z. Ren. Ultrasensitive voltammetric detection of trace heavy metal ions using carbon nanotube nanoelectrode array. *Analyst*, **130** (7), 1098-1101 (2005).

99. PK. Sahoo, B. Panigrahy, S. Sahoo, AK. Satpati, D. Li, D. Bahadur. In situ synthesis and properties of reduced graphene oxide/Bi nanocomposites: As an electroactive material for analysis of heavy metals. *Biosensors and Bioelectronics*, **43** (0):293-296 (2013).

100. EA. Hutton, B. Ogorevc, SB. Hočevar, MR.Smyth. Bismuth film microelectrode for direct voltammetric measurement of trace cobalt and nickel in some simulated and real body fluid samples. *Analytica Chimica Acta,* **557** (1–2), 57-63 (2006).

101. P. Jothimuthu, RA. Wilson, J. Herren, X. Pei, W. Kang, R. Daniels, *et al*. Zinc Detection in Serum by Anodic Stripping Voltammetry on Microfabricated Bismuth Electrodes. *Electroanalysis*, **25** (2), 401-407 (2013).

102. Z. Zhang, K. Yu, D. Bai, Z. Zhu. Synthesis and Electrochemical Sensing Toward Heavy Metals of Bunch-like Bismuth Nanostructures. *Nanoscale Research Letters*, **5** (2), 398–402 (2009).

103. J. Li, S. Guo, Y. Zhai, E. Wang, High-sensitivity determination of lead and cadmium based on the Nafion-graphene composite film. *Analytica Chimica Acta,* **649** (2), 196-201 (2009).

104. RO. Kadara, IE. Tothill. Development of disposable bulk-modified screen-printed electrode based on bismuth oxide for stripping chronopotentiometric analysis of lead (II) and cadmium (II) in soil and water samples. *Anal Chim Acta*, **623** (1), 76-81 (2008).

105. R. Pauliukaitė SB. Hočeva, B. Ogorevc, J. Wang. Characterization and Applications of a Bismuth Bulk Electrode. *Electroanalysis*, **16** (9), 719-723 (2004).

106. Ü. Anik, S. Marín, M.Pumera M, A. Merkoçi, S. Alegret. Stripping Voltammetry with Bismuth Modified Graphite-Epoxy Composite Electrodes. *Electroanalysis*, **17** (10), 881-886 (2005).

107. DE. Mays, A. Hussam. Voltammetric methods for determination and speciation of inorganic arsenic in the environment—A review. *Analytica Chimica Acta,* **646** (1–2), 6-16 (2009).

108. L. Jiajie, Y. Nagaosa. Cathodic stripping voltammetric determination of As(III) with in situ plated bismuth-film electrode using the catalytic hydrogen wave. *Analytica Chimica Acta,* **593** (1), 1-6 (2007).

109. P. Zong, J. Long, Y. Nagaosa. Determination of total antimony(III,V) by square-wave anodic stripping voltammetry with in situ plated bismuth-film electrode. International Journal of *Environmental Analytical Chemistry*, **91** (5), 421-430 (2011).

110. Q. Zhang, SW. Zhong, JL. Su, XJ. Li, H. Zou, Determination of Trace Chromium by Square-Wave Adsorptive Cathodic Stripping Voltammetry at an Improved Bismuth Film Electrode. *Journal of the Electrochemical Society*, **160** (4), H237-H42 (2013).

111. EO. Jorge, MM. Neto, MM. Rocha . A mercury-free electrochemical sensor for the determination of thallium(I) based on the rotating-disc bismuth film electrode. *Talanta*, **72** (4), 1392-1399 (2007).

112. J. Wang, D. Lu, Thongngamdee S, Lin Y, Sadik OA. Catalytic adsorptive stripping voltammetric measurements of trace vanadium at bismuth film electrodes. *Talanta*, **69** (4), 91491-7 (2006).

113. GMS. Alves, JMCS. Magalhães, HMVM. Soares, Simultaneous Determination of Nickel and Cobalt Using a Solid Bismuth Vibrating Electrode by Adsorptive Cathodic Stripping Voltammetry. *Electroanalysis*, **25** (5), 1247-1255 (2013).

114. C. Kokkinos, A. Economou, I. Raptis, T. Speliotis. Disposable lithographically fabricated bismuth microelectrode arrays for stripping voltammetric detection of trace metals. *Electrochemistry Communications*, **13** (5), 391-395 (2011).

115. S. Zhong, J. Su, L. Chen, J. Tong, W. Jia, X. Li, H. Zou, Determination of Total Germanium in Chinese Herbal Remedies by Square-Wave Catalytic Adsorptive Cathodic Stripping Voltammetry at an Improved Bismuth Film Electrode, *International Journal of Electrochemistry*, 735019 (2013).

116. L. Lin, S. Thongngamdee, J. Wang, Y. Lin, OA. Sadik, SY. Ly. Adsorptive stripping voltammetric measurements of trace uranium at the bismuth film electrode. *Analytica Chimica Acta*, **535** (1–2), 9-13 (2005).

117. P. Zong, Y. Nagaosa. Determination of antimony(III) and (V) in natural water by cathodic stripping voltammetry with in-situ plated bismuth film electrode. *Microchim Acta*, **166** (1-2), 139-144 (2009).

118. C. Kokkinos, A. Economou, I. Raptis, T. Speliotis. Disposable mercury-free cell-on-a-chip devices with integrated microfabricated electrodes for the determination of trace nickel(II) by adsorptive stripping voltammetry. *Analytica Chimica Acta*, **622** (1–2), 111-118 (2008).

119. L. Lin, NS. Lawrence, S. Thongngamdee, J. Wang, Y. Lin. Catalytic adsorptive stripping determination of trace chromium (VI) at the bismuth film electrode. *Talanta*, **65** (1), 144-148 (2005).

120. C. Kokkinos, A. Economou, M. Koupparis. Determination of trace cobalt(II) by adsorptive stripping voltammetry on disposable microfabricated electrochemical cells with integrated planar metal-film electrodes. *Talanta*, **77** (3), 1137-1142 (2009).

121. Niu X, Zhao H, Lan M. Disposable screen-printed bismuth electrode modified with multi-walled carbon nanotubes for electrochemical stripping measurements. Analytical Sciences. 2011;27(12):1237-1241.

122. R. Pauliukaite, R. Metelka, I. Švancara, A. Królicka, A. Bobrowski, K. Vytřas K, *et al*. Carbon paste electrodes modified with Bi_2O_3 as sensors for the determination of Cd and Pb. *Anal Bioanal Chem*, **374** (6), 1155-1158 (2002).

123. D. Pan, L. Zhang, J. Zhuang, T. Yin, W. Lu, W. Qin. On-Line Determination of Lead in Tap Waters at Two-Step Prepared Bismuth Electrode. *International Journal of Electrochemical Science*, **6** (7), 2710-2717 (2011).

124. ME. Conti, F. Botrè. Honeybees and their products as potential bioindicators of heavy metals contamination. *Environmental Monitoring and Assessment*, , **69** (3), 267-282 (2001).

125. S. Bogdanov. Contaminants of bee products. *Apidologie*, **37** (1), 1-18 (2006).

126. GD. Pierini, AM. Granero, MS. Di Nezio, ME. Centurión, MA. Zon, H. Fernández, Development of an electroanalytical method for the determination of lead in Argentina raw propolis based on bismuth electrodes. *Microchemical Journal*, **106**, 102-106 (2013).

127. DQ. Huang, BL. Xu, J. Tang, LL. Yang, ZB. Yang, SP. Bi. Bismuth Film Electrodes for Indirect Determination of Sulfide Ion in Water Samples at Trace Level by Anodic Stripping Voltammetry. *International Journal of Electrochemical Science*, **7** (4), 2860-2873 (2012).

128. M. Bučková, P. Gründler, GU. Flechsig. Adsorptive Stripping Voltammetric Detection of Daunomycin at a Bismuth Bulk Electrode. *Electroanalysis*, **17** (5-6), 440-4 (2005).

129. JA. Rodríguez, E. Barrado, Y. Castrillejo, JR. Santos, JLFC Lima, Validation of a tubular bismuth film amperometric detector: Determination of diclofenac sodium by multisyringe flow injection analysis. *Journal of Pharmaceutical and Biomedical Analysis*, **45** (1), 47-53 (2007).

130. M. Moreno, E. Bermejo, M. Chicharro, A. Zapardiel, AS. Arribas. Cathodic Electrochemical Determination of Herbicides in Acid Media Using a Bismuth Film Electrode. *Electroanalysis*, **21** (3-5), 415-421 (2009).

131. AS. Arribas, E. Bermejo, M. Chicharro, A. Zapardiel. Voltammetric Detection of the Herbicide Metamitron at a Bismuth Film Electrode in Nondeaerated Solution. *Electroanalysis*, **18** (23), 2331-2336 (2006).

132. V. Guzsvány, M. Kádár, Z. Papp, L. Bjelica, F. Gaál, K. Tóth, Monitoring of Photocatalytic Degradation of Selected Neonicotinoid Insecticides by Cathodic Voltammetry with a Bismuth Film Electrode. *Electroanalysis*, **20** (3), 291-300 (2008).

133. W. Zhang, H. Tang, P. Geng, Q. Wang, L. Jin, Z. Wu. Amperometric method for rapid detection of Escherichia coli by flow injection analysis using a bismuth nano-film modified glassy carbon electrode. *Electrochemistry Communications*, **9** (4), 833-838 (2007).

134. S. Timur, Ü. Anik. α-Glucosidase based bismuth film electrode for inhibitor detection. *Analytica Chimica Acta*, **598** (1), 143-146 (2007).

135. Ü. Anık, S. Timur, M. Çubukçu, A. Merkoçi. The usage of a bismuth film electrode as transducer in glucose biosensing. *Microchim Acta*,**160** (1-2), 269-273 (2008).

136. WY. Su, SM. Wang, SH. Cheng. Electrochemically pretreated screen-printed carbon electrodes for the simultaneous determination of aminophenol isomers. *Journal of Electroanalytical Chemistry*,**651** (2), 166-172 (2011).

137. A. Merkoçi, Ü. Anik, S. Çevik, M. Çubukçu, M. Guix. Bismuth Film Combined with Screen-Printed Electrode as Biosensing Platform for Phenol Detection. *Electroanalysis*, **22** (13), 1429-1436 (2010).

138. D. Shan, J. Zhang, HG. Xue, YC. Zhang, S. Cosnier, SN. Ding. Polycrystalline bismuth oxide films for development of amperometric biosensor for phenolic compounds. *Biosensors and Bioelectronics*,**24** (12), 3671-3676 (2009).

139. Ü. Anik, S. Cevik, S. Timur, Bismuth Film Electrode as Sensing Platform for IgE–anti-IgE Interactions. *Electroanalysis*, **23** (10), 2379-2385 (2011)

CHAPTER 3: SYNTHESIS OF BISMUTH NANOPARTICLES WITH INTEREST FOR SENSING APPLICATION

Between their many applications bismuth nanoparticles (BiNPs) are showing interest as pre-concentrators in heavy metals detection while being applied as working electrode modifiers used in electrochemical stripping analysis. From the different reported methods to synthesize BiNPs we are focused on the typical polyol method, largely used in these types of metallic and semi-metallic nanoparticles. This study presents the strategy for an easy control of the shape and size of BiNPs including nanocubes, nanosferes and triangular nanostructures. To improve the BiNP size and shape different reducing agents (ethylene glycol or sodium hypophosphite) and stabilizers (polyvinyl pyrrolidone, PVP, in different amounts) have been studied. The efficiency of BiNPs for heavy metals analysis in terms of detection sensitivity while being used as modifiers of screen-printed carbon electrodes including the applicability of the developed device in real sea water samples is shown. A parallel study between the obtained nanoparticles and their performance in heavy metal sensing has been described in this chapter.

3.1 Introduction

From the early 2000, bismuth has emerged as a promising electrode material in electroanalysis field being with interest overall in electrochemical stripping, voltammetric and amperometric based sensors[1–3]. The interest comes from the environmentally friendly ("green") character of bismuth electrodes in comparison to mercury (the most used in voltammetric techniques) and its good performance in heavy metal detection applications.

Due to these properties, bismuth has become the most used candidate to substitute mercury as a working electrode modifier in electrochemical stripping analysis[4]. As it is well reported, bismuth electrodes offer a well-defined, undistorted, and highly reproducible stripping response, excellent resolution of neighbouring peaks, high hydrogen evolution, wide linear dynamic range, with signal-to-background characteristics comparable to those of common mercury electrodes[5].

Different types of bismuth-based sensors have been reported but the most used configurations are based on the co-deposition (*in situ*) of bismuth during electrochemical stripping analysis and the use of bismuth modified (*ex situ*) electrodes. Bismuth films are normally generated by its electroplating onto electrode surfaces such as glassy carbon electrodes[6], boron doped diamond electrodes[7], gold microelectrodes[8] and screen-printed electrodes[9].

Attempt for the modification of SPCEs with metallic nanoparticles before stripping analysis of heavy metals, in order to benefit from unique advantages over electrodes, such as, enhancement of mass transport, catalysis, high effective surface area and control

over electrode microenvironment also has been reported[10]. Bismuth nanoparticles used as electrode modifiers have proven to be highly sensitive and reliable for trace analysis of heavy metals in conjunction with anodic stripping voltammetry[11]. The attractive and unique behaviour of BiNP modified electrodes is attributed to the formation of multicomponent alloys, as well as the enhanced sensibility coming from the combination of the great properties of the nanostructured material.

Different ways to obtain bismuth nanostructures have been reported. On one hand, the obtaining of BiNPs can be performed form bulk metallic bismuth by using thermal decomposition method usually not efficient enough in terms of production yield[12]. On the other hand reductive methods to synthetize BiNPs also have been reported. Various reducing agents, including ethylene-glycol[13], sodium borohydride[14], aqueous hydrazine solution[15], ethylene-diammine and, recently, sodium hyposphite[16] have been used to prepare Bi crystals. The use of an organometallic complex of bismuth as a precursor for the decomposition also has been reported[17,18]. In addition, photochemical activation has been used to synthesize bismuth nanoparticles[19,20]. The use of reductive methods provides some advantages in terms of size and shape control, and, usually, it leads to the increase of the efficiency of BiNPs preparation in terms of massive production.

We study now different chemical reducing strategies to synthetize bismuth nanoparticles for a better efficiency in heavy metal analysis by using electrochemical stripping analysis. To improve the sensing capability of the synthetized BiNPs interesting and novel modifications of its preparation procedures are now introduced. In addition, the use of bismuth nanoparticles is combined with screen-printed electrodes including

their operation in flow-through mode that may offer better cost-efficient devices with interest for future applications that would include automated and miniaturized measuring systems for environmental control and other fields.

3.2 Experimental Section

3.2.1 Chemicals

For the synthesis of bismuth nanoparticles the following reagents were used: Bismuth (III) nitrate pentahydrate, reagent grade, 98% from Aldrich, potassium hydroxide, ACS-ISO-for analysis, from Carlo Ebra reagents, poly(vinyl pyrrolidone) (PVP, M_W~30.000) from Aldrich, ethylene glycol from J. T. Baker Chemicals B. V. and acetone, isopropanol and ethanol were supplied by Panreac.

Heavy metals stock solutions were prepared by diluting lead (II) and cadmium (II) standard solutions AA grade (1000 ± 2 mg/l, Panreac). The water used for preparation of all solutions was from Milli-Q system (>18.2MΩcm^{-1}, Millipore). Seawater used was from Catalan coast. Acetate buffer was made using sodium acetate (Sigma-Aldrich) and acetic acid (Sigma-Aldrich). The pH was adjusted and determined using the pH-meter (BASIC 20+, from Crisom). All glass material used has been cleaned using diluted nitric acid (65% PA, Panreac).

3.2.2 Preparation of Screen Printed Carbon Electrodes (SPCE)

The SPCEs consist of a single strip with three electrodes: working, reference and counter electrode. Three different inks were used: graphite ink for the working and counter electrode (Electrodag 423SS ink), silver/silver chloride for the reference electrode layer (Electrodag 6037SS ink) and finally an insulating layer (Minico M-7000 Blue) to better define the working electrode area and avoid the undesirable contacts of the liquid with the internal connections. All the inks were purchased from Acheson Industries. After

the deposition of each layer, a drying process is followed by keeping the polyester substrate at 120 °C for 45 min (graphite) and 30 min (Ag/AgCl and insulating inks).

3.2.3 Electrochemical analysis

For the electrochemical measurements a computer-controlled Autolab PGSTAT-12 (302 N-High performance) (potentiostat/galvanostat) with general-purposes electrochemical software operating system (GPES version 4.9.007, from Eco Chemie B.V., Utrecht, The Netherlands) was used. The integrated three electrodes strips were connected to the Autolab PGSTAT-12 with a specially adapted electrical edge connector. The flow-through system consists of a peristaltic pump (PERIMAX 12) used for pumping the measuring solutions to a flow cell adapted to the SPCEs. The flow cell enables the use of SPCEs for flow-through applications. The SPCE is inserted into the slit/opening of the cell and tightened by a screw. The cell assures the wall-jet flow around the working electrode.

All electrochemical experiments were carried out at room temperature and no oxygen removal was performed. Heavy metal concentrations were determined by square wave voltammetry (SWV). The voltammetric parameters for the experiments were as follows: conditioning potential -0.5 V for 60 s, deposition potential -1.1 V for 120 s, equilibration time 30 s, SW amplitude 28 mV, step potential 3 mV, and frequency 15 Hz. Flow-through conditions were used during the conditioning and the accumulation step, whereas the equilibration step and the square wave scan were performed in a quiescent solution. Before using a new SPCE, repeated blank measurements in seawater were carried out (usually ten times) up to obtaining a stable background current. A new sensor

was used for each experiment. The range of concentration selected is 10 to 100 ppb of each metal in seawater at pH=4.5, adjusted using 0.1 M acetate buffer.

To evaluate the working range of the sensors, ASW responses toward Cd and Pb concentration changes have been studied. The modification of SPCEs has been performed by simple drop casting of BiNPs suspension of 0.1 mg BiNPs/mL onto the WE of the SPCE.

3.2.4 Characterization

Scanning electron microscope (SEM) analyses were performed by using an EVO (Carl Zeiss NTS GmbH. Germany). Transmission electron microscope (TEM) images were taken with a JEM-2011 (Jeol, Ltd., Japan). X-ray powder diffraction patterns were collected on a Siemens D-5000 diffactometer (German) using Cu Kα radiation.

Synthesis of BiNPs: All reactions were performed with magnetic stirring at >1000rpm in a 50 ml two-necked flask. During the reactions, the temperature was held constant by a temperature-controlled heating system with an aluminum support. All the synthesis were protected with a continue flow of nitrogen gas.

3.2.5 Polyol method

Bismuth nanoparticles were synthetized following a modification of the polyol method described by Y. Wang et al.[22] In a typical synthesis, 0,1g of $Bi(NO_3)_3$, KOH and Poly(vinyl pyrrolidone) in different amounts were dissolved in 25 mL ethylene glycol. This reaction mixture was heated up to 185^{o}C and kept during 2 h under constant stirring. At 80^{o}C a white solid, due to $Bi(OH)_3$ precipitation was observed, but the solution turns to transparent at higher temperature. Black BiNPs were isolated and sequentially washed

with *iso*-propanol and mili-Q water by centrifugation. The effect of the amounts of KOH (from 0.19g to 0.24g) and the PVP (from 0.1g to 0.05g) and their role in the synthesis was investigated.

3.2.6 Reduction with sodium hypophosphite

A solution of 0.1 g of $Bi(NO_3)_3$ and 0.1 g of PVP in 15 mL of ethylene glycol and a solution of 0,035 g of NaH_2PO_2 in 10 mL of ethylene glycol were heated to 60^{o}C. Both solutions were mixed and kept at this temperature for 60 min under stirring. The formed dark product was collected from the resultant solution by centrifugation. The black solid was sequentially washed using ethanol and mili-Q water.

3.3 Results and Discussion

3.3.1 Synthesis and characterization of bismuth nanoparticles

Among the different strategies described in the literature for BiNPs preparation, considering the good performance and solubility in water of the formed nanoparticles, polyol method has been selected as the most adequate for the modification of electrodes in heavy metal sensors. Bismuth nanoparticles were synthesized according to the literature references[21].

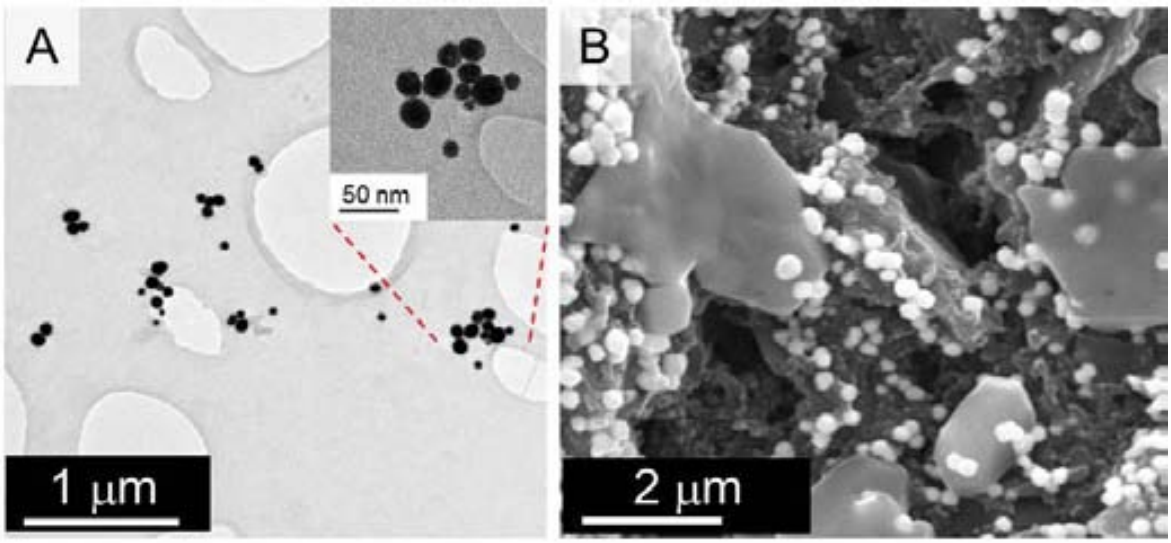

Figure 3.1 (A): TEM micrograph of bismuth nanoparticles synthesized with 0.1g $Bi(NO_3)_3$, 0.19g KOH and 0.1g PVP. The inset shows a zoom. (B): SEM image of these nanoparticles onto screen-printed carbon electrode.

Mixtures of $Bi(NO_3)_3$, KOH and PVP in ethyleneglycol gave spherical Bi nanoparticles with different diameters and appearances and dispersible in water and alcohols. In a standard synthesis 0,1g PVP and 0,19g KOH in the reaction media were used. Spherical nanoparticles of 400nm diameter with defined edges were obtained. The figure 3.1 shows the TEM images of the resultant nanoparticles. Although sedimentation

was observed in aqueous and alcoholic media, these particles were used in sensing application with good performance as it will be discussed below.

The role of KOH in the mixture is to promote the formation of the bismutate anion (BiO^{3-}) which, seems to be more reactive versus to the reduction to Bi(0)[22]. In aim to increase the reactivity of bismuth an excess of KOH (0.27g) was added to the reaction medium. This excess of alkaline salt produces large particles with different shapes, from spherical to cubic particles, with a diameter of around 1,2µm, as is shown in the figure 3.2. Although their high stability in water or alcoholic solutions and towards air oxidation; the big size causes a rapid sedimentation in any solvent. Due to the poor stability of the dispersions their application in heavy metal analysis was discarded.

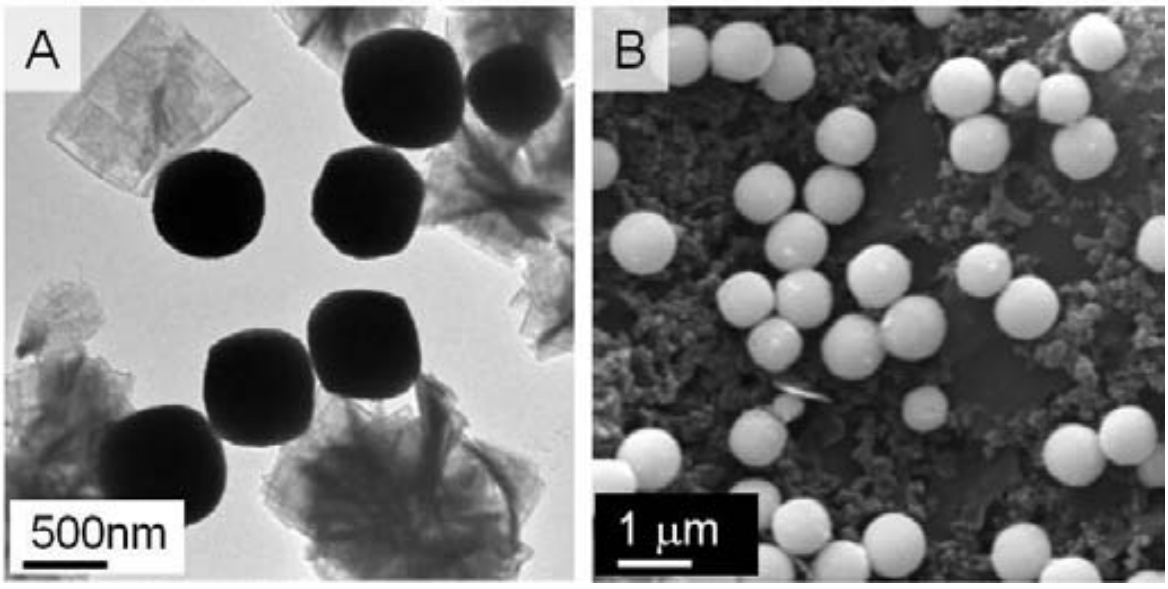

Figure 3.2 (A): TEM micrograph of bismuth nanoparticles synthesized with 0.1g $Bi(NO_3)_3$, 0.27g KOH and 0.1g PVP. (B): SEM image of these nanoparticles onto screen-printed carbon electrode.

As it is well known, PVP is a very good agent to promote nucleation and prevent aggregation of different kind of nanoparticles[23,24] However, the amount of PVP on the

nanparticles surface has to be limited in case of their use for electrochemical sensing applications. For this reason the quantity of PVP in the formation of BiNPs was reduced to amounts within 0.01 to 0.05g. The obtained nanoparticles were studied in order to visualize their morphology by SEM and TEM. Nanoparticles with limited amount of PVP resulted in spherical shapes and diameters of approximately 240nm (See Figure 3.3 A) with a wrinkled surface; this particular surface can be also seen in the SEM images in the Figure 3.5 D. The same reaction but in the absence of basic edia were also checked and 400nm nanoparticles with poor stability and poor size control were obtained.

An alternative method for BiNPs synthesis was a modified polyol process that includes chemical reduction at low temperature that was applied for the synthesis of copper nanoparticles[25]. This method is based on the chemical reduction of copper sulfate by sodium hypophosphite in ethylene glycol within the presence of PVP, to control the size of nanoparticles, prevent their aggregation and improve the stability of the resulting colloidal nanoparticles. Due to the similar standard reduction potential of copper and bismuth (+0.34 V and +0.32 V vs. SHE respectively), this methodology was chosen for the synthesis of bismuth nanoparticles as well. Using this method, relatively smaller BiNPs were obtained. TEM of dispersions shows triangular 70 nm nanoparticles with a mass of PVP residue of the reaction, as is shown by the spherical shapes in the Figure 3.4 A. SEM image shows the large amount of PVP present in the bismuth nanoparticle dispersion, after 10 washing steps (figure 3.4 B). One of the advantages of this synthetic procedure is the use of lower temperature and shorter synthesis time. The presence of large amounts of PVP before the cleaning procedure shows a principal drawback of this synthesis strategy: it causes lower conductivity of the SPCE and

therefore, poor response in sensing applications. When the amount of PVP was reduced below 0.05g, the nanoparticles weren't formed.

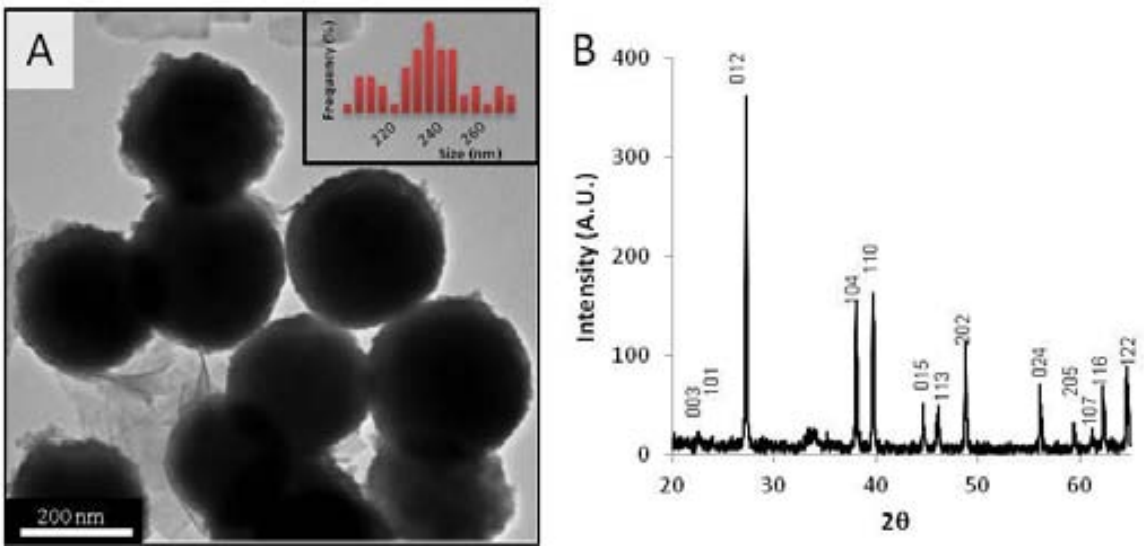

Figure 3.3 TEM micrograph of bismuth nanoparticles synthesized with 0.1g $Bi(NO_3)_3$, 0.19g KOH and 0.05g PVP. The inset shows the histogram of size distribution. (B): XRD pattern, of the same nanoparticles.

The XRD pattern of BiNPs, obtained with 0.1 g $Bi(NO_3)_3$, 0.19 g KOH and 0.05 g PVP, is shown in the part B of figure 3.3. It can be seen that all the diffraction peaks can be perfectly indexed to the rhombohedral phase of bismuth (Bi^0) (JCPDS No. 04-006-7762, R3m). Sharp peaks with high intensity reveal good crystallization of these nanoparticles. From the various nanoparticles synthetized the PVP based ones (at the optimal synthesis conditions), given the good performance (as discussed below) have been used to modify the SPCE for further application in heavy metal detection.

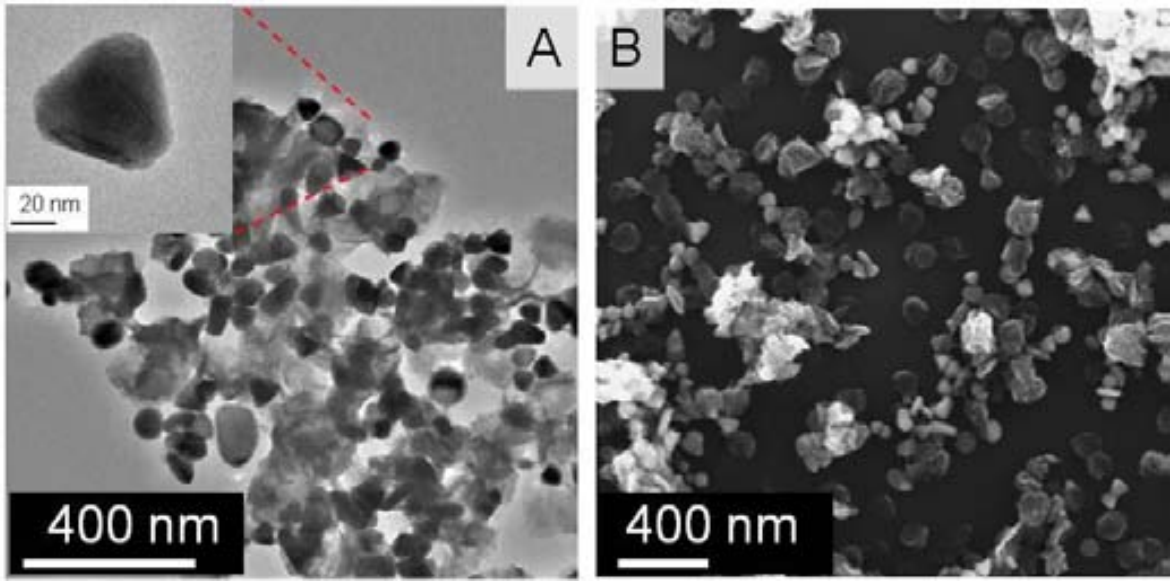

Figure 3.4 (A) TEM micrograph of bismuth nanoparticles synthesized using hypophosphite as a reducing angent. The inset shows the histogram of size distribution. (B): SEM image of these nanoparticles onto silicon wafer platform.

3.3.2 Evaluation of BiNPs prior electrochemical measurements

The measuring system used for SWV measurements is schematically represented in figure 4.5 A. The modification of the electrodes has been made by simple drop casting deposition onto working electrode; 5 µL drop of solution of bismuth nanoparticles (0.1 mg/mL) was found the best to cover the whole working electrode area and avoid either excess or uncovered areas. Figure 3.5 B shows pictures of a 45 SPCE units including a single one prepared by screen-printing technology. Homogeneous distribution of the BiNPs, drop casted onto the electrodes surface, can be observed by Scanning Electron Microscopy (SEM) image (see the figure 3.5 D) although some agglomerated particles can also be observed due probably to different adhesion properties of the electrode surface (carbon and polymer of the printed ink). BiNP show a well adhesion onto SPCE without the need for using any cross-linking agent. Figure 3.5 C is the SEM image of the bare

surface of SPCE. A uniform binding of carbon onto polyester substrate as a result of the printing process can be observed. This polyester platform used for SPCE is transparent and flexible and is made in large arrays of electrodes, providing advantages in terms of low cost and mass production beside application versatility. The possibility to integrate this simple electrochemical cell in a fluidic system is another great advantage in terms of stability and reproducibility.

The electrochemical response of SPCE is strongly affected by the quality of the used BiNPs including the on-top remaining/stabilizing compounds during their synthesis. Between various factors to be considered PVP seems to play an important role. Besides the role in synthesis (promote nucleation and prevent nanoparticles aggregation), PVP helps BiNPs in their better sticking onto the carbon electrode surface (ensuring a better immobilization) and protecting them from possible oxidation. Because that, the cleaning process must be exhaustively controlled.

As it is discussed previously, the use of PVP at amounts lower than 0.05 g in the synthesis medium reduces dramatically the stability of the nanoparticles and, subsequently, their future uses in SPCE modification. The increasing of the amount of PVP at levels higher than 0.1 g has a negative effect upon the conductivity in electrochemical applications discarding these samples for future heavy metal electrochemical stripping analysis applications.

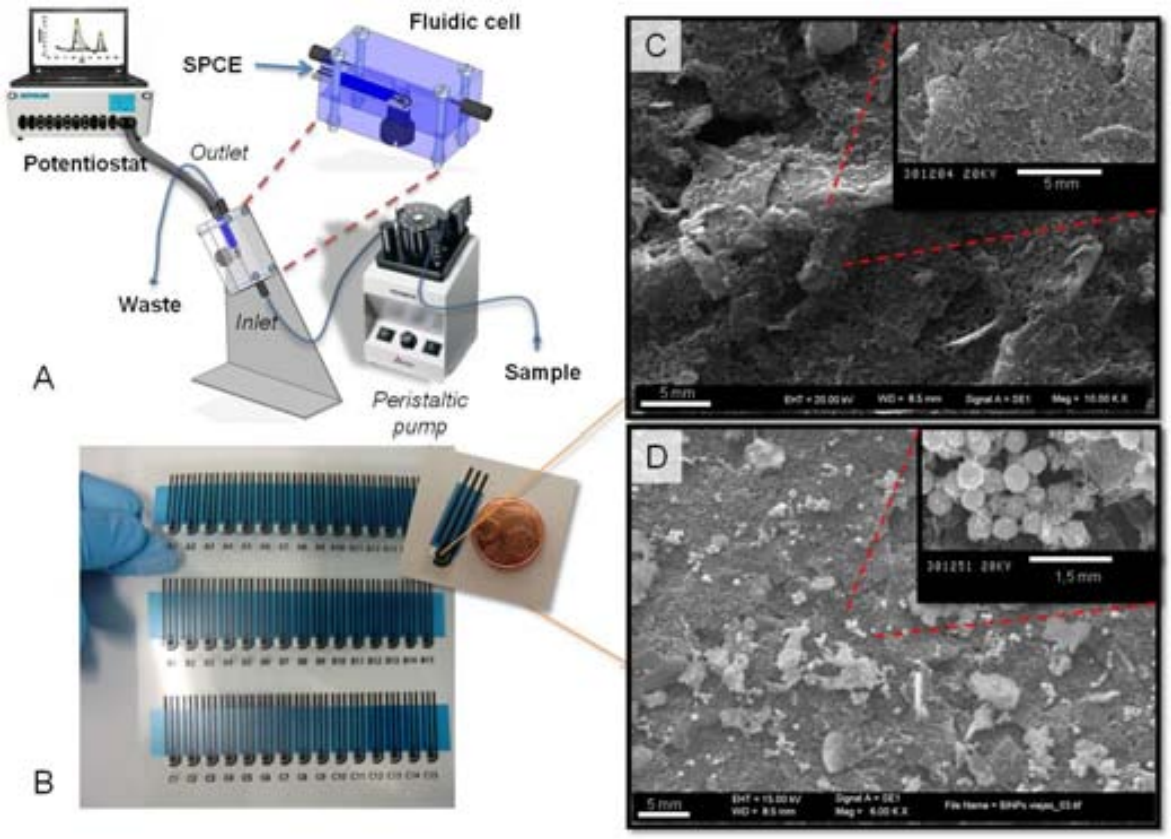

Figure 3.5 The scheme (A) shows the flow through system for heavy metal detection, the inset is a zoom of cell design. Picture (B) shows a sheet of 45 SPCE units and a single SPCE. The SEM images, including zooms, of the working electrode surface of (C) non-modified SPCE and (D) SPCE modified with BiNPs are shown.

3.3.3 Sensing application

Heavy metals detection was studied so as to evaluate the performance of the sensor. Lead and cadmium, given the importance of their detection in polluted water samples, have been chosen for these studies. To evaluate the working range of the sensors, the calibration curves that correspond to ASW peak current versus the Pb or Cd concentration have been obtained. The use of BiNP modified SPCE is expected to achieve at least a similar response as mercury modified ones previously reported for the monitoring of heavy metals in seawater but with the advantage of being mercury-free

devices[26]. Carbon-based SPCEs make use of the large available surface area and porosity of the working electrode area so as to exhibit an attractive electro-analytical performance with well-separated stripping signals for each metal[27]. While bare screen-printed carbon electrodes (bare-SPCE) show good response for lead, however a poor sensibility for cadmium detection, as we can see from figure 3.6 A, including even splitting of lead's peaks were observed (results are not shown).

The relatively poor response obtained by the use of bare SPCE is now increased by the presence of bismuth nanoparticles introduced by a simple casting of a drop of BiNPs dispersion of 0.1 mg BiNPs/mL. These nanoparticles are obtained using polyol method in presence of 0.05 g PVP in the synthesis, as is described previously. Figure 3.6 shows the SWV curves obtained for cadmium detection (with concentrations from 10 to 100 ppb) using bare-SPCE (3.6 A) and bismuth modified ones (3.6 B) including the corresponding calibration curves (3.6 C) plotted together for comparison purpose. In a similar mode the same results obtained for lead detection in seawater samples are also given (see Figure 3.6 D, E and F). The obtained results show a linear range of response for both cadmium and lead from 10 to 100 ppb. Clear increases of the responses (the sensitivities have been increased by 80% for cadmium and 40% for lead) when bismuth nanoparticles modify the working electrode surface can be appreciated. In addition, the repeatability is one of the strong points of this system, RSD are below 5% in both cadmium and lead measurements.

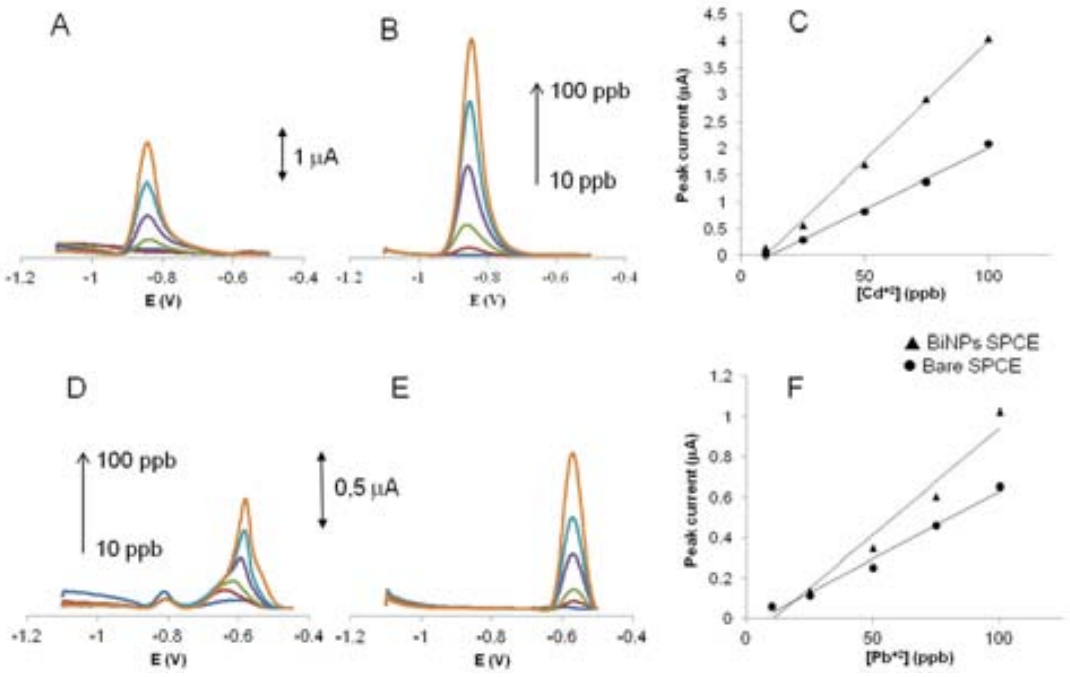

Figure 3.6 Typical SWV stripping response curves for cadmium using bare-SPCE (A) and Bi NPs modified SPCE (B), and the comparison of calibration curves at 0 to 100ppb range (C). (D) and (E) shows the same SWV responses of bare and bismuth modified SPCE to lead and (F) the corresponding calibrations at 0 to 100ppb range. Experimental details as described in the text.

To evaluate the selectivity of the BiNP modified SPCE the simultaneous detection of Cd and Pb also have been tested. Using BiNPs modified SPCE, clear differentiation between cadmium and lead with corresponding peaks appearing at -0,9 and -0,6 V respectively has been observed. In the case of unmodified electrodes, the presence of lead reduces dramatically the cadmium sensing capability (see figure 3.7 B). In this case, the oxidation peak of cadmium appears at -0,65 V and the peak at -0,45 V correspond to lead, with poor performance in both cases.

The effect of the amount of the PVP present in the synthesis through the performance of the SPCE modified with the resulting BiNPs by SWV detection of Cd and Pb was previously studied. Different sets of bismuth nanoparticles were also tested in

parallel with the optimization of the synthesis in aim to found the best nanoparticles for heavy metals sensing. Table 3.1 summarizes the sensibilities and limits of detection of the different modified SPCEs. The sensibility towards Cd was higher for the lowest amounts of PVP (0.05 g); in fact, its value was found 35% bigger than when 0.1 g PVP is used. In spite of, in the case of lead detection the effect of the amount of PVP in the synthesis is less critical and significant differences in terms of sensibility and limits of detection can't be seen. The presence of PVP offers good stabilization of BiNPs and contributes to improvements in terms of the control of the stripping curves shapes. However increased concentrations of PVP have a negative effect upon the SWV curves due to the decrease of the conductivity as well as of the catalytic effect during electroplating step (passivation effect).

Type of sensor	Analyte	Sensibility	LOD
Bare SPCE	Pb, Cd	0.0053 and 0.036 mA/ppb	13 and 18 ppb
Bi NPs, with low amount of PVP	Pb, Cd	0.018 and 0.0153 mA/ppb	8 and 12 ppb
Bi NPs	Pb, Cd	0.013 and 0.0444 mA/ppb	15 and 11 ppb
Bi NPs, Hypophosphite as a reducing agent	Pb	0.008 mA/ppb	20 ppb

Table 3.1 Resume of heavy metal detection performance. Measures in seawater spiked samples at pH 4,5 with acetate buffer.

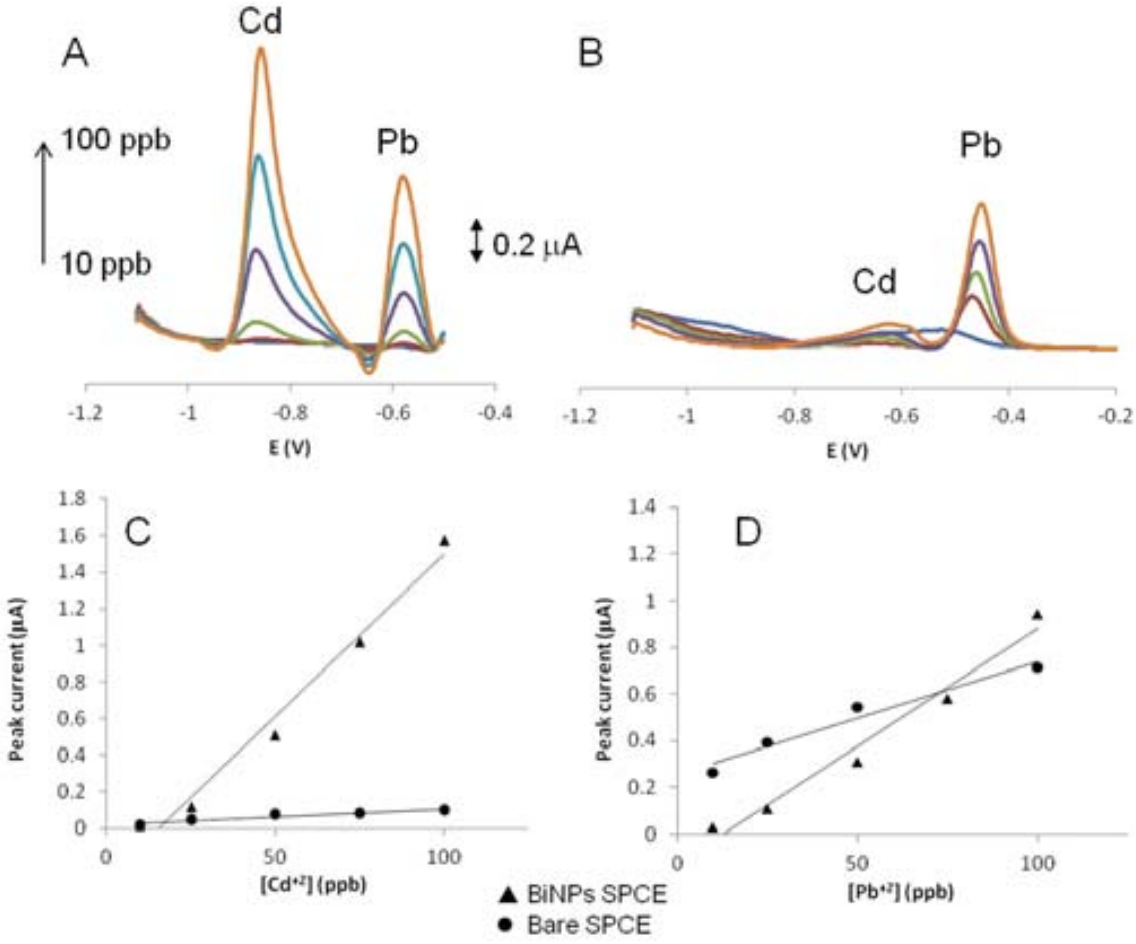

Figure 3.7 Typical SWV stripping response curves for the simultaneous detection of cadmium and lead using Bi NPs modified SPCE (A) and bare-SPCE (B). In the bottom the corresponding calibration curves in the range of 0 to 100ppb for cadmium (C) and lead (D) are shown. Experimental details as described in the text.

3.4 Conclusions

Different reductive methods to synthesize bismuth nanoparticles (BiNP) with interest for applications in electrochemical stripping analysis of heavy metals have been studied. The kind of reductive methods directly affects the morphology of BiNPs in terms of shape and size. In addition, the synthesis was optimized to found the best nanoparticles for heavy metal detection and their integration in an electrochemical sensing platform.

The obtained BiNP using polyol method with the lower concentration of PVP (0.05 g in the synthesis) have shown to be effective enough in improving the efficiency of screen-printed electrodes while being used in square wave anodic stripping voltammetry of heavy metals. The use of these BiNPs has clearly contributed to reach detection limits as low as 5 and 9ppb for lead and cadmium respectively.

The reducing in PVP quantity during BiNP synthesis didn’t bring significant loss of BiNP stability keeping the compromise with the sensor performance improvement. This PVP based reductive method seems to be the most adequate to obtain BiNP with interest for electrochemical stripping analysis of heavy metals. Further applications of these nanoparticles in biosensing field are also previewed and will be object of future communications

3.5 References

(1) Svancara, I.; Prior, C.; Hocevar, S. B.; Wang, J. *Electroanalysis* **2010**, 22, 1405.

(2) Wang, J. *Electroanalysis* **2005**, 17, 1341.

(3) Mayorga-Martinez, C. C.; Cadevall, M.; Guix, M.; Ros, J.; Merkoci, A. *Biosens. Bioelectron*. **2013**, 40, 57.

(4) Arduini, F.; Calvo, J. Q.; Amine, A.; Palleschi, G.; Moscone, D. *Trac-Trends in Analytical Chemistry* **2010**, 29, 1295.

(5) Wang, J.; Lu, J.; Hocevar, S. B.; Farias, P. A. M. *Anal. Chem*. **2000**, 72, 3218.

(6) Kefala, G.; Economou, A.; Voulgaropoulos, A.; Sofoniou, M. *Talanta* **2003**, 61, 603.

(7) Toghill, K. E.; Xiao, L.; Wildgoose, G. G.; Compton, R. G. *Electroanalysis* **2009**, 21, 1113.

(8) Zou, Z.; Jang, A.; MacKnight, E.; Wu, P.-M.; Do, J.; Bishop, P. L.; Ahn, C. H. *Sensors and Actuators B-Chemical* **2008**, 134, 18.

(9) Lezi, N.; Economou, A.; Dimovasilis, P. A.; Trikalitis, P. N.; Prodromidis, M. I. *Analytica Chimica Acta* **2012,** 728, 1.

(10) Aragay, G.; Pons, J.; Merkoçi, A. *Chemical Reviews* **2011**, 111, 3433.

(11) Granado, M. A.; Olivares-Marín, M.; Pinilla, E. *Talanta* **2009**, 80, 631.

(12) Zhao, Y.; Zhang, Z.; Dang, H. *Materials Letters* **2004**, 58, 790.

(13) Wang, W. Z.; Poudel, B.; Ma, Y.; Ren, Z. F. *The Journal of Physical Chemistry B* **2006**, 110, 25702.

(14) Wang, Y.; Chen, J.; Chen, L.; Chen, Y.-B.; Wu, L.-M. *Crystal Growth & Design* **2010**, 10, 1578.

(15) Ma, D.; Zhao, J.; Li, Y.; Su, X.; Hou, S.; Zhao, Y.; Hao, X.; Li, L. *Colloids and Surfaces a-Physicochemical and Engineering Aspects* **2010**, 368, 105.

(16) Ma, D.; Zhao, J.; Chu, R.; Yang, S.; Zhao, Y.; Hao, X.; Li, L.; Zhang, L.; Lu, Y.; Yu, C. *Advanced Powder Technology* **2013**, 24, 79.

(17) Carotenuto, G.; Hison, C. L.; Capezzuto, F.; Palomba, M.; Perlo, P.; Conte, P. *Journal of Nanoparticle Research* **2009**, 11, 1729.

(18) Son, J. S.; Park, K.; Han, M.-K.; Kang, C.; Park, S.-G.; Kim, J.-H.; Kim, W.; Kim, S.-J.; Hyeon, T. *Angewandte Chemie-International Edition* **2011**, 50, 1363.

(19) Luz, A.; Feldmann, C. *Journal of Materials Chemistry* **2009**, 19, 8107.

(20) Warren, S. C.; Jackson, A. C.; Cater-Cyker, Z. D.; DiSalvo, F. J.; Wiesner, U. *Journal of the American Chemical Society* **2007**, 129, 10072.

(21) Wang, Y. W.; Kim, K. S. *Nanotechnology* **2008**, 19.

(22) Lee, Y.; Choi, J.-R.; Lee, K. J.; Stott, N. E.; Kim, D. *Nanotechnology* **2008**, 19.

(23) Aragay, G.; Puig-Font, A.; Cadevall, M.; Merkoci, A. *J. Phys. Chem. C* **2010**, 114, 9049.

(24) Aragay, G.; Pons, J.; Merkoci, A. *Journal of Materials Chemistry* **2011**, 21, 4326.

CHAPTER 4: MAGNETIC CORE-SHELL NANOPARTICLES FOR DIGITAL-LIKE HEAVY METAL SENSING

Herein a novel magnetic core-bismuth shell nanoparticles-based platform for heavy metal detection is presented. These particles are proposed as electrode modifiers due to their magnetic core (constituted by magnetite) which can facilitate their immobilization onto the electrode by placing a permanent magnet behind it, and the bismuth oxide containing shell. This bismuth-based shell that enhances the heavy metals capture and detection offers a digital-like sensing device achieving a very good limit of detection with a good analytical performance. This digital-like behaviour can be accomplished by a simple displacement of the nanoparticles from the electrode, making it a reusable and easy to be cleaned platform.

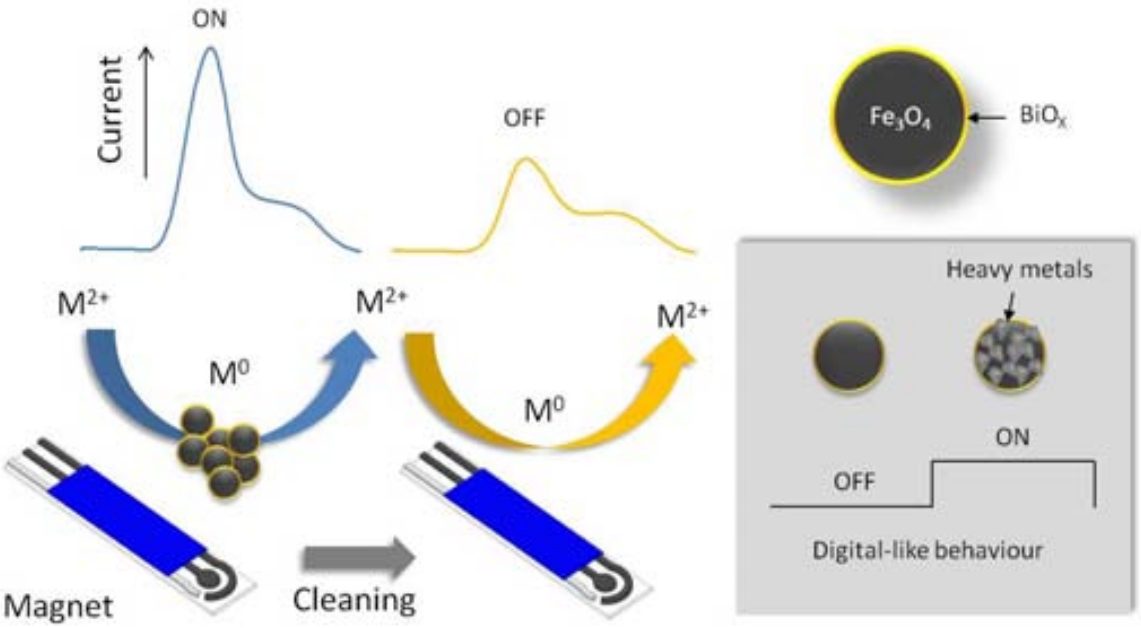

Graphical abstract Schematic representation of digital-like behaviour of magnetically modified heavy metal sensors.

4.1 Introduction

Historically, stripping voltammetry for heavy metal detection has been performed at mercury-based electrodes, due to its unique electrochemical properties[1,2]. Nevertheless, the toxicity of mercury has strongly limited its use for real time or laboratory analysis due to the current strict environmental regulations leading to the investigation of alternative materials. Bismuth can compete with mercury in terms of potential window, sensitivity, resolution of the voltammetric responses, dynamic range and limit of detection[3,4].

The selective modification of electrodes is not a trivial issue. Different types of bismuth-based sensors have been reported, but the most used configurations are based on the co-deposition (*in situ*) of bismuth during electrochemical analysis and the use of bismuth modified (*ex situ*) electrodes[5]. Different sources of bismuth such as bismuth (III) saline solution[6], bismuth nanoparticles[7,8] or bismuth oxide particles[9,10] are reported for both approaches. The application using bismuth oxide is particularly interesting in modifying of electrode substrate with bismuth; it is well documented to improve the electroanalytical performance and can act akin to a mercury modified electrode yet having negligible toxicity.

The modification of electrode surface involves careful preparation of the samples and different methodologies have been used to achieve it. The use of films[11], polymers[12], screen printing ink[13] or dropping a nanoparticles solution[8] are some examples. Bismuth oxide is incorporated into the bulk of the screen printed electrode in a way that when the potential is held sufficiently negative, bismuth oxide at the electrode surface is electrochemically reduced forming bismuth metal.

Looking for novel flexible and efficient heavy metal detection alternative we propose a new way to selectively modify electrodes with interest in heavy metal detection by using magnetic core-shell nanoparticles. This novel platform takes advantages of the magnetic core and the unique electrochemical properties of bismuth in the nanoparticles shell. This represents a simple and efficient way to modify electrodes with interest for portable microfluidics in order to detect heavy metals with high sensitivity, selectivity and in a short time.

4.2 experimental section

4.2.1 Chemicals

For the synthesis of nanoparticles iron (II) sulfate heptahydrate and bismuth (III) nitrate pentahydrate were used. Potassium nitrate, with reagent grade of 98% was purchased from Sigma Aldrich. Sodium hydroxide, ACS-ISO-for analysis, ethanol and sulfuric acid were obtained from Panreac. The water used for preparation of all solutions was from Milli-Q system (>18.2 $M\Omega cm^{-1}$, Millipore).

Heavy metals stock solutions were prepared by diluting lead (II) and cadmium (II) standard solutions AA grade (1000 ± 2 mgL^{-1}, Panreac, Spain). Acetate buffer was made using sodium acetate and acetic acid (both were purchased in Sigma-Aldrich, Spain); this buffer contains sodium chloride (Panreac). The pH was adjusted at 4.5 and determined using the pH-meter (BASIC 20+, from Crison). All glass material used has been cleaned using diluted nitric acid (65% PA, Panreac).

For the preparation of chip devices, SU-8 (Microchem) was used as a photoresist and XP SU8 Developer (Microchem) as a developing solvent. Polydimethylsiloxane (PDMS, from SYLGARD 184) and polycarbonate substrate (Corning, USA) were used for the chip fabrication.

4.2.2 Preparation of Screen Printed Carbon Electrodes (SPCE)

The SPCEs consist of a single polycarbonate substrate with three electrodes: working, reference and counter electrode. Two different inks were used: graphite ink for the working and counter electrode (Electrodag 423SS ink) and silver/silver chloride for

the reference electrode layer (Electrodag 6037SS ink). All the inks were purchased from Acheson Industries. After the deposition of each layer, a drying process is followed by keeping the polyester substrate at 60°C for 15 min after each layer.

4.2.3 Fabrication of chips

The chips consisted of a lineal channel as a cell chamber detection. Microchips were fabricated by rapid prototyping and PDMS technologies as described in the literature[14]. Briefly, a 4 inch silicon wafer was spin coated for 50s at 2000 rpm with a negative photoresist (SU8-50) and patterned by photolithography by an exposure of UV light for 50s by using a plastic mask and revealed conveniently. All the procedure was carried out in a cleaning room environment. Then PDMS was poured onto the resulting SU8 master and cured at 65°C for 4hr. The channels were 500 mm wide by 50 mm depth and 5 cm long (Figure 4.1 B).

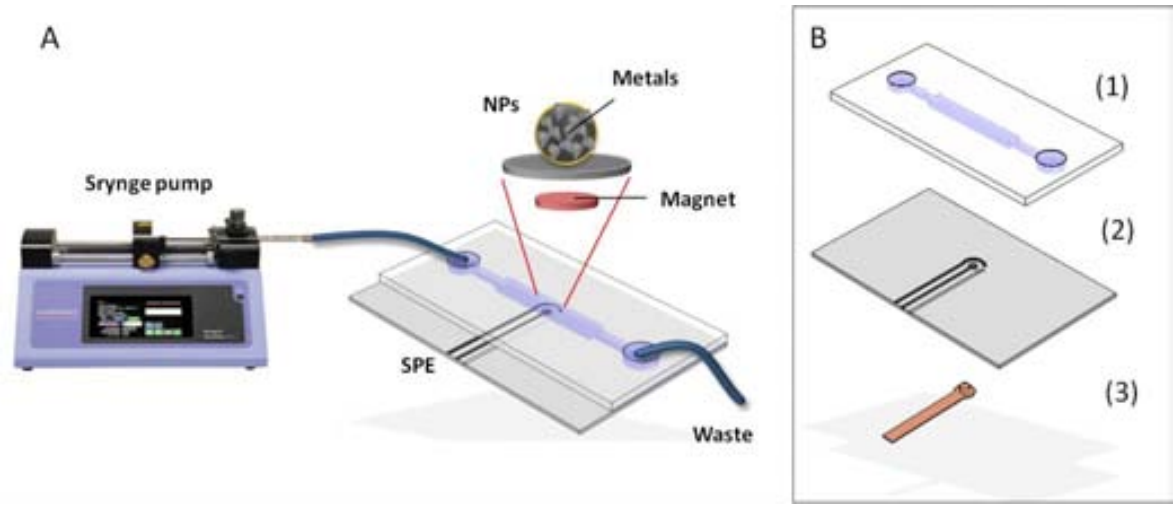

Figure 4.1 A scheme of microfluidic sensing system and the different parts of the cell (B): 1) PDMS master, 2) polycarbonate substrate with the printed SPCE and c) the magnet.

The flow-through system consists of a syringe pump used for introducing the solutions to a microfluidic channel, as is shown in the figure 4.1 A. This microfluidic chip has been prepared by soft lithography techniques.

Finally, the PDMS channel and the PC substrate were assembled using a previously reported protocol[15-16]. The polycarbonate substrate was treated by air-plasma for 1 min and then immersed into a 2% (v/v) 3-aminopropyltriethoxylane (APTES) (Sigma Aldrich) solution in water for 1 h in order to functionalize the surface with amino groups. The surface of the PDMS channel was also activated for 1min by plasma, and put into contact with the PC sheet to achieve irreversible bonding. Finally, a homemade connector was used to connect it to the potentiostat.

4.2.4 Electrochemical analysis

For the electrochemical measurements was used a computer-controlled Autolab PGSTAT-12 (302 N-High performance) (potentiostat/galvanostat) with general-purposes electrochemical software operating system (GPES version 4.9.007, from Eco Chemie B.V., Utrecht, The Netherlands). The integrated three electrodes strips were connected to the Autolab PGSTAT-12 with a specially adapted electrical edge connector. The SPCE sensors consisted of a screen-printed electrochemical cell with three electrodes in one single slide: a graphite working electrode, a graphite counter electrode and a silver pseudo-reference electrode.

All electrochemical experiments were carried out at room temperature and no oxygen removal was performed. Heavy metal concentrations were determined by square wave voltammetry (SWV). The voltammetric parameters for the experiments were as

follows: conditioning potential -0.5 V for 60s, deposition potential -1.1 V for 120s, equilibration time 30s, SW amplitude 28 mV, step potential 3 mV, and frequency 15 Hz. Flow-through conditions were used during the conditioning and the accumulation step, whereas the equilibration step and the square wave scan were performed in a quiescent solution. Before using a new SPCE, the working electrode was then activated by cyclic voltammetry (10 cycles at a potential range from -0.8 V to 0.8 V and a scan rate of 100 mV s^{-1} in PBS buffer). Then, repeated blank measurements in seawater were carried out (usually ten times) up to obtaining of a stable background current. A new sensor was used for each experiment, except the studies of modification and cleaning of the electrodes. The range of concentration selected is 10 to 100ppb of each metal in 0.1M acetate buffer (pH=4.5) and 0.1M NaCl as electrolyte support[2,17].

To evaluate the working range of the sensors, calibration curves that correspond to ASW peak current versus the Cd and Pb concentration have been obtained. The modification of home-made SPCEs (HM-SPCE) in chip has been optimized by flowing a suspension of 0.1 mg NPs/mL performed at 50 µL of flow with the magnet under the working electrode. Then -1.1 V was applied for 3min to generate the bismuth electrode.

4.2.5 Characterization

Transmission electron microscope (TEM) images were taken with a JEM-2011 (Jeol, Ltd., Japan). X-ray powder diffraction patterns were collected on a X¨Pert MPDP analytical diffractometers (Panalytical) using Cu Kα radiation. Patterns were recorded over the 2θ range 20–95^{o} at 40kV and 40 mA.

4.2.6 Synthesis of nanoparticles

Magnetite@bismuth oxide core@shell nanoparticles were synthesized by previously published procedure with modifications[18]. All reactions were performed with magnetic stirring at >1000 rpm in a 500 mL tree-necked flask under nitrogen flow. During the reactions, the temperature was held constant by a temperature-controlled reactor and a silicon bath. The synthesis consists of iron (II) sulphate and bismuth (III) nitrate co-precipitation in a basic and oxidant medium[18]. In a typical experiment, a solution of 5.7 mmol of iron sulphate and 0.3 mmol of bismuth nitrate were dissolved in 20 mL of water containing 0.02 M of H_2SO_4 in a 250 mL three naked flask. After 1 hour with nitrogen bubbling, 180mL (water–ethanol 80:100) of NaOH and KNO_3 (0.07 M and 0.1 M, respectively) were added slowly at room temperature. When the precipitation was completed, the system was heated to 90^{o}C and kept for 24 h under stirring conditions. Then the suspension was cooled at room temperature, and the solid was separated by magnetic decantation with a magnet and washed several times with distilled water. The final water dispersion obtained is stable in water and alcohols.

4.3 Results and discussion

4.3.1 Synthesis and characterization of core-shell nanoparticles

Nanoparticles were synthesized following a described method by M. Andrés-Vergés, *et.al*[18], where bismuth was used to control the particle size and the colloidal properties. Nanoparticles prepared by this method contain a magnetic magnetite core and a bismuth oxide shell. Using aqueous bismuth nitrate with a Bi(III)/Fe(II) ratio of 5%,

nanoparticles of 14±3 nm diameter were obtained. Figure 4.2 shows TEM images of the typical nanocrystals, showing octahedral shape nanoparticles with homogenous size, as is shown in the histogram. The XRD pattern of solid nanoparticles confirms the magnetite core, but surface bismuth oxide diffraction peaks are not observed due to their thickness, just like was described in the former publication[18], however the effect of superficial bismuth was clearly demonstrated in further electrochemical studies.

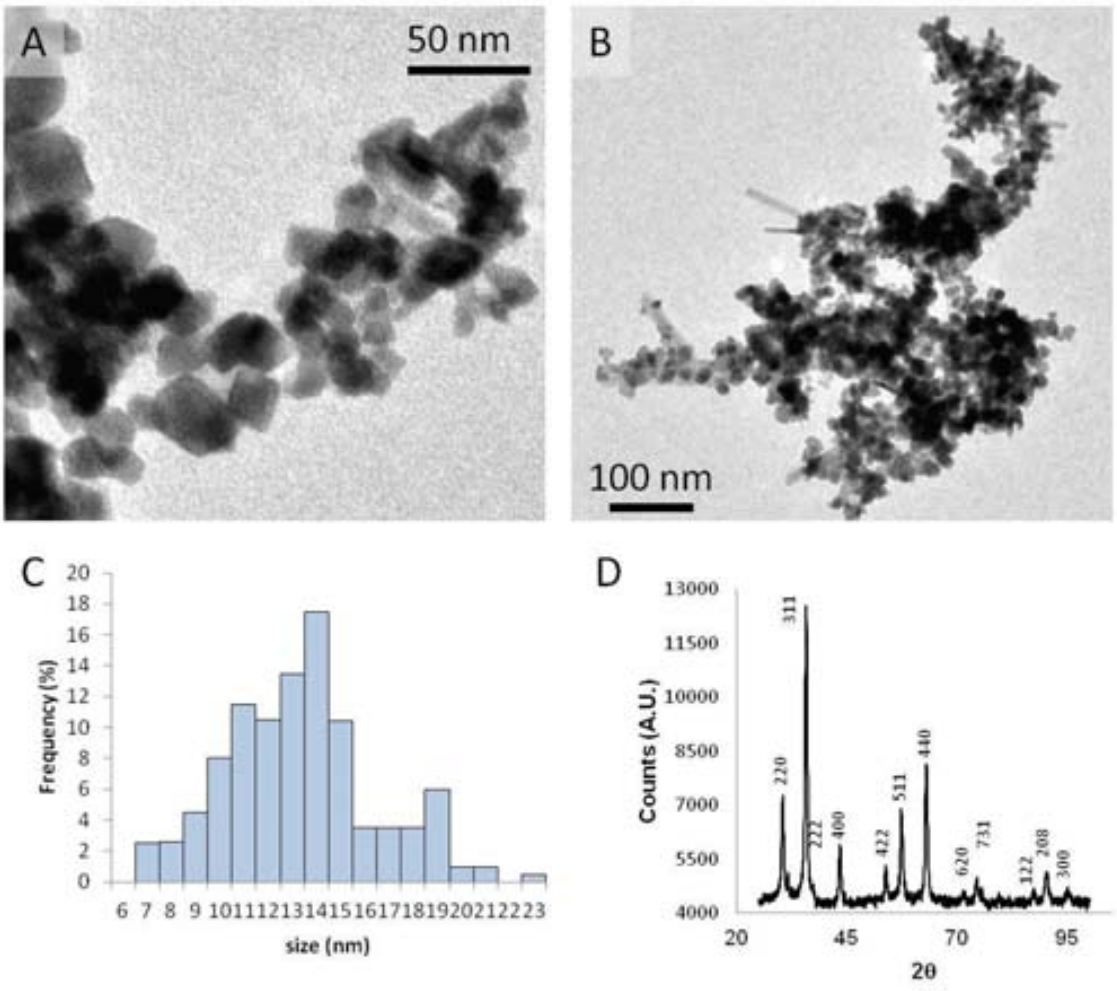

Figure 4.2 TEM images of the obtained magnetic nanoparticles (A and B), the size distribution (C) and the XRD patter (D).

4.3.2 Heavy metal detection

To confirm the usability of these nanoparticles, lead detection using electrochemical stripping was tested. Initially, a drop of 100 mL of metal solution was poured onto the electrode strip (covering all electrodes). Then, magnetic nanoparticles of different concentrations were tested and 100 ppb of lead have been detected. The amount of nanoparticles used for this test was from 0.01 µg to 0.5 µg mL^{-1}. Nanoparticle amount higher than 0.25 µg didn't bring any improvement (saturation of the signal; results not shown) while those lower than 0.01 µg didn't show any change of the signal. In resume, the best amount of magnetic particles was found to be 0.05 µg mL^{-1}. Using this concentration, different concentrations of lead solutions have been measured and a calibration curve has been obtained for modified and unmodified electrodes.

Figure 4.3 shows the calibration curves and the voltammograms of lead detection. In this case, the modification doesn't show improvements in the intensity of the peaks. However, better electrochemical behaviour of modified electrodes can be seen in terms of baseline and signal / noise ratio; the baseline is more flat and the peaks can be easily observed. Therefore, these nanoparticles can be used in a flow system being more efficient in heavy metals detection.

Using this optimization, a simple sensing system that operates in flow conditions was designed. Microfluidic system given its interesting applications in biosensing including biomarkers[16], phenols[19], pesticides[20] detection was chosen.

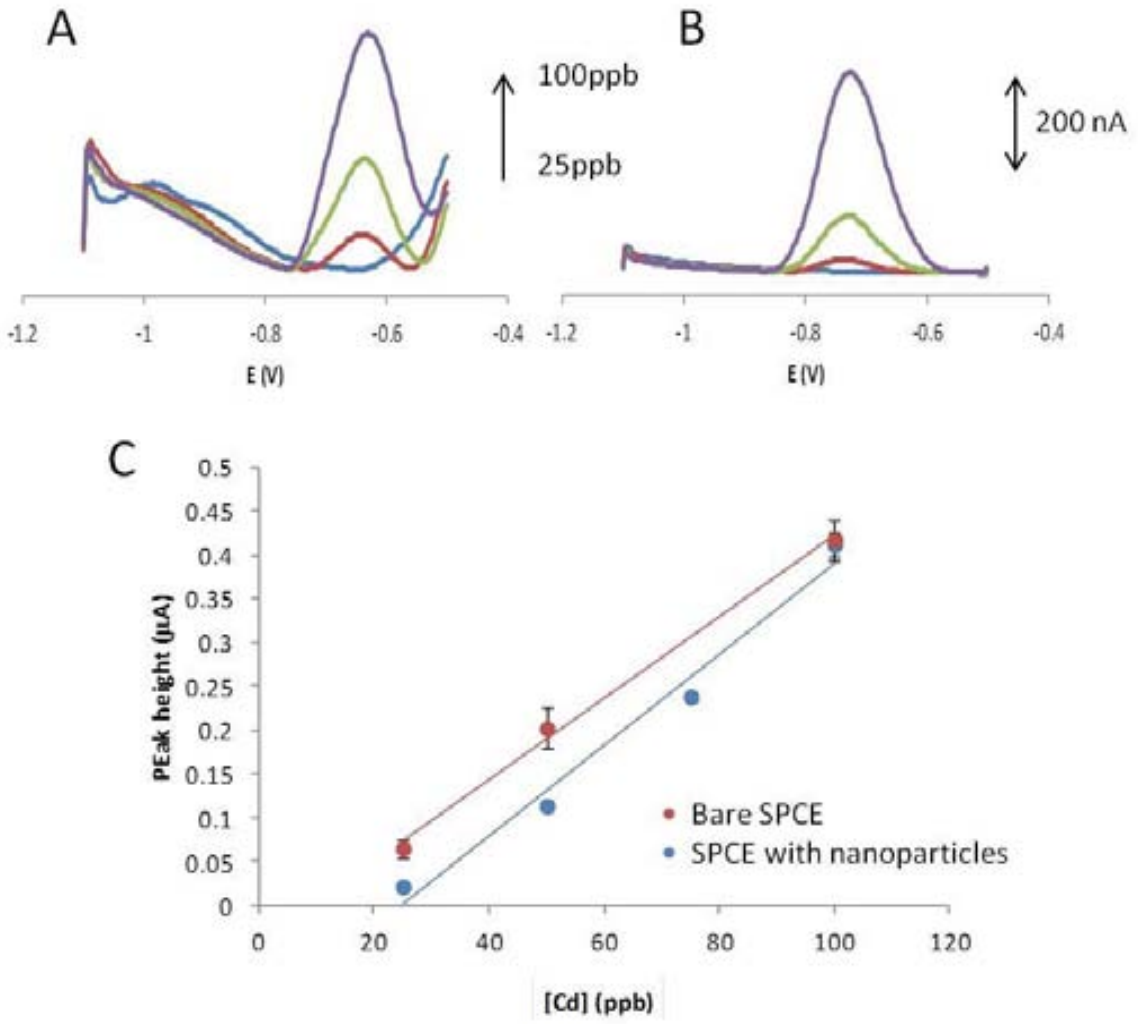

Figure 4.3 SW-ASV voltammograms of lead detection using bare electrode (A) and modified electrode (B) in drop detection mode. Comparison of both calibration curves (C).

The heavy metal detector was fabricated using magnetic nanoparticles as modifier of the electrodes. A solution of magnetic particles was flown and the magnetic nanoparticles were captured onto the electrode surface by placing a permanent magnet behind it. This immobilization can be seen visually due to the brown colour of the nanoparticles solution appeared on top of the working electrode area. As in the case of batch measurements (in drop detection), successive heavy metal standard solutions were

measured and a calibration curve for modified and unmodified electrodes were plotted. It is clearly observed (see figure 4.4) that the use of nanoparticles clearly increases the sensibility (limit of detection reaming the same). The increase in the sensitivity is due to the presence of bismuth which in turn attracts heavy metals due to alloy formation. Such heavy metal accumulation enhances the electrochemical stripping signal during heavy metal detection.

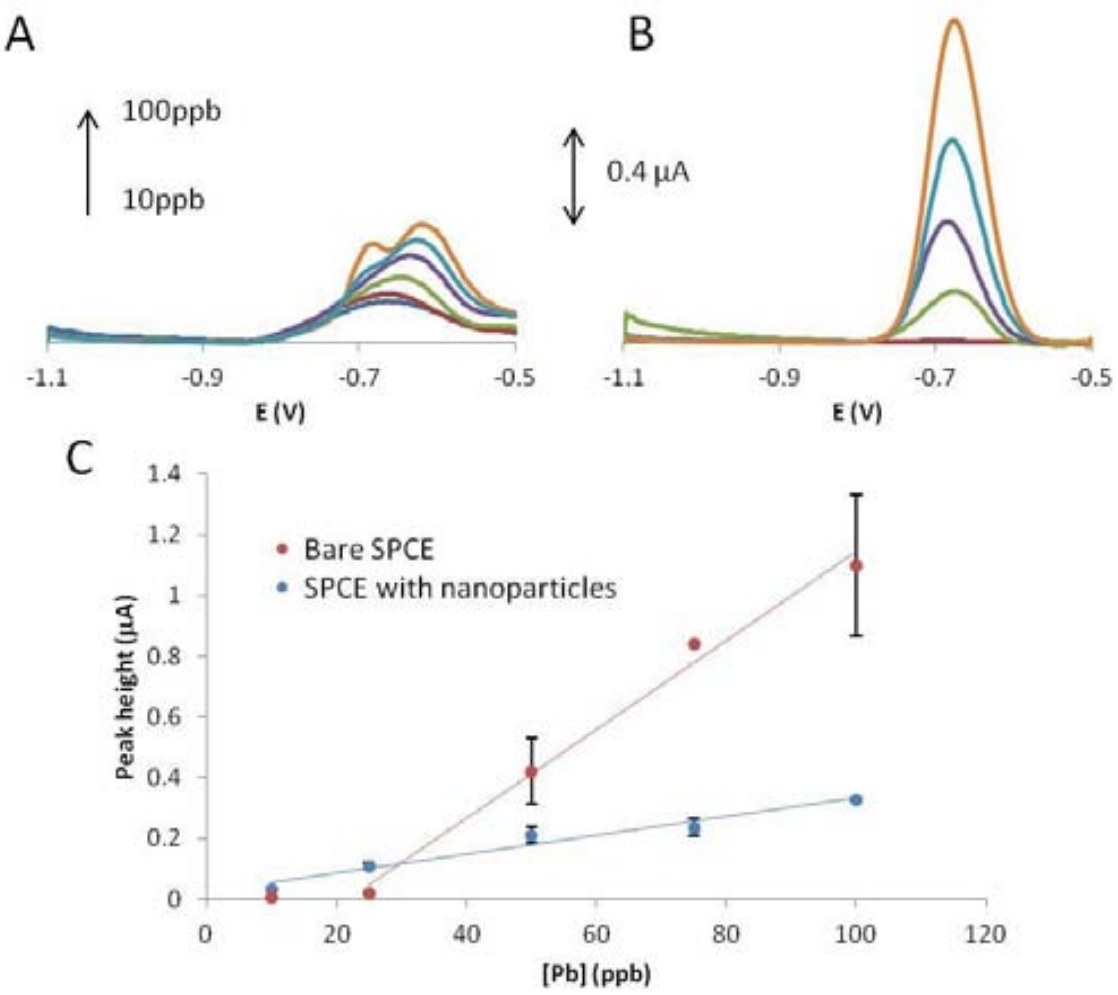

Figure 4.4 SW-ASV voltammograms of lead detection using bare electrode (A) and modified electrode (B) in microfuidic cell. Comparison of both calibration curves (C).

4.4.3 Selective electrode modification and reusability studies

The main objective was developed a new method to modify selectively the electrodes surface. The nanoparticles were easily removed from the electrode just taking out the magnet and flowing new buffer solution; the removing can be increased using a magnet on the upper part. For better cleaning of the electrode (removing all the bismuth) large amount of acidic solutions were needed.

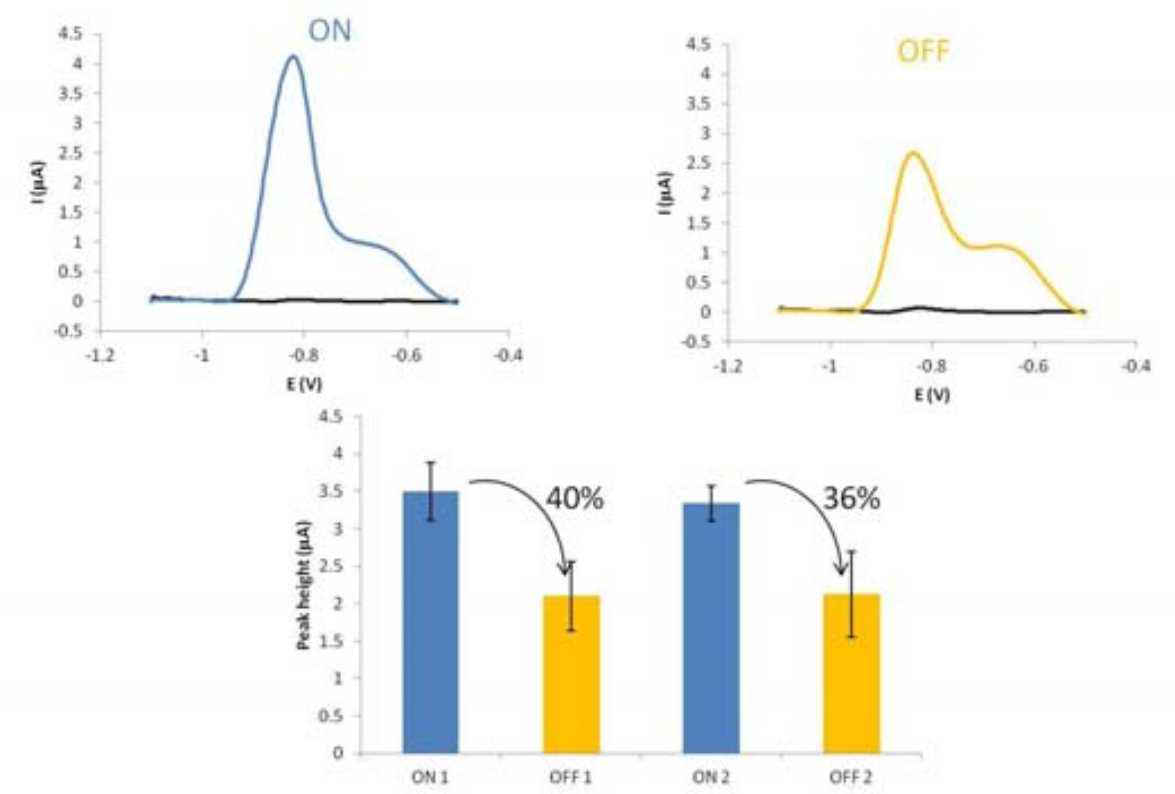

Figure 4.5 Example of 100 ppb of Cd SW-ASV measurement using modified (ON) and unmodified (OFF) electrodes and the intensity of the peaks for different ON/OFF cycles.

The main objective was to develop a new method to selectively modify the electrodes surface. The nanoparticles were easily removed from the electrode by a simple removing of the magnet and flowing of a new buffer solution. For a better

cleaning of the electrode (removing of all the bismuth) large amount of acidic solutions (i.e. acetate buffer) were needed. Figure 4.5 shows the typical response of 100 ppb of cadmium by using the modified and unmodified electrodes. The change of the peak intensity when the nanoparticles are removed is shown (an approximate 40% reduction of the peak intensity). Before cleaning of the electrode, the nanoparticles were poured onto the electrode again and the signal was restored during two cycles (damage of the electrode couldn't allow for more cycles).

4.5 Conclusions

Magnetic core-shell nanoparticles of 15 nm diameter that contain bismuth have been used as on-off inducing electrochemical stripping signal for heavy metals detection. The electrochemical stripping performance was studied and an enhancement in the sensibility of heavy metal sensing in a simple microfluidic cell were observed.

The sensibility of this system to the lead detection increases in 78% due to the bismuth based modification. The study of reusability of this easy electrode modification has been satisfactorily tested. In summary, the selective modification was clearly demonstrated in terms of heavy metal sensing. In addition, these nanoparticles seem to be useful for further digital-like sensing and biosensing applications due to the versatility of bismuth oxide and their properties.

4.6 Bibliography

(1) Güell, R.; Aragay, G.; Fontàs, C.; Anticó, E.; Merkoçi, A. *Anal. Chim. Acta* **2008**, *627*, 219–224.

(2) G. Aragay; A. Puig-Font; M. Cadevall; Merkoçi, A. *J. Phys. Chem. C* **2010**, *114*, 9049–9055.

(3) Wang, J. *Electroanalysis* **2005**, *17*, 1341–1346.

(4) Švancara, I.; Prior, C.; Hočevar, S. B.; Wang, J. *Electroanalysis* **2010**, *22*, 1405–1420.

(5) Arduini, F.; Calvo, J. Q.; Palleschi, G.; Moscone, D.; Amine, A. *TrAC Trends Anal. Chem.* **2010**, *29*, 1295–1304.

(6) Kefala, G.; Economou, a; Voulgaropoulos, a; Sofoniou, M. *Talanta* **2003**, *61*, 603–610.

(7) Saturno, J.; Valera, D.; Carrero, H.; Fernández, L. *Sensors Actuators B Chem.* **2011**, *159*, 92–96.

(8) Rico, M. A. G.; Olivares-Marín, M.; Gil, E. P. *Talanta* **2009**, *80*, 631–635.

(9) Sahoo, P. K.; Panigrahy, B.; Sahoo, S.; Satpati, A. K.; Li, D.; Bahadur, D. *Biosens. Bioelectron.* **2013**, *43*, 293–296.

(10) Lezi, N.; Economou, A.; Dimovasilis, P. a; Trikalitis, P. N.; Prodromidis, M. I. *Anal. Chim. Acta* **2012**, *728*, 1–8.

(11) Rehacek, V.; Hotovy, I.; Vojs, M.; Mika, F. *Microsyst. Technol.* **2007**, *14*, 491–498.

(12) Li, J.; Guo, S.; Zhai, Y.; Wang, E. *Anal. Chim. Acta* **2009**, *649*, 196–201.

(13) Kadara, R. O.; Tothill, I. E. *Anal. Chim. Acta* **2008**, *623*, 76–81.

(14) Xia, Y.; Whitesides, G. M. *Annu. Rev. Mater. Sci.* **1998**, 153–184.

(15) Tang, L.; Lee, N. Y. *Lab Chip* **2010**, *10*, 1274–1280.

(16) Medina-Sánchez, M.; Miserere, S.; Morales-Narváez, E.; Merkoçi, A. *Biosens. Bioelectron.* **2014**, *54*, 279–284.

(17) Mirceski, V.; Hocevar, S. B.; Ogorevc, B.; Gulaboski, R.; Drangov, I. *Anal. Chem.* **2012**, *84*, 4429–4436.

(18) Andrés-Vergés, M.; del Puerto Morales, M.; Veintemillas-Verdaguer, S.; Palomares, F. J.; Serna, C. J. *Chem. Mater.* **2012**, *24*, 319–324.

(19) Mayorga-Martinez, C. C.; Hlavata, L.; Miserere, S.; López-Marzo, A.; Labuda, J.; Pons, J.; Merkoçi, A. *Biosens. Bioelectron.* **2014**, *55*, 355–359.

(20) Llopis, X.; Pumera, M.; Alegret, S.; Merkoçi, A. *Lab Chip* **2009**, *9*, 213–218.

CHAPTER 5: ECO-FRIENDLY ELECTROCHEMICAL LAB-ON-PAPER FOR HEAVY METAL DETECTION

A disposable electrochemical lateral flow paper-based sensing device for heavy metal detection is proposed. The detection of metals such as lead and cadmium in aqueous samples in a range from 10 to 100 ppb with very good analytical performance (LOD is 7 and 11 ppb for lead and cadmium respectively) is demonstrated. Moreover the platform was used as a sample pretreatment thanks to the paper filtering properties. Real samples, especially in which the matrix usually is turbid and would in principle need a previous filtration, are successfully analyzed. This lab-on-paper device is simple, low-cost, easy-to-fabricate and portable, being a promising tool for new point-of-care applications in environmental monitoring, public health and food safety.

5.1 Introduction

It is very well known, that a heavy metal contamination causes critical problems for the ecological systems, most of times due to human activity[1,2]. For this reason, safe limits or maximum contaminant levels have been defined for drinking water by different organizations (World Health Organization, WHO, and Environmental Protection Agency, EPA) from all over the world[3]. For this reason, there is an ongoing trend to develop sensing strategies for the early detection of pollution by heavy metals, even at trace levels, in various chemical systems, including living systems and environment.

Simple devices with interest on the heavy metals detection in environmental samples are mainly based on colorimetric assays. Different strategies to increase the sensibility are being developed, as for example the use of nanomaterials as transducer modifiers or as labels. Most of lateral flow assays use gold nanoparticles[4] or chromogenic reagents[5] as colorimetric markers. However, the cost of reagents and materials for these assays, including related detectors (if not a naked eye platform) may be a drawback which has make electrochemical methods to be integrated in such sensing platforms[6,7].

Among the disposable platforms, paper-based sensors can be an interesting alternative for low-cost and eco-friendly analytical platforms. Paper is an inexpensive and abundant material, flexible, light and easy to use. In addition, due to its porosity, it has the capability to transport fluids via capillarity forces. The platforms based on paper can acquire different functionalities through the creation of different patterns or structures onto them. For example fluidics in the paper can be achieved by printing of hydrophobic

channels[8]. Integration of transducers or conductive contacts in the paper platform can also be performed by using conventional printing technologies such as inkjet[9], wax printing[10] or screen printing[11], making them amenable to in-situ, low-cost and friendly fabrication[12].

The integration of screen-printed carbon electrodes (SPCEs) in a point-of-care platform, such as lateral flow sensor, is easier, resulting a device easy to fabricate and to be used[13]. On the other hand, by using electrodes fabricated by screen printing technology, the resulting device is cheaper in comparison to other kind of electrodes, such as those based on sputtering or other micro and nanofabrication technologies[14,15]. SPCEs are usually printed onto polymeric materials, such as polyester[16], due to overall the mechanical properties of this platform, beside their low cost.

The detection of heavy metals, among other pollutants has been previously addressed by our group through different nano and micromaterials-based strategies[17] such lateral flow[18] and electrochemical based platforms[19,20]. Electrochemical methods are interesting due to the possibility of miniaturization in order to produce portable devices with great sensitivity and selectivity.

Based on the advantages of paper-based platforms and electrochemical detection and their simple integration using screen-printed technology for heavy metal detection in complex and turbid samples[13] we propose now a simple and easy alternative that represents an eco-friendly electrochemical lab-on-paper for heavy metals detection. It is a disposable platform with filtering and heavy metal electrochemical stripping/based

detection capability that takes advantages of the membranes themselves, the wax printing and screen-printing technologies.

5.2 experimental part

5.2.1 Materials and Reagents

For the preparation of lab-on-paper, filter paper (Whatman filter paper No. 1, from VWR, USA) was used as platform. The screen-printed carbon electrodes (SPCE), consisting of three electrodes: working, reference and counter electrode were produced by screen printing technology using a screen-printing machine (DEK 248, DEK International, Switzerland). Two different inks were used: graphite ink for the working and counter electrode (Electrodag 423SS ink) and silver/silver chloride for the reference electrode layer (Electrodag 6037SS ink). All the inks were purchased from Acheson Industries. After the deposition of each layer, a drying process is followed by keeping the paper substrate at 60°C for 45min (graphite) and 30min (Ag/AgCl and insulating inks). To print the wax ink onto the paper Xerox colorcube 8570 wax printer (Xerox Corp., USA) was used. Hot plate (VWR, USA) was used to melt the wax and generate the hydrophobic walls.

Heavy metals stock solutions were prepared by diluting lead (II) and cadmium (II) standard solutions AA grade (1000 ± 2 mg/L, Panreac). The water used for preparation of all solutions was from Milli-Q system (>18.2 Mωcm−1, Millipore). For the calibration curves experiments, acetate saline buffer (0.1 M, pH = 4.5) was made using sodium

chloride (Sigma-Aldrich) sodium acetate (Sigma-Aldrich) and acetic acid (Sigma-Aldrich). The pH was adjusted and determined using the pH-meter (BASIC 20+, from Crison). To prepare the spiked samples, 900 µL of sample (seawater or mud) was mixed with 100 µL of this buffer, which contains the metal solution. All glass material used has been cleaned using diluted nitric acid (65% PA, Panreac).

5.2.2 Preparation of the lab-on-paper device

First of all, the channel geometry was designed with a graphic software (Corel Draw X4), taking into account the dimensions of the channel (3 mm wide and 25 mm length, widened in the end part), in order to align in a reproducible way the electrode position onto the channel, as well as ensure the electrode wettability just in the active detection zone, as well as the required fluid trajectory for the proper metal deposition onto the working electrode. Once the design was performed, it was printed onto the paper with a wax printer machine, and then it was heated in order to melt the wax across the paper to create a hydrophobic barrier that defines the fluid confinement. This melting process was performed at 150^{o}C for 10s by using a hot plate. After the channel preparation, the electrochemical detector was printed onto the channel. It consisted of a set of three electrodes of 500 µm width separated by 500 µm with an approximated thickness of 4 µm, produced by screen printing technology. The fabrication process involved two steps. In the first step the graphite layer (that creates WE and CE) was printed onto the paper sheet. Secondly, a layer of silver/silver chloride ink was printed as a reference electrode.

In order to avoid liquid leakages, a second paper layer closing the bottom part of the paper channel was needed. This layer was also printed with the wax printer machine, but in this case it was not necessary to melt the wax, because the printed surface area (also hydrophobic) was big enough to close the channel. Both paper layers (channel and substrate) were attached by using adhesive glue. Finally, the absorbent pad (CFSP001700, from Millipore (Billerica, USA) cut in pieces of 5 x 10 mm was located at the end of the channel (See Figure 5.1). The function of the absorbent pad is to wick the fluid through the membrane, increasing the amount/volume of the sample and the sensitivity due to a continuous sample renovation in the electrochemical cell during the preconcentration step. The figure 5.1 shows the scheme of layer by layer chip building and the look of the final device.

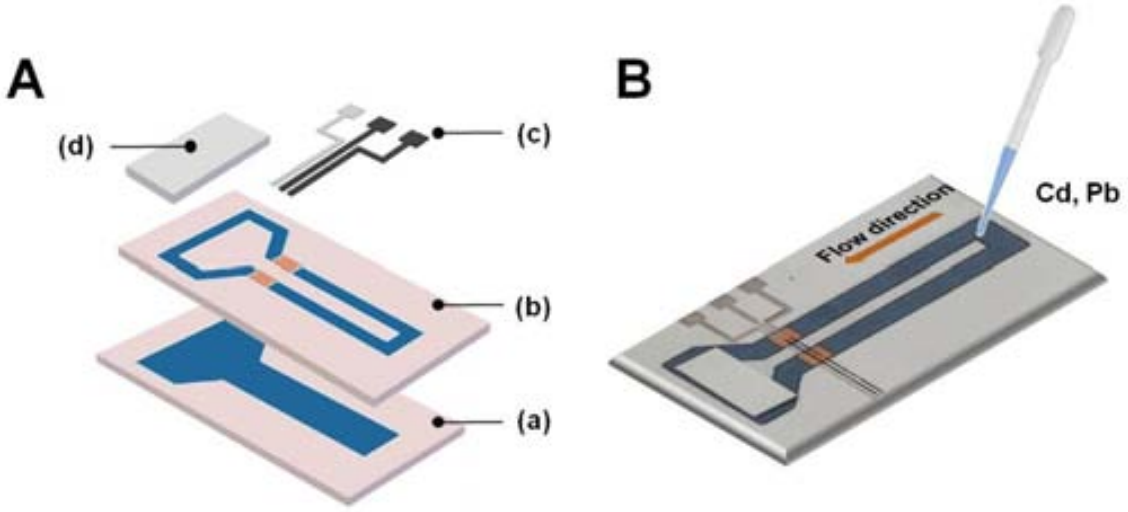

Figure 5.1 Schematic of a lab-on-paper device. (A) Different components of the chip: a) bottom layer, b) channel layer, c) RE (grey color), WE (in center) and CE and d) absorbent pad. (B) Picture of the fabricated device.

5.2.3 Electrochemical analysis

For the electrochemical measurements, a computer-controlled Autolab PGSTAT-12 (302 N-High performance) (potentiostat/galvanostat) with general-purposes electrochemical software operating system (GPES version 4.9.007, from Eco Chemie B.V., Utrecht, The Netherlands) was used. The integrated three electrodes strips were connected to the Autolab PGSTAT-12 with a specially adapted electrical edge connector. All electrochemical experiments were carried out at room temperature and no oxygen removal was performed. Heavy metal concentrations were determined by square wave voltammetry (SWV). The voltammetric parameters for the experiments were as follows: deposition potential -1.1 V for 120s, SW amplitude 28 mV, step potential 3 mV, and frequency 25 Hz. The measurement was manually started when the liquid flow arrived to the electrodes. A new sensor was used for each measurement, due to the impossibility to clean it. After several optimizations 25 µL of sample was dropped in the initial part of the channel which contains acetate buffer and the adequate amount of surfactant.

5.3 Results and discussion

5.3.1 Paper-based platform: previous optimizations

To achieve good sensing performance in general, and particularly repeatability, of the device, a study of the composition of the sample solution and its volume was firstly studied. The use of acidic media for the detection of heavy metal in saline solutions is commonly used so as to obtain sharp intensity peaks. For these experiments, an acetate

saline buffer, pH 4.5, was selected. Nevertheless, the use of a surfactant in the flowing solution / sample is crucial to obtain good results. The presence of surfactant species in the solution causes a decreasing of surface tension and increase the wetting capability; this facilitates the absorption and diffusion of the solution through the channel ensuring a better efficiency and reproducibility during measurement. For this reason the use of Triton X-100 and Tween-20 at different concentrations was evaluated. For these experiments several levels of concentration have been chosen: 0.01, 0.05 and 0.1% of both surfactants; the flow rate was determined by visual inspection with the aim to select the best options, considering the time needed to wet the entire chip. As it is shown in the figure 5.2 A, a highest peak current of around 0.27 µA with a relative standard deviation of 12% was observed when a measuring solution containing 0.01% Triton was used.

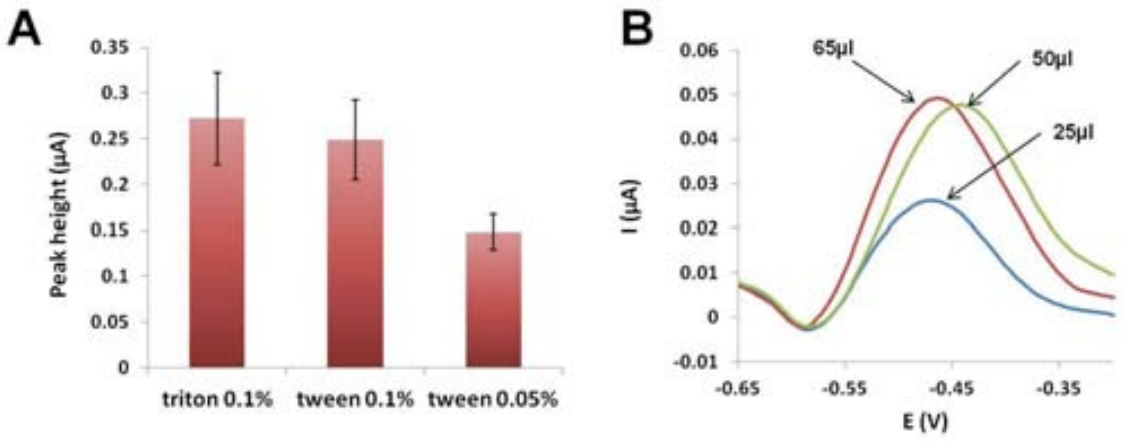

Figure 5.2 (A) Peak intensity measurements of lead (100 ppb) in buffer solution using different surfactants, and (B) measurements of 100 ppb of lead in acetate saline buffer using different sample volumes. All the experimental details as given in the text.

The amount of sample is crucial to ensure repeatability and use this device in real applications. Different sample volumes have been tested: 25, 50 and 65 µL. As it is shown

in figure 5.2 B sample volumes of 65 and 50 µL have similar response, nevertheless 50 µL was chosen for further applications. Higher volumes were not considered due to the channel dimensions and the capability of the pad to absorb the introduced sample volume.

5.3.2 Electrochemical measurements evaluation

All the previous optimizations, such us the chip geometry, injection volume and buffer composition, are discussed in supporting information. Therefore, in order to evaluate the sensing capability of the device, a calibration curve of lead in the range of 5 to 100 ppb was performed. A lineal correlation between the concentration and the measured peak intensity was found using buffered solutions (figure 5.3). The sensibility of this sensor is 2.4 nA/ppb Pb and the limit of detection 7 ppb Pb calculated as a 3 times the blank standard deviation. A buffer acetate (pH 4.5) was used for the detection of heavy metal in saline solutions being this the commonly reported in the literature[21,22].

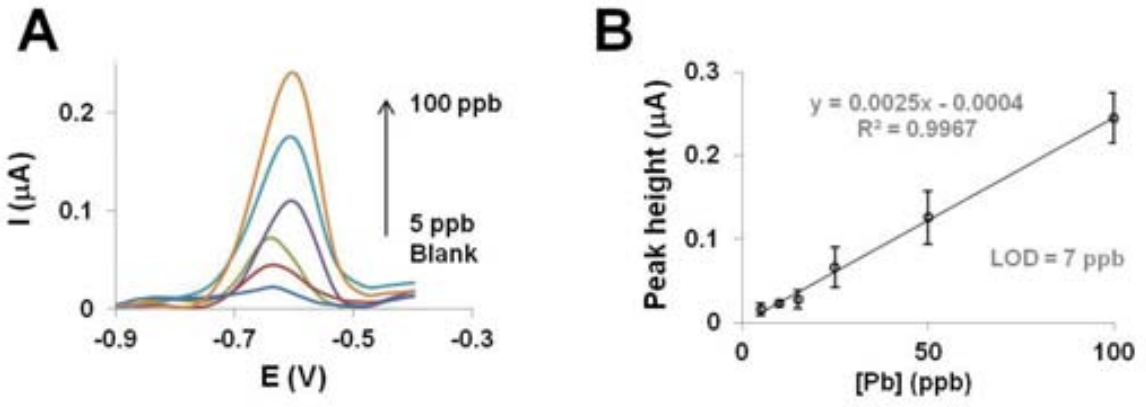

Figure 5.3 Lead detection using paper chips. (A) Typical SWV stripping response curves for lead (from 5 to 100 ppb) and (B) calibration curve; experimental details as given in the text.

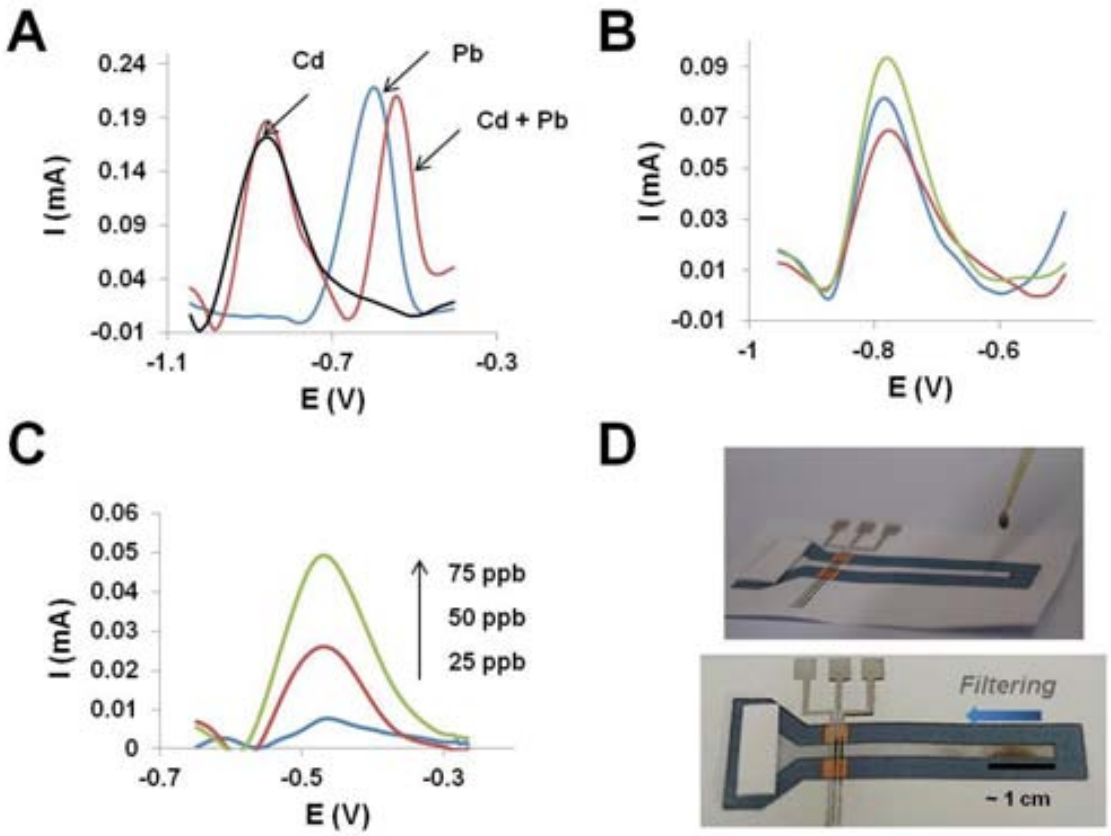

Figure 5.4 Detection of lead and cadmium in both single and multidetection in spiked samples (A), detection of lead in seawater samples (B) and detection of lead in mud samples (C). Photographs during the sampling (inset) and the measuring steps of mud samples (D). All the experimental details are described in the text.

To evaluate the performance of this sensor a multidetection test was also carried out. In this case, lead and cadmium were analyzed in both single and multidetection modes. Figure 5.4 shows a comparison of the peak size in these cases: lead in single detection at 100 ppb and the detection of both metals in the same spiked sample at this concentration. The shift of around 50 mV of lead peak can be attributed to the effect of cadmium during the reduction and the stripping steps. In addition, similar peak intensity height was observed when the peak of 100 ppb of lead in single detection is compared with the same concentration detected by multidetection mode. The same behaviour was

observed for cadmium. Therefore, the possible effects derived from the interference between lead and cadmium can be considered as negligible.

Seawater is a well known and interesting/convenient matrix to detect heavy metals using electrochemical stripping analysis due to their high salinity. On the contrary it gives problems in conventional analysis techniques such as optical methods. Using this simple system it is possible to detect correctly samples with 100 ppb of lead, as it is shown in the figure 5.4 B. Thanks to the filtering capability of the paper platform the device is capable to detect heavy metals in water samples containing solids (this can be with interest for example for sewage sludge in water treatment system or eutrophic water samples, very rich in microalgae) with interest in various environment study & control scenario in industrial and coastal waters.

Regarding the filtering capability of the paper, an analysis of mud spiked sample was made. As it is discussed before, acidic media and surfactant must be used for the heavy metal detection. For this reason a buffer solution, which also contains the surfactant (Triton X-100, at a concentration of 0.1%), was added to the sample solution in low amount. As shown in figure 5.4 C and D the channel is long enough to efficiently filter the sample.

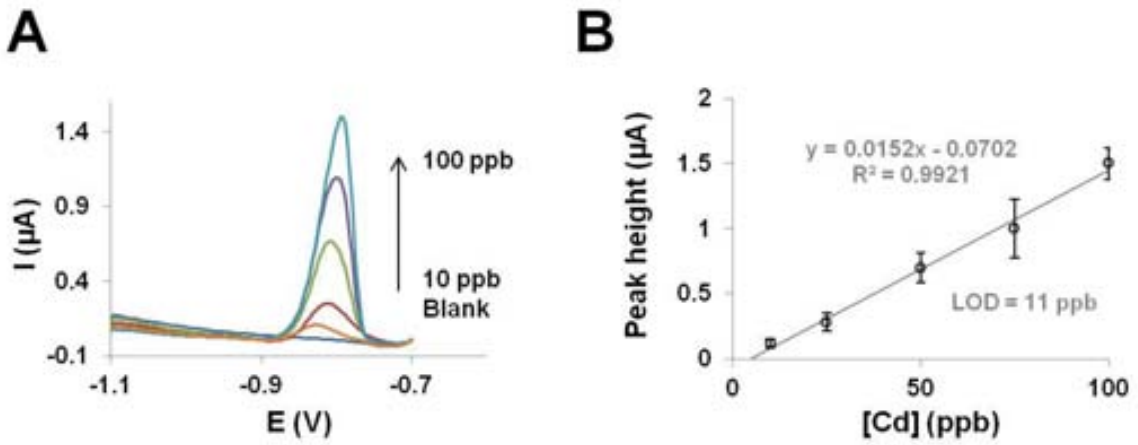

Figure 5.5 Cadmium detection. (A) Typical SWV stripping response curves for cadmium (from 0 to 100ppb), and (B) lineal correlation using lab on a paper devices. Experimental details in the text.

As the multidetecton tests show, cadmium can also be detected using this device. To evaluate the sensibility of this system to the cadmium, measurements of different concentrated samples were performed in buffer conditions, as it is shown in the figure 5.5. From these measurements a calibration curve can be obtained: in this case the sensibility is 15.2 nA/ppb and the calculated limit of detection is 11 ppb.

5.4 Conclusions

A new platform for heavy metal sensing was designed and applied. The developed device is able to filter water samples in presence of solid particles and detect heavy metals in a point of care sensing tool which doesn't need any previous pre-treatment. The sensing of lead and cadmium has been made with satisfactory results; the limits of detection obtained are 7 and 11 ppb respectively, including the multidetection analysis. The detection of pollutants also has been made in complex matrixes such as mud and seawater. In both cases, the detection of lead is possible without needing pre-treated

samples. Such detection efficiency in such complex samples has been achieved thanks to the filter capability of the paper platform. The obtained results are of interest for many other applications in the future such as detection of heavy metals in biological samples (i.e. blood) beside others.

5.5 References

(1) Vallee, B. L.; Ulmer, D. D. *Annu. Rev. Biochem.* **1972**, *41*, 91–128.

(2) Partanen, T.; Heikkila, P.; Hernberg, S.; Kauppinen, T.; Moneta, G.; Ojajarvi, a. *Scand. J. Work. Environ. Health* **1991**, *17*, 231–239.

(3) U.S. Environmental Protection Agency. *Risk Assessment. Management and Communication of Drinking Water Contamination*; 1989; Vol. US EPA 625.

(4) López Marzo, A. M.; Pons, J.; Blake, D. a; Merkoçi, A. *Anal. Chem.* **2013**, *85*, 3532–3538.

(5) Wang, H.; Li, Y.; Wei, J.; Xu, J.; Wang, Y.; Zheng, G. *Anal. Bioanal. Chem.* **2014**, *406*, 2799–2807.

(6) Feng, Q.-M.; Zhang, Q.; Shi, C.-G.; Xu, J.-J.; Bao, N.; Gu, H.-Y. *Talanta* **2013**, *115*, 235–240.

(7) Shi, J.; Tang, F.; Xing, H.; Zheng, H.; Bi, L.; Wang, W. *J. Braz. Chem. Soc.* **2012**, *23*, 1124–1130.

(8) Dossi, N.; Toniolo, R.; Pizzariello, A.; Impellizzieri, F.; Piccin, E.; Bontempelli, G. *Electrophoresis* **2013**, *34*, 2085–2091.

(9) Su, S.; Ali, M. M.; Filipe, C. D. M.; Li, Y.; Pelton, R. *Biomacromolecules* **2008**, *9*, 935–941.

(10) Carrilho, E.; Martinez, A. W.; Whitesides, G. M. *Anal. Chem.* **2009**, *81*, 7091–7095.

(11) Savolainen, A.; Zhang, Y.; Rochefort, D.; Holopainen, U.; Erho, T.; Virtanen, J.; Smolander, M. *Biomacromolecules* **2011**, *12*, 2008–2015.

(12) Martinez, A. W.; Phillips, S. T.; Whitesides, G. M.; Carrilho, E. *Anal. Chem.* **2010**, *82*, 3–10.

(13) Parolo, C.; Medina-Sánchez, M.; Montón, H.; de la Escosura-Muñiz, A.; Merkoçi, A. *Part. Part. Syst. Charact.* **2013**, *30*, 662–666.

(14) Ge, L.; Yan, J.; Song, X.; Yan, M.; Ge, S.; Yu, J. *Biomaterials* **2012**, *33*, 1024–1031.

(15) Wang, P.; Ge, L.; Yan, M.; Song, X.; Ge, S.; Yu, J. *Biosens. Bioelectron.* **2012**, *32*, 238–243.

(16) Aragay, G.; Pons, J.; Merkoçi, A. *J. Mater. Chem.* **2011**, *21*, 4326.

(17) Aragay, G.; Pons, J.; Merkoçi, A. *Chem. Rev.* **2011**, *111*, 3433–3458.

(18) López Marzo, A. M.; Pons, J.; Blake, D. A.; Merkoçi, A. *Biosens. Bioelectron.* **2013**, *47*, 190–198.

(19) Güell, R.; Aragay, G.; Fontàs, C.; Anticó, E.; Merkoçi, A. *Anal. Chim. Acta* **2008**, *627*, 219–224.

(20) Güell, R.; Fontàs, C.; Aragay, G.; Merkoçi, A.; Anticó, E. *Int. J. Environ. Anal. Chem.* **2013**, *93*, 872–883.

(21) G. Aragay; A. Puig-Font; M. Cadevall; Merkoçi, A. *J. Phys. Chem. C* **2010**, *114*, 9049–9055.

(22) Mirceski, V.; Hocevar, S. B.; Ogorevc, B.; Gulaboski, R.; Drangov, I. *Anal. Chem.* **2012**, *84*, 4429–4436.

5.6 Supporting information

The first lateral flow chips designs and optimizations are described in this part of the chapter.

5.6.1 Design optimization

Initially, a single and straight channel were designed, see figure SI1. This design provides some advantages such as, easy fabrication and manipulation, but finally was dismissed. The main drawback is the poor reproducibility and the great dependence between the drop place injection and the electrodes position. Figure SI 1 shows the different response between the injections in the initial (B) or final (A) part of the channel. Despite the altitude of the peak A is much higher than the case of B, in this position the filtering process can't occur. The second option was chosen for all the analysis.

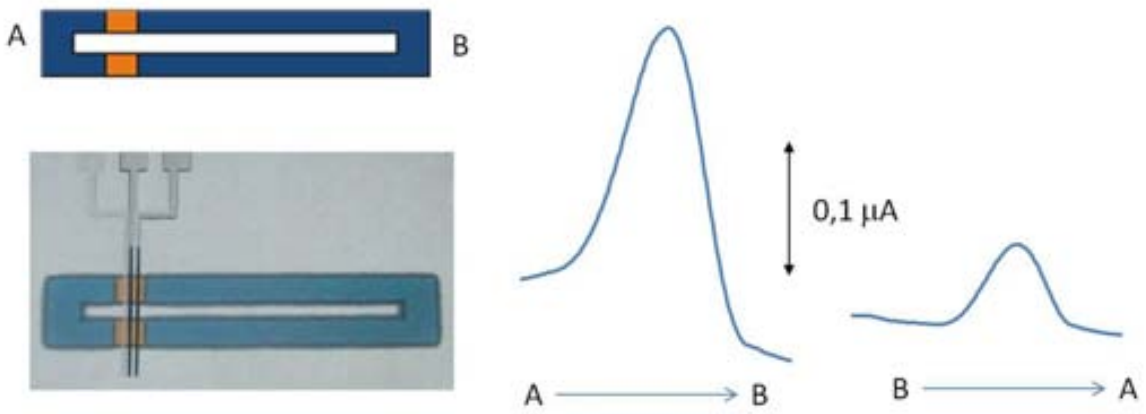

Figure 6.SI1 Design of a first proposal for the *lab-on-paper* device. In the upper part the design and in the bottom, a photograph of the final device. In the left part the different response between the injections in the initial (A) or final (B) part of the channel.

Moreover, this design has a very critical drawback: the maximum volume accepted was 10 µL, leading to a poor limit of detection. Due to this problem, the new design (and used for all the studies) was proposed. In this case the channel was widened in the end part and incorporated an adsorbent path, creating a homogeneous and contiguous flow. This design was selected as a best for our proposal thanks to their simplicity.

CHAPTER 6: BISMUTH NANOPARTICLES FOR PHENOLIC COMPOUNDS BIOSENSING APPLICATION

The rapid determination of trace phenolic compounds is of great importance for evaluating the total toxicity of contaminated water samples. Nowadays, electrochemical tyrosinase (Tyr) based biosensors constitute a promising technology for the *in situ* monitoring of phenolic compounds because of their advantages such as high selectivity, promising response speed, potential for miniaturization, simple instrumentation and easy automatization. The detection of phenolic compounds is based on the combination of bismuth nanoparticles (BiNPs) and Tyr for phenol detections will be hereby reported. This is achieved through the integration of BiNPs/Tyr onto the working electrode of a screen printed electrode (SPE) by using glutaraldehyde as a cross-linking agent. The biosensor shows good performance and good selectivity for phenolic compounds.

6.1 Introduction

The determination of trace phenol compounds released into the ground and surface water is of special importance. Phenolic compounds are widely used in petrochemical products and in wood preservatives, textiles, plastics, dyes, paper, herbicides and pesticides[1,2]. Most of them can be highly toxic and many health problems are related to them, as they could be absorbed through oral, dermal, or respiratory tracts[1,3]. The development of methods to identify and quantify phenolic compounds in various samples to evaluate their total toxicity in environmental and human health problems is of great relevance. Therefore, numerous analytical methodologies for detecting phenolic compounds, such as, ultraviolet spectrophotometric analyses, gas chromatography, liquid chromatography, or capillary electrophoresis have been developed. These methods offer good limits of detection (LODs) and wide working concentration ranges. However, they need the use of sophisticated and relatively costly apparatus and they generally require complicated pretreatment procedures. Recently, large efforts have been focused on the development of simple and effective analytical methods for the determination of phenolic compounds[2,4].

Nowadays, electrochemical enzyme-based biosensors constitute promising technology for the *in situ* monitoring of phenolic compounds because of the advantages that they present, such as high selectivity, low production cost, promising response speed, potential for miniaturization, simple instrumentation and easy automation[2,3]. Among the developed electrochemical methods, amperometric biosensors based on

tyrosinase (Tyr) and polyphenol oxidase (PPO) have proved to be sensitive and convenient for the determination of phenolic compounds[1,4,5]. In particular, tyrosinase (Try) enzyme catalyzes the hydroxylation of monophenols to o-diphenols (monophenolase activity) by oxygen, and also catalyzes the oxidation of o-diphenols to o-quinones (catecholase activity). O-quinones can be later electrochemically reduced to catechol without any mediator on the electrode surface. The detection of phenol derivates thus relies on monitoring the catechol product[3,4,6]. The effective immobilization of tyrosinase on the electrode surface is considered a key step in the development of tyrosinase biosensors for phenolic compounds determination[2]. More recently, various supporting materials have been successfully used to immobilize tyrosinase (Tyr) on the electrode. In addition, there are several related works reporting the development of biosensors where tyrosinase is immobilized onto the screen printed electrode (SPE)[5] that can be implemented in portable systems as an alternative detection method for the direct on-site analysis.

Nanomaterials have also been used to fabricate tyrosinase-based biosensor, especially nanoparticles, such as ZnO nanoparticles[7], calcium carbonate nanoparticles[8], gold nanoparticles[5,9], or hydroxyapatite nanoparticles[2]. On the other hand bismuth[10], and bismuth oxide[1] films have recently been reported for the detection of phenolic compounds by using amperometric biosensors. These materials applied to electroanalysis have opened a new range of possibilities for the construction of phenolic electrochemical biosensors based on these nanomaterials.

In addition to its regular size bismuth nanoparticules (BiNP) shows other advantages such as a larger specific surface area and biocompatibility. These properties provide an excellent platform for enzyme and protein immobilizations.

In the current study, we propose the development of an amperometric BiNP/Tyr-based biosensor. This is achieved through BiNP/Tyr integration onto the working electrode of a screen printed electrode (SPE) by using glutaraldehyde as a cross-linking agent. The resulting BiNP/Tyr-based biosensor exhibited high sensitive response toward phenol and catechol detection with very low detection limits (26 nM for catechol and 62 nM for phenol) and showing a linear response up to 100 µM and 71 µM for catechol and phenol, respectively.

6.2 Materials and methods

6.2.1 Apparatus and reagents

Electrochemical measurements were performed with a model CH-Instrument potentiostat 660 A electrochemical workstation from CH Instruments Inc., Austin, TX. Impedance analysis of the prepared SPE modified electrodes was performed by using an Autolab302 potentiostat/galvanostat/frequency-response analyzer PGST30, controlled by GPES/FRA Version 4.9. Magnetic stirrer was used to provide the convective transport during the amperometric measurements. Scanning electron microscope (SEM) analysis were performed by using a EVO (Carl Zeiss NTS GmbH. Germany). Transmission electron microscope (TEM) images were taken with a JEM-2011 (Jeol, Ltd., Japan). X-ray powder diffraction patterns were collected on a Siemens D-5000 diffactometer (German) by using Cu Kα radiation. Patterns were recorded over the 2ϑ range 20–65° at 40 kV and 40 mA. Z-Potential measurements were made with a Malvern ZetaSizer Nano ZS instrument operating at a light source wavelength of 532 nm and a fixed scattering angle of 173° for detection.

Glutaraldehyde (at 25%), tyrosinase from mushroom (≥1000 unit/mg), phenol, potassium dihydrogen phosphate, potasium monohydrogen phosphate dehydrate and potassium chloride were purchased from Sigma Aldrich. For the synthesis of bismuth nanoparticles, bismuth (III) nitrate pentahydrate (reagent grade, 98%) from Aldrich was used. Potassium hydroxide, ACS-ISO-For analysis and isopropanol (synthesis grade) were obtained by Carlo Ebra reagents. Poly (vinyl pirrolidone) (PVP, MW∼30.000) was

acquired from Aldrich. J. T. Baker Chemicals B. V. supplies ethylene glycol. All solutions were prepared with ultra-pure water from a Millipore-MilliQ system.

6.2.2 Synthesis of bismuth nanoparticles

One-step bismuth (III) nitrate reduction method has been used in order to obtain bismuth nanoparticles[11]. In this synthesis, 0.1 g of $Bi(NO_3)_3$, 0.19 g KOH and 0.05 g of Poly(vinyl pirrolidone) (PVP, MW≈30.000) were dissolved in 25 mL of ethylene glycol (EG). The mixture was heated up to 185 °C and kept under nitrogen atmosphere and constant stirring during 2 h. The obtained nanoparticles were cleaned with isopropanol and milli-Q water by centrifugation. The obtained nanoparticles were dried by nitrogen airflow. These nanoparticles can also be partially dispersed in water and ethanol.

6.2.3 Preparation of Screen Printed Electrode and modification with BiNP and Tyr

Screen printing electrodes fabrication is based on the sequential deposition of a graphite ink, Ag/AgCl ink and insulating ink on a polyester substrate. After the deposition of each layer, a drying process is followed by keeping the polyester substrate at 120 °C for 45 min (graphite) and 30 min (Ag/AgCl and insulating). A 5 µL BiNP at 1 mg/ml solution drop was deposited onto the working SPE electrode surface and allowed to dry at room temperature for 20 min. 1 mg of tyrosinase (Tyr) enzyme was dissolved in 50 µL of 0.1 M phosphate buffer at pH 6.5. A 7 µL drop of Tyr solution was deposited onto the working SPE/BiNP electrode surface and allowed to dry at room temperature for 3 h. Finally, 5 µL drop of glutaraldehyde (Glu) solution at 1% was casted onto the SPE/BiNP/Tyr electrode surface and let to dry at 40 °C for 30 min. The prepared SPE/BiNP/Tyr/Glu sensor was kept at 4 °C.

6.2.4 *O*-quinone synthesis

As to determine phenol detection mechanism *o*-quinone was synthesized following the method described by Laird et al.[12]. A solution composed of catechol (0.1 g), acetone (10mL) and silver oxide (0.4 g) was stirred during 10 min. The obtained solution was immediately filtered and dried. To purify this product it was dissolved in water and extracted again by using chloroform. After the extraction, the product is dried under vacuum.

6.2.5 Electrochemical experiments

All electrochemical experiments were carried out at room temperature. In order to study the characteristics of the BiNPs/Tyr modified electrodes, electrochemical impedance spectroscopy (EIS) studies were performed in 1 mM $[Fe(CN)_6]^{3-/4-}$ (1:1) mixture with KCl 0.1 M as redox probe. The AC frequency range studied was from 0.1 Hz to 100 kHz, with logarithmic scale of 10 points per decade and an applied potential of 50 mV of AC Potential. Nyquist (imaginary impedance versus real impedance) diagrams were also recorded. CV measurements were carried out at the potential range of −0.8 to 0.8 V vs. Ag/AgCl with an scan rate of 50 mv/s. All electrochemical experiments were carried out in 0.1 M phosphate buffer (PB) at pH 6.5 with 0.1 M KCl.

6.3 Results and discussion

6.3.1 Morphological studies

A homogeneous distribution of the BiNP on the electrodes surface can be observed by Scanning Electron Microscopy (SEM) image (see Figure 5.1A). Morphological and structural studies of bismuth nanoparticles were performed by Transmission Electron Microscopy (TEM). Highly regular and uniform average diameter of around 244 nm (see Figure 5.1B) can be measured.

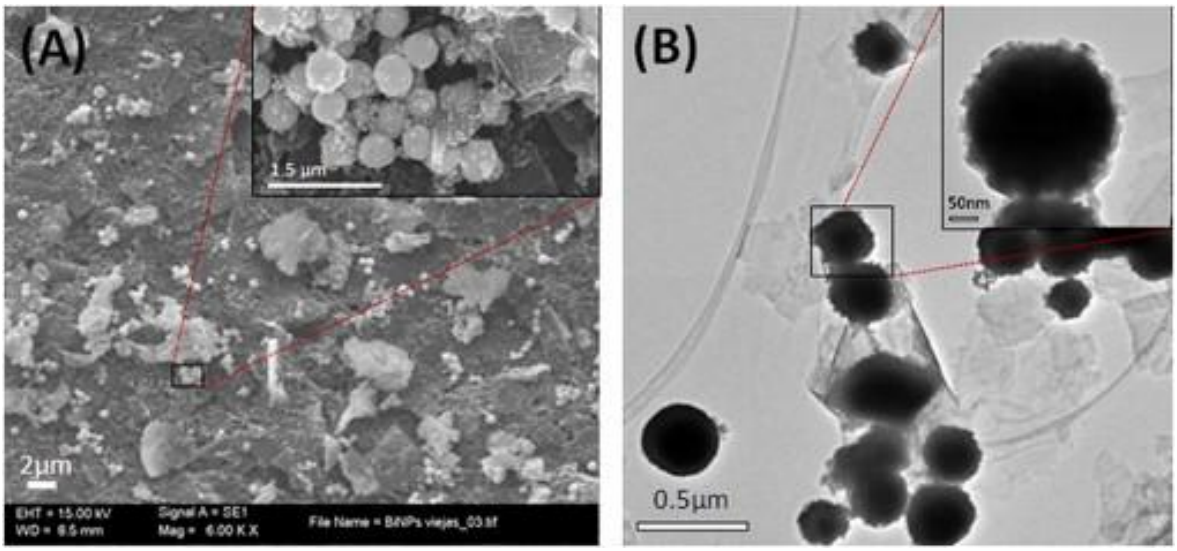

Figure 6.1 SEM micrographs of BiNP modified SPE (A). TEM image of BiNP dispersed in milli-Q water.

Z-potential (surface charge) measurements are a commonly used tool to determine the stability of a colloidal suspension of electrostatically stabilized nanoparticles. Dynamic light scattering (DLS) allows the determination of the hydrodynamic diameter of colloidal particles and conjugates, which is the diameter of the sphere with the same Brownian motion of the analyzed particle. According to the

DLS measurements, particles with 460 nm of hydrodynamic range with high homogeneous sizes have been synthetized, although z-potential analysis shows poor electrostatic stabilization of these nanoparticles in water medium. If we compare the values obtained by TEM and by Z-potential studies, BiNP diameters are similar.

The crystalline structure and the phase composition of bismuth nanoparticles were characterized by X-ray diffraction (XRD). Figure 5.2A shows the typical XRD patterns of the bismuth nanoparticle powder synthesized. All diffraction peaks can be perfectly indexed to the rhombohedral phase of bismuth (Bi°), which is consistent with the already reported phase for bismuth nanopowders[13]. Phase identification was performed by comparing the obtained XRD with the standard data facilitated by Joint Committee on Powder Diffraction Standards (JCPDS no. 04-006-7762, R3m).

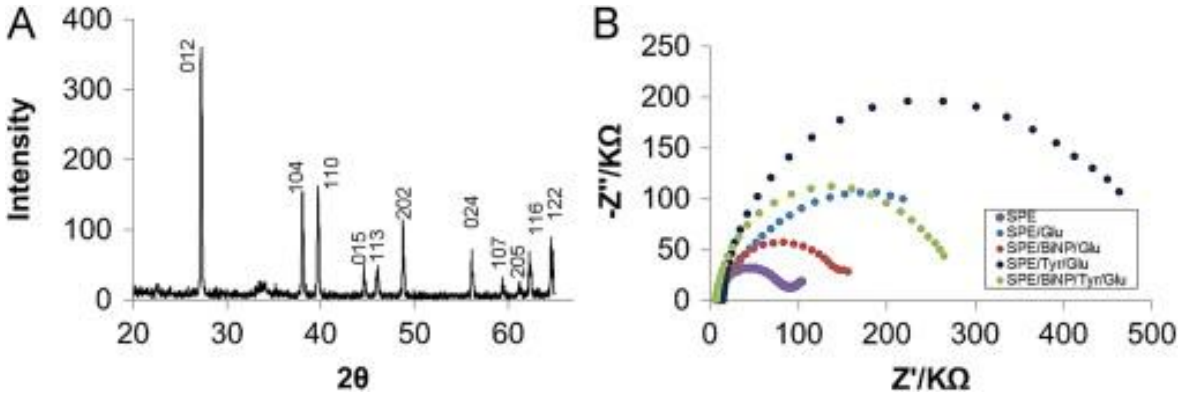

Figure 6.2 (A) X-ray diffraction pattern recorded from the synthesized BiNP. (B) Argand diagram of: bare SPE, SPE/Glu, SPE/BiNP/Glu and SPE/BiNP/Tyr/Glu modified electrodes in 1 mM $[Fe(CN)_6]^{3-/4-}$ (1:1) containing 0.1 M KCl.

6.3.2 EIS characterization of bismuth nanoparticles SPE/BiNP/Tyr biosensor

Electrochemical impedance spectroscopy (EIS) is a well known method used to study the surface features of modified electrodes. The curve of EIS presented as Nyquist

plot consists in two parts: one part is the semicircle section, located at higher frequencies corresponding to the electron transfer limited process. The electron-transfer resistance (Rct) can be obtained by measuring its diameter. The other part of Nyquist plot is the linear section, which brings the information related to the diffusion process held in solution and located at lower frequencies. This second section is used as to analyze the detailed electrochemical response of the modified electrodes by using individual or mixed Nyquist components. EIS of bare SPE (with and without glutaraldehyde), and SPE/BiNP, SPE/Tyr and SPE/BiNP/Tyr, all surfaces modified with glutaraldehyde were firstly evaluated in a 1 mM $[Fe(CN)_6]^{3-/4-}$ (1:1) with 0.1 M KCl as a redox probe by using (EIS) as to confirm the BiNP/Tyr immobilization (see Figure 2B). The Rct of the glutaraldehyde modified SPE increased in comparison with the bare SPE, which indicates that glutaraldehyde film was an obstacle for the electron transfer at the interface region. The result is consistent with the already reported ones by using similar systems[14,15]. With BiNP assembled within the glutaraldehyde film, the obtained Rct decreased. The lower charge transfer resistance is probably due to the faster ion diffusion/migration in the BiNP/Glu film in comparison with the glutaraldehyde film only. On the other hand, when the enzyme was immobilized through glutaraldehyde the charge transfer resistance increased, which not only indicates the efficient enzyme absorption but at the same time that both materials hinder the electron transfer. Finally it can be observed that the adsorption of Tyrosinase onto BiNP is related to the decrease of the semicircle, indicating that Tyrosinase had been successfully immobilized onto de SPE modified with BiNP.

6.3.3 Evaluation of the electrochemical sensing capability of SPE/BiNP/Tyr/Glu biosensor.

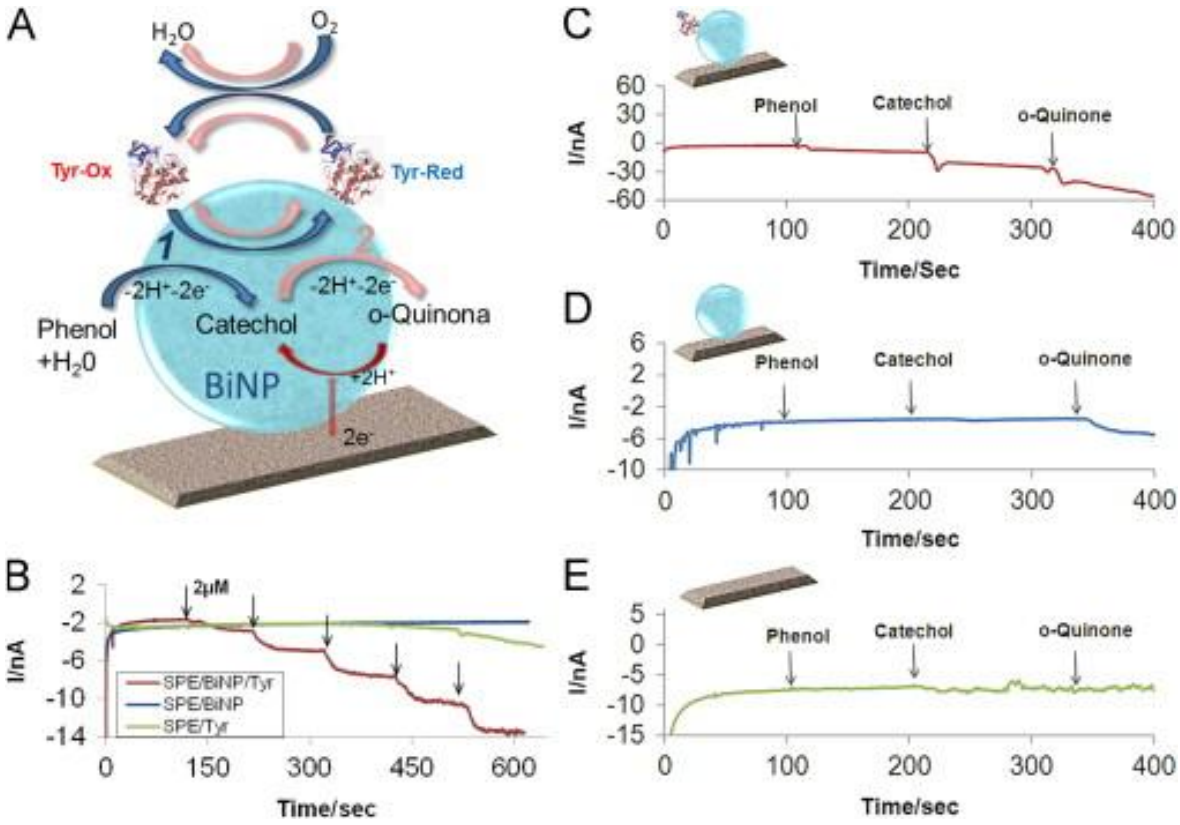

Figure 6.3 Proposed mechanism for the phenol and catechol electrocatalytic detection by using BiNP based biosensor (A). Current–time response curves of bare SPE, SPE/BiNP and SPE/BiNP/Tyr modified electrodes upon successive additions of 2 µM phenol (B). Chronoamperometric responses of SPE/BiNP/Tyr (C), SPE/BiNP (D), SPE (E) biosensors upon successive additions of 10 µM Phenol, catechol and o-quinone. All the experiments were carried at −200 mV, without nitrogen saturation.

Figure 6.3B depicts the chrono-amperometric responses for the different enzyme modified sensors, and using 0.1 M phosphate buffer (PB) at pH 6.5 with 0.1 M KCl upon successive addition of 2 µM phenol. The SPE/BiNP/Tyr biosensor showed a higher current change than the SPE/Tyr one (Figure 3B). The observed reduction current was attributed to the direct reduction of o-quinone to cathecol, released from the enzyme-

catalyzed reaction on the electrode surface (see Figure 6.3A). Only a background current was observed in the SPE/Glu sensor.

Tyrosinase (Tyr) has hydroxylase activity, by which phenol can be hydroxylated to catechol using molecular oxygen (Eq. 6.1), and also oxidase activity that can catalyze the oxidation of catechol to o-quinone (Eq. 6.2). At moderately negative potential (−200 mV) the o-quinone product of phenol oxidation may be electrochemically reduced to catechol (Eq. 6.3). Oxidation process by the enzyme, followed by the reduction at the electrode surface, may result in cycling between catechol and o-quinone yielding a catalytically amplified current. Therefore, what is occurring at the electrode surface is the reduction of o-quinone to catechol (working electrode is acting as a cathode)[16].

$$\text{Phenol} + \text{Tyr}_{(\text{ox})} + \text{H}_2\text{O} \rightarrow \text{Catechol} + \text{Tyr}_{(\text{red})} + 2\text{H}^+ + 2\text{e}^- \quad (6.1)$$

$$\text{Catechol} + \text{Tyr}_{(\text{ox})} \rightarrow o\text{-quinone} + \text{Tyr}_{(\text{red})} + 2\text{H}^+ + 2\text{e}^- \quad (6.2)$$

$$o\text{-quinone} + 2\text{H}^+ + 2\text{e}^- \xrightarrow{-200\text{mV}} 200\text{mV catechol} \quad (6.3)$$

For a better elucidation of the phenolic compounds detection mechanism (Figure 6.3A), amperometric measurements were carried out. Measurements were performed under different experimental conditions. The first one (Figure 6.3C) was carried out using a SPE/BiNP/Tyr, while the second case (Figure 6.3D) corresponded to SPE sensor modified only with BiNP. Finally, a bare SPE was also checked (Figure 6.3E). The current responses of each electrode toward 10 µM phenol, 10 µM catechol and 10µM o-quinone (synthesized in our laboratory by the method already described in the materials and methods section) additions were recorded. A decrease of current of 1.72 and 15.4 nA

was recorded for SPE/BiNP and SPE/BiNP/Tyr, respectively. This behavior shows an appropriate current response to o-quinone (see Figure 6.3C and D). In addition, the mentioned current response in both electrodes may be attributed to the presence of BiNP in the surface, which seems to bring an electron transfer kinetic enhancement in the reduction current of o-quinone.

SPE/BiNP/Tyr biosensor is the only one which exhibits response to phenol and catechol addition, showing a current increase of 4.34 and 12.43 nA, respectively (see Figure 6.3C). This sensor can detect phenolic compounds because of the presence of both tyrosinase and BiNP. Using this sensor the following reactions can be coupled: phenol hydroxilation to catechol occurs first, followed by the catechol oxidation to o-quinone and o-quinone reduction to catechol due to the presence of BiNP. SPE modified only with glutaraldehyde (Figure 6.3E) doesn't show any response toward either phenol, catechol or o-quinone.

6.3.4 SPE/BiNP/Tyr biosensor calibration and evaluation of interferences

The amperometric response of the SPE/BiNP/Tyr to successive additions of phenol and catechol were further evaluated under the optimized experimental conditions (data not shown). Figure 6.4A and B show the typical current–time dynamic responses of the SPE/BiNP/Tyr towards phenol and catechol, respectively. The electrode showed a rapid and sensitive bioelectrocatalytic response, reaching about 95% of the steady-state current within 15 and 50 s after each addition of catechol and phenol, respectively. The different response times are due to the fact that phenol has to be firstly hydroxilated to catechol, which in turn needs then to be oxidized to o-quinone

and this last one to be reduced afterwards to catechol in presence of BiNP (Figure 6.4A).

In the case of catechol detection the first step is omitted (Figure 6.4B).

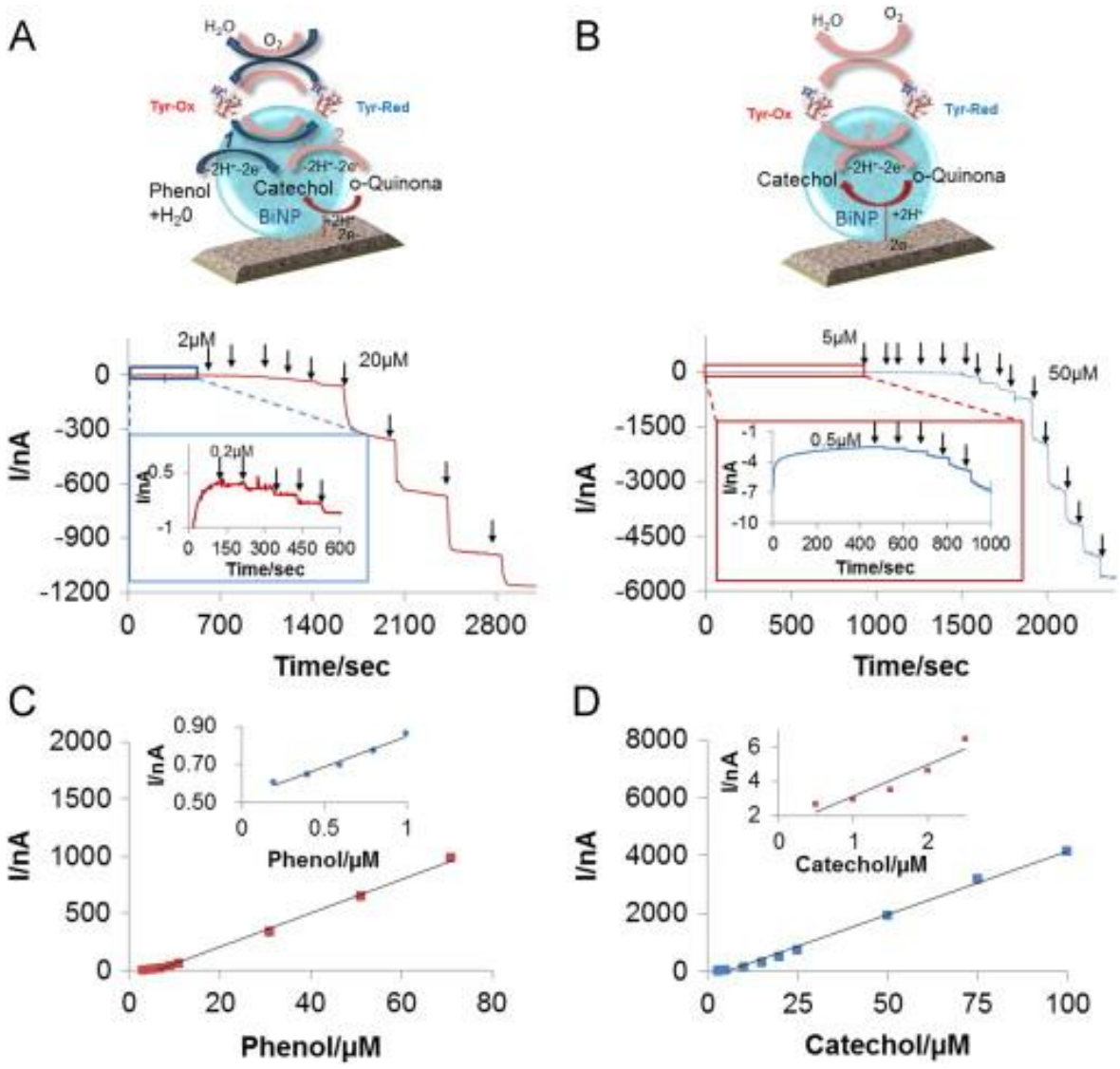

Figure 6.4 Typical current–time response curves for the successive additions of 0.2, 2 and 20 µM of phenol (A) and 0.5, 5 and 50 µM of catechol (B); inset: magnification of the initial steps. Sensor calibration given as current versus phenol (B) and catechol (D) concentration; inset: magnification at low concentration range for phenol and catechol.

Figure 6.4C and D show the typical calibration curves of the SPE/BiNP/Tyr toward phenol and catechol, respectively. The biosensing performance present two linear

response ranges at low and high concentrations for both phenolic compounds. The phenol detection shows a linear response range from 0.2 to 1 µM (r^2=0.974) and 3–71 µM (r^2=0.995) for low concentration and high concentration ranges, respectively. While for catechol detection the linear response ranges are from 0.5 to 2.5 µM for low concentration and 3–100 µM for the high concentration range, both with a similar linearity. On the other hand SPE/BiNP/Tyr biosensor shows LOD of 26 nM and 62 nM for catechol and phenol, respectively. The sensitivities in the linear calibration regions for low concentration shows the following order: 44.056 nA/µM (catechol)>14.025 nA/µM (phenol). The difference in sensitivity might depend on the catalytic selectivity of tyrosinase for different phenolic compounds[2].

Moreover, the Michaelis–Menten constants (K_M^{app}) obtained for phenol and catechol are 0.063 mM and 0.083 mM, respectively. The lower K_M^{app} is estimated from the data obtained from the amperometric response, indicating that the immobilized tyrosinase is strongly adsorbed onto the working electrode surface of the SPE modified with BiNPs, and a good affinity of the enzyme for phenol and catechol is shown.

The lower K_M^{app} value may be related to an efficient recycling process of the substrate process, by electrochemically reducing the o-quinone to catechol, which serves as tyrosinase substrate[1].

Analytical performance of the proposed biosensor was compared with other reported tyrosinase biosensors based in SPE. The proposed SPE/BiNP/Tyr biosensor exhibited improved analytical performances in terms of linear range of response and limit of detection in comparison with other reported biosensors, such as

SPE/MWCNT/Bi/Tissue[10], SPE/MWCNT/Tyr/Glu[14] and Tyr–Au/PASE–GO/SPE[5]. All these results indicate that the developed BiNP based electrochemical biosensor is an excellent candidate for phenol and catechol detection.

The reproducibility of the fabrication process was evaluated by the comparison of the current responses obtained for 0.5 µM phenol using 3 different biosensors. The results of the triplicate sets, indicated by error bars, reveal the repeatability and reproducibility (Figure 6.5A) of the measurements with a relative standard deviation (RSD) of less than 15% within a 0.5–2.5 µM phenol concentration range.

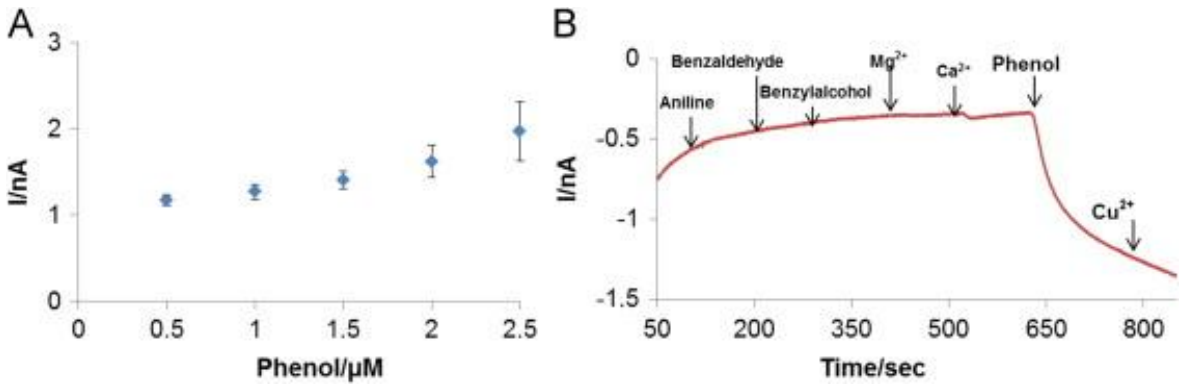

Figure 6.5 Triplicate sets, indicated by error bars, of the measurements with a relative standard deviation (RSD) less than 15% for 0.5–2.5 µM phenol concentration (A). SPE/BiNP/Tyr biosensor response upon successive additions of 50 µM aniline, benzaldehyde, benzylalcohol, Mg^{2+}, Ca^{2+}, 5 µM of phenol and 25 µM Cu^{+2} (B).

Selectivity is a very important parameter to be considered for biosensors detecting phenol derivates. To evaluate the selectivity of the biosensor, chrono-amperometric response toward aniline, benzaldehyde, benzylalcohol, Mg^{2+},Ca^{+2} (each one in a concentration 10 times higher than phenol concentration) and Cu^{+2} (5 times higher than phenol concentration) were measured (see Figure 6.5B). The selected species for interference studies seem to be the ones usually present with the phenolic

compounds in contaminated samples[17]. A good selectivity of the SPE/BiNP/Tyr biosensor toward phenol detection is evident by the neglected responses toward interfering species.

6.4 Conclusions

A novel electrochemical biosensor based on bismuth nanoparticles and tyrosinase for the determination of phenolic compounds is developed. The suggested bionanocomposite matrix provides mild and efficient immobilization process for tyrosinase and BiNPs ensuring at the same time an enhanced sensibility and fast response. These qualities may be ascribed to an efficient process of enzyme substrates recycling (electrochemical reduction of the enzymatically generated o-quinone by producing catechol, the tyrosinase substrate). It must be noted that the enzyme recycling of the phenolic compounds is dependent on the electrode matrix used. The biosensor exhibited good analytical performances to phenolic compounds in terms of sensitivity, low detection limit, reproducibility and fabrication simplicity and can be used for the accurate determination of several phenolic compounds without the need to use extra mediators. This sensor uses a very low DC potential, decreasing this way the effect of interferences such as aniline, benzaldehyde, benzylalcohol, Mg^{2+}, Ca^{2+} and Cu^{+2}. Phenol and catechol detections mechanisms associated to the designed biosensor are also evaluated.

6. 5 References

(1) Shan, D.; Zhang, J.; Xue, H.-G.; Zhang, Y.-C.; Cosnier, S.; Ding, S.-N. *Biosens. Bioelectron.* **2009**, *24*, 3671–3676.

(2) Lu, L.; Zhang, L.; Zhang, X.; Huan, S.; Shen, G.; Yu, R. *Anal. Chim. Acta* **2010**, *665*, 146–151.

(3) Apetrei, C.; Alessio, P.; Constantino, C. J. L.; de Saja, J. A.; Rodriguez-Mendez, M. L.; Pavinatto, F. J.; Ramos Fernandes, E. G.; Zucolotto, V.; Oliveira, O. N. *Biosens. Bioelectron.* **2011**, *26*, 2513–2519.

(4) Tsai, Y.-C.; Chiu, C.-C. *Sensors Actuators B Chem.* **2007**, *125*, 10–16.

(5) Song, W.; Li, D.-W.; Li, Y.-T.; Li, Y.; Long, Y.-T. *Biosens. Bioelectron.* **2011**, *26*, 3181–3186.

(6) Cosnier, S.; Popescu, I. C. *Anal. Chim. Acta* **1996**, *319*, 145–151.

(7) Li, Y.-F.; Liu, Z.-M.; Liu, Y.-L.; Yang, Y.-H.; Shen, G.-L.; Yu, R.-Q. *Anal. Biochem.* **2006**, *349*, 33–40.

(8) Shan, D.; Zhu, M.; Han, E.; Xue, H.; Cosnier, S. *Biosens. Bioelectron.* **2007**, *23*, 648–654.

(9) Pingarrón, J. M.; Yáñez-Sedeño, P.; González-Cortés, A. *Electrochim. Acta* **2008**, *53*, 5848–5866.

(10) Merkoçi, A.; Anik, U.; Çevik, S.; Çubukçu, M.; Guix, M. *Electroanalysis* **2010**, *22*, 1429–1436.

(11) Wang, Y.; Kim, K. S. *Nanotechnology* **2008**, *19*, 265303.

(12) Aebisher, D.; Brzostowska, E. M.; Mahendran, A.; Greer, A. **2007**, 2951–2955.

(13) López-Salinas, F. I.; Martínez-Castañón, G. A.; Martínez-Mendoza, J. R.; Ruiz, F. *Mater. Lett.* **2010**, *64*, 1555–1558.

(14) Alarcón, G.; Guix, M.; Ambrosi, A.; Ramirez Silva, M. T.; Palomar Pardave, M. E.; Merkoçi, A. *Nanotechnology* **2010**, *21*, 245502.

(15) Mayorga-Martinez, C. C.; Guix, M.; Madrid, R. E.; Merkoçi, A. *Chem. Commun. (Camb).* **2012**, *48*, 1686–1688.

(16) Guix, M.; Pérez-López, B.; Sahin, M.; Roldán, M.; Ambrosi, A.; Merkoçi, A. *Analyst* **2010**, *135*, 1918–1925.

(17) Cosnier, S.; Fombon, J.-J.; Labbé, P.; Limosin, D. *Sensors Actuators B Chem.* **1999**, *59*, 134–139.

7. GENERAL CONCLUSIONS AND FUTURE PERSPECTIVES

7.1 General conclusions

In this PhD thesis, new platforms based on bismuth nanoparticles and other materials including paper with interest in heavy metals and phenol compound detection have been developed.

4.1.1 Bismuth nanoparticles with interest in heavy metal detection

Different methods of synthesis of bismuth nanoparticles (BiNPs) with potential interest for applications in electrochemical stripping analysis of heavy metals have been studied. From the obtained results it is concluded that the chemical nature of the reducing agent directly affect the morphology of BiNPs in terms of shape and size. In addition, the synthesis, based on polyol method, was optimized in order to find the most active bismuth nanoparticles for heavy metal detection and their integration in an electrochemical sensing platform.

The most efficient nanoparticles are obtained using polyol method with the lowest amount of PVP (0.05g in the synthesis). Approximately 240nm BiNPs with a wrinkled surface are obtained under these synthetic conditions as confirmed by TEM and SEM analyses.

BiNPs have shown to be effective enough in the improvement of the efficiency of screen-printed electrodes while being used in square wave anodic stripping voltammetry of heavy metals. The use of BiNPs has clearly contributed to reach very low detection limits such as 5 and 9ppb for lead and cadmium respectively. In addition, the presence of

BiNPs substantially improves the performance of the screen-printed electrode heavy metal sensor in seawater samples.

The reducing in PVP quantity during BiNPs synthesis did not bring significant loss of BiNPs stability keeping the compromise with the sensor performance improvement. This PVP based reductive method seems to be the most adequate to obtain BiNPs with interest for electrochemical stripping analysis of heavy metals.

7.1.2 Bismuth magnetic nanoparticles for heavy metal sensors

Magnetic core-shell nanoparticles modified with bismuth were synthesized following a modified previously published method. These nanoparticles have been successfully used for the electrode modification through application of a magnetic field reaching interesting performance in heavy metals sensing.

The developed synthesis gives nanoparticles of 14±3 nm diameter. These nanoparticles were characterized by TEM and XRD techniques. The presence of superficial bismuth was also detected due to their electrochemical properties. These electrochemical properties were studied and an enhancement in the sensibility of heavy metal sensing in a simple electrochemical cell was observed.

With an optimized amount of nanoparticles good calibration curves were obtained. The modification improves the sensing capability in both in-drop and in.chip detection formats. The sensibility of this system toward lead detection is increased up to 78 % due to the bismuth-based modification.

The study of the reusability of this simple sensing format has been satisfactorily tested. These nanoparticles seem to be useful for further digital-like sensing and biosensing applications due to the versatility of bismuth oxide and their properties.

7.1.3 Paper based heavy metal sensor

A new platform for heavy metal sensing was designed and applied. The developed device is able to filter water samples containing solid particles and detect afterwards heavy metals in without the need of any previous pretreatment.

The analytical performance for sensing of lead and cadmium using this platform was satisfactory achieved. The limits of detection for lead and cadmium obtained were 7 and 11 ppb respectively, including their detection in a multidetection analysis. The detection of these analytes also has been shown in complex matrixes such as mud and seawater. In both cases, the detection without the need of previous pre-treatment of samples is shown. Such detection efficiency even in complex samples has been achieved thanks to the filtering capability of the paper platform. The obtained results are of interest for many other applications in the future that may include heavy metals detection in biological samples (i.e. blood) beside others.

7.1.4 Phenols detection using BiNPs

A novel electrochemical biosensor based on bismuth nanoparticles and tyrosinase for the determination of phenolic compounds is developed. The biosensor exhibited good analytical performances to phenolic compounds in terms of sensitivity, low detection limit, reproducibility and fabrication simplicity and can be used for the

accurate determination of several phenolic compounds without the need to use extra mediators.

The suggested bionanocomposite matrix provides mild and efficient immobilization process for tyrosinase and BiNPs ensuring at the same time an enhanced sensibility and fast response with good limits of detection (62 and 26 nM for phenol and catechol respectively). These qualities may be ascribed to an efficient process of enzyme substrates recycling (electrochemical reduction of the enzymatically generated o-quinone by producing catechol, the tyrosinase substrate). It must be noted that the enzyme recycling of the phenolic compounds is dependent on the electrode matrix used. In addition, this sensor uses a very low DC potential, decreasing in this way the effect of interferences such as aniline, benzaldehyde, benzylalcohol, Mg^{2+}, Ca^{2+} and Cu^{+2}. Phenol and catechol detections mechanisms associated to the designed biosensor are also evaluated.

7.2 Future perspectives

The applicability of the reported technologies, especially considering the use of bismuth nanoparticles, is one of the most interesting achievements which can be used for sensing and biosensing applications. The developed bismuth-based technologies may be easy adapted for their mass production leading to cost-efficient sensing and biosensing devices.

An important improvement in heavy metals detection is related to the use of bismuth nanoparticles that can be easily employed to modify electrodes even integrated

within chip systems. The low toxicity of bismuth nanoparticles is advantageous for their use in sensing and biosensing. The application of these nanoparticles can also be extended in bioanalytical platforms that use heavy metals containing quantum dots as labels for DNA, protein or cells detection.

The integration of screen-printed electrodes in a lateral flow for heavy metal sensor may open new perspectives for electrochemical stripping analysis of heavy metals. Of special interest should be the applicability of these paper-based platforms in clinical analysis. The use of bismuth modified paper-based platforms may open new perspectives for multi detection of proteins, DNA and other biomolecules through using of quantum dots.

ANNEX I: SCIENTIFIC PRODUCTION

The research work accomplished, resulted in several publications and manuscripts that were submitted, or in near future, to international peer-reviewed scientific journals, and also in a book chapter by invitation of the editor. In addition, the work done has been presented in different nationals and international workshops.

Collaboration in congress

XVII Trobada Transfronterera sobre Sensos i Biosensors, Tarragona (Catalonia), 20-21st September 2013, Poster presentation: "*Bismuth nanoparticles for phenolic compounds biosensing application*"

Jornades Doctorals 2013, Bellaterra (Catalonia), 15-17th June 2013, Poster and oral presentation: "*Synthesis of Bismuth Nanoparticles with interest for sensing application*"

Rethinking Nano Workshop: From discovery to design. Barcelona (Catalonia), 8th November 2012, Poster Presentation: "*Bismuth nanoparticles for phenolic compounds biosensing application*"

Biosensors 2012, Cancun (Mexico), 15-18th May 2012, Poster presentation: "*Bismuth nanoparticles for phenolic compounds biosensing application*"

XVI Trobada Transfronterera sobre Sensos i Biosensors, Toulouse (France), 29-30th September 2011, Poster presentation: "*Synthesis of bismuth nanoparticles for sensing applications*"

NANOJASP 2010 - Nanomaterials based biosensors and biosystems. Improving the quality and security of citizen's life Workshop: Spain-Japan, Barcelona (Catalonia), 29-30th November 2011, Poster presentation: "*Heavy metals monitoring using Screen-Printed Electrodes*"

XV Trobada Transfronterera sobre Sensos i Biosensors, Sant Carles de la Ràpita (Catalonia), 16-17th September 2010, Poster presentation: "*Synthesis and application of bismuth nanoparticles fin metal sensing*"

Publications

Published works

"*Bismuth nanoparticles for phenolic compounds biosensing application*" C. C. Mayorga-Martinez, M. Cadevall, M. Guix, J. Ros, A. Merkoci. **Biosensors & Bioelectronics**, 2013. 40, 57-62.

In preparation papers

"*Bismuth based nanomaterials and platforms for sensing and biosensing applications*", M. Cadevall, J. Ros, A. Merkoçi. Functional and PhysicalProperties of Polymer Nanocomposites edited by Aravind Dasari and James Njuguna, Willey Online Library -*in press*-

"Synthesis of bismuth nanoparticles with interest for sensing application", M. Cadevall, J. Ros, A. Merkoçi, **Chemistry: An Eurpean Journal**, 2014, -submited-

"Eco-friendly electrochemical lab-on-paper for heavy metal detection", M. Cadevall, M. Medina-Sánchez, J. Ros. A. Merkoçi,

"Magnetic core-shell nanoparticles for digital-like heavy metal sensing" M. Cadevall, M. Medina-Sánchez, J. Ros. A. Merkoçi,

Additional publications

"Enhanced detection of quantum dots labeled protein by simultaneous bismuth electrodeposition into microfluidic channel" M. Medina-sánchez, S. Miserere, M. Cadevall, A. Merkoçi –submitted-

"*Surface Characterizations of Mercury Based Electrodes with the Resulting Micro and Nano amalgam Wires and Spheres Formations May Reveal Both Gained Sensitivity and Faced Non-Stability in Heavy Metal Detection*", Gemma Aragay, Anna Puig-Font, Miquel Cadevall, and Arben Merkoçi, **Journal of Physical Chemistry C**, 2010, 114, 9049 – 9055

ANNEX II: TECHNIQUES USED

In this thesis some different techniques have been used. Examples of that are screen printed technology, wax printing or soft lithography, for the fabrication of the different sensing platforms. Now, in this part, I would describe briefly all of these techniques in aim to give the reader complementary tools for better text understanding.

AII .1 Preparation techniques

AII .1.1 Screen printed electrodes fabrication

In this thesis work all the electrodes, which conform the electrochemical cells, have been fabricated using screen printed technology. Screen printing technology is a printing technique that uses a woven mesh to support an ink-blocking stencil to receive a desired image. The attached stencil forms open areas of mesh that transfer ink onto a substrate. The substrates used in this work have been printed onto polyester, polycarbonate and filter paper, depending on the final application. The figure AII.1 shows schematically the printing principle and the electrodes printing.

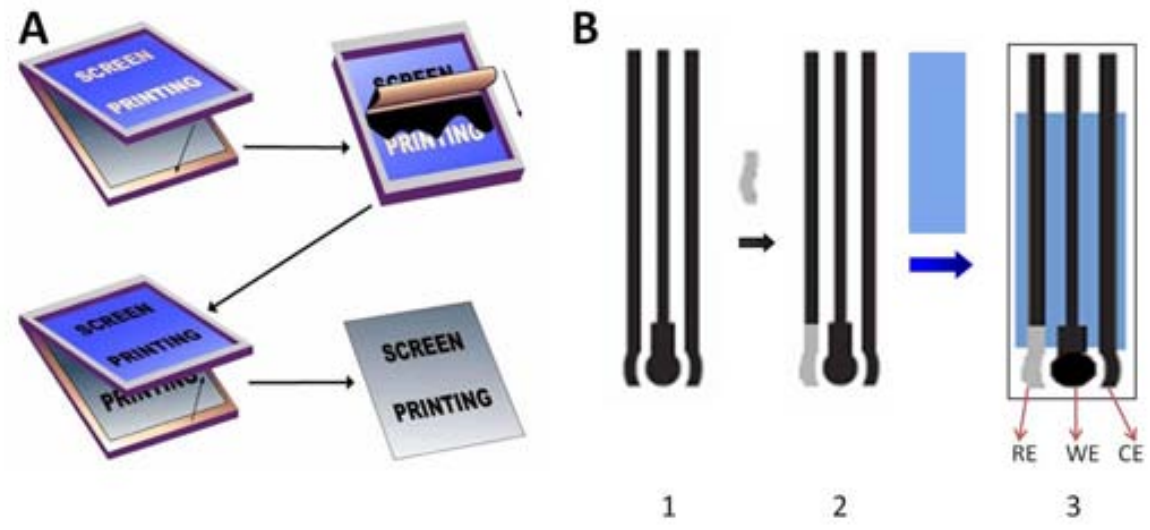

Figure AII .1 Schematic screen printing procedure (A) and the different ink layers to fabricate the electrodes. 1) Carbon ink, 2) Silver/silver chloride ink and 3) Insulator ink. RE is the reference electrode, WE is the working electrode and CE is the counter electrode.

Three different inks have been used: graphite ink for the working and counter electrode (Electrodag 423SS ink), silver/silver chloride for the reference electrode layer

(Electrodag 6037SS ink) and finally an insulating layer (Minico M-7000 Blue) to better define the working electrode area and avoid the undesirable contacts of the liquid with the internal connections. All the inks have been purchased from Acheson Industries. After the deposition of each layer onto polyester substrate, a drying process was followed by keeping the polyester substrate at 120^{o}C for 45 min (graphite) and 30 min (Ag/AgCl and insulating inks).

The printing of SPCE onto polycarbonate or paper follows a relatively differnt procedure. First, the insutaing ink was not used due to PDMS or wax acts as a insulator avoiding the undesirable contacts of the liquid with the internal connections. The other relevant change is in the drying temperature; for both substrates have been reduced to 60^{o}C due to polycarbonate deforms and wax melts at higher temperatures.

For these work two different electrodes geometries have been used. For the studies of modification of electrodes using bismuth nanoparticles (for both heavy metal and phenols sensing) and modification with magnetic core shell nanoparticles, for lead detection, type A in the figure AII. 2 have been used. This geometry is commonly used in our group for different kind of applications due to their large versatility and easy implementation in different cell detection systems[1–3]. The type B has been used in the lab on paper application; this geometry is more appropriated for chip applications[4,5].

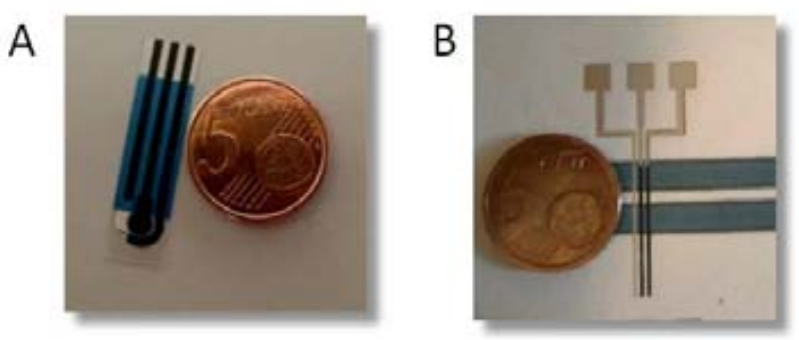

Figure AII. 2 Screen printed electrode onto polyester (A) and screen printed electrode printed onto paper; with the wax channel (B).

AII .1.2 Chip fabrication

Fast and cheap prototyping methods for the design and fabrication of polymeric microfluidic systems have been developed. Traditionally, microfluidic systems have been fabricated in glass, defined by photolithography or micromachining; however, there are limitations with glass substrate, especially for the rapid prototyping. Indeed fabrication process of glass chips is very slow, expensive, and requires special facilities. Instead, polymers (i.e. thermoplastics such as polymethyl methacrylate (PMMA) or elastomers as poly (dimethylsiloxane) (PDMS)) offer an attractive alternative to glass as microsystems substrates. In our case we use PDMS due to their easy integration with the substrate and the chemical resistance to the solutions.

The microchannel design and fabrication process was performed in four steps: 1) design of the microfluidic network and printing onto a transparency mask using a high resolution printing machine, 2) master fabrication through photolithography, using cleaning room facilities; 3) PDMS channel replication and finally 4) the bonding with the substrate. The fabrication steps are explained in the next paragraphs and summarized in the Figure AII .3.

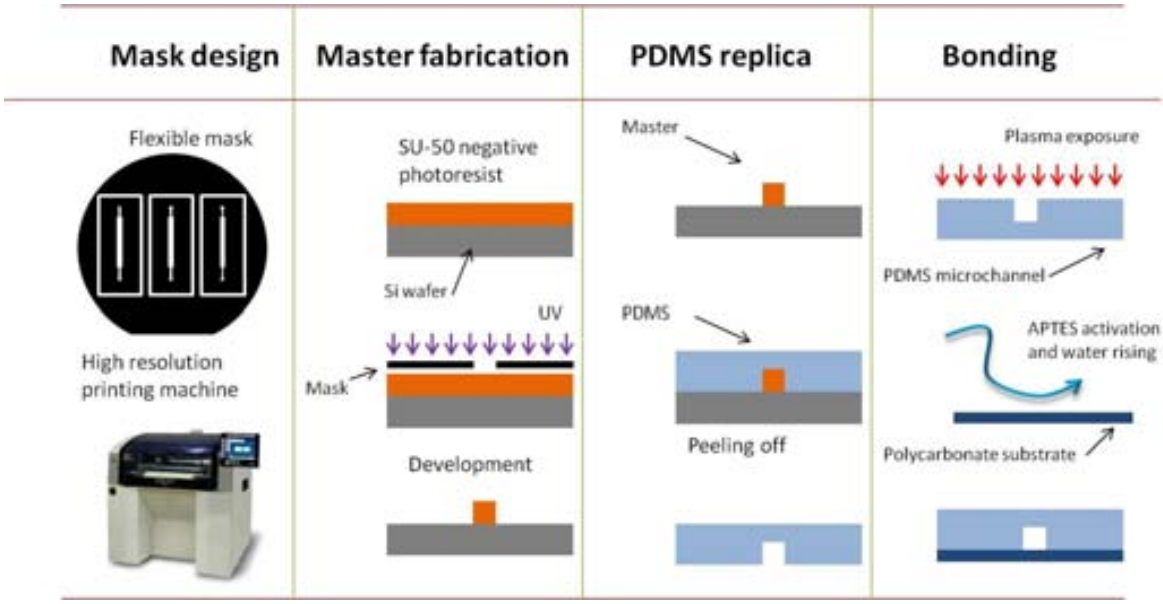

Figure AII .3 Microchannel fabrication steps: mask design, master fabrication, PDMS replication and bonding.

The most critical step in the fabrication of PDMS microfluidic device is the manufacture of a high quality master. This involves spin coating of the substrate (in our case 4' silicon wafer) with photoresist to ensure uniform thickness of the master, pre-exposure bake to evaporate the excess of the solvent from the photoresist, exposure of the resist to UV through a mask, post-exposure bake to promote polymerization in irradiated areas, and development of the master to remove unexposed photoresist, leaving only the desired positive structure.

To design the microchannels computer assisted design software (QCAD) with high resolution (24000 dpi) has been used. The design proposed is a single and RECTE channel, the central part, where there is the electrochemical cell, is larger than the inlet or the outlet. This design was printed onto a transparent film by using a high resolution printing machine. Then, in a cleaning room lab, a silicon wafer was cleaned and a solution of 4' SU8-50 photoresist was deposited in a uniform thickness layer by using a

spin coating machine. In our case 2000rpm, during 50s, were needed to obtain a 50 µm master. Before to perform the photolithography step, a pre-baking time was made at 95^{o}C during 40min. Then the photoresist was exposit for 50s using UV light and was cured at 65^{o}C for 4h. XP SU8 Developer was used as a revelat agent.

Before pouring PDMS onto the silicon wafer, it is important to accurately clean its surface to avoid possible dust that can lead to deformities on the final PDMS microchannel. PDMS oligomer and crosslinking agent were mixed in the weight ratio of 10:1 and degassed. The pattern for the PDMS device is created by pouring the liquid PDMS onto a surface containing the negative of the pattern. After pouring it, it is cured for 2 h at 65^{o}C. Then, the PDMS layer with the pattern of the negative relief was peeled off from the master. The reservoirs were made by punching holes in the structured PDMS.

The integration of the electrodes to the chip and the closing of the channel have 3 steps: printing the electrodes onto a polycarbonate substrate, preparing both surfaces for the bonding and attaching both parts. First the polycarbonate substrate, with the printed electrodes, were cleaned with *iso*-propanol, deionized water and dried with a stream of air. Then the substrate was treated oxygen plasma treatment (60 W, 1min) and was immersed in 2% v/v aqueous (3-Aminopropyl)triethoxysilane (APTES) solution for 60min. After that, the excess of APTES solution was rinsed with water while an oxygen plasma treatment was made to the PDMS. Finally, the activated thermoplastic and PDMS substrate were kept in conformal contact at room temperature for 1h and bonding was evaluated by a manual peeling test.

AII .1.3 Wax channel development

Among the disposable platforms, paper-based sensors can be an interesting alternative for low-cost and eco-friendly analytical platforms. As will be discussed bellow, the platforms based on paper can acquire different functionalities through the creation of different patterns or structures onto them. For example fluidics in the paper can be achieved by printing of hydrophobic channels[6]. Integration of transducers or conductive contacts in the paper platform can also be performed by using conventional printing technologies such as inkjet[7], wax printing[8] or screen printing[9], making them amenable to in-situ, low-cost and friendly fabrication[10]. In our case, we propose to use wax printing due to the group experience.

First of all, the channel geometry was designed with a graphic software (Corel Draw X4), taking into account the dimensions of the channel (3 mm wide and 25 mm length, widened in the end part), in order to align in a reproducible way the electrode position onto the channel, as well as ensure the electrode wettability just in the active detection zone, as well as the required fluid trajectory for the proper metal deposition onto the working electrode. Once the design was performed, it was printed onto the paper with a wax printer machine, and then it was heated in order to melt the wax across the paper to create a hydrophobic barrier that defines the fluid confinement. This melting process was performed at 150^{o}C for 10s by using a hot plate. After the channel preparation, the electrochemical detector was printed onto the channel. It consisted of a set of three electrodes of 500 µm width separated by 500 µm with an approximated thickness of 4 µm, produced by screen printing technology. The fabrication process involved two steps. In the first step the graphite layer (that creates WE and CE) was

printed onto the paper sheet. Secondly, a layer of silver/silver chloride ink was printed as a reference electrode.

In order to avoid liquid leakages, a second paper layer closing the bottom part of the paper channel was needed. This layer was also printed with the wax printer machine, but in this case it was not necessary to melt the wax, because the printed surface area (also hydrophobic) was big enough to close the channel. Both paper layers (channel and substrate) were attached by using adhesive glue. Finally, the absorbent pad (CFSP001700, from Millipore (Billerica, USA) cut in pieces of 5 x 10 mm was located at the end of the channel (See Figure AII. 4). The function of the absorbent pad is to wick the fluid through the membrane, increasing the amount/volume of the sample and the sensitivity due to a continuous sample renovation in the electrochemical cell during the pre-concentration step.

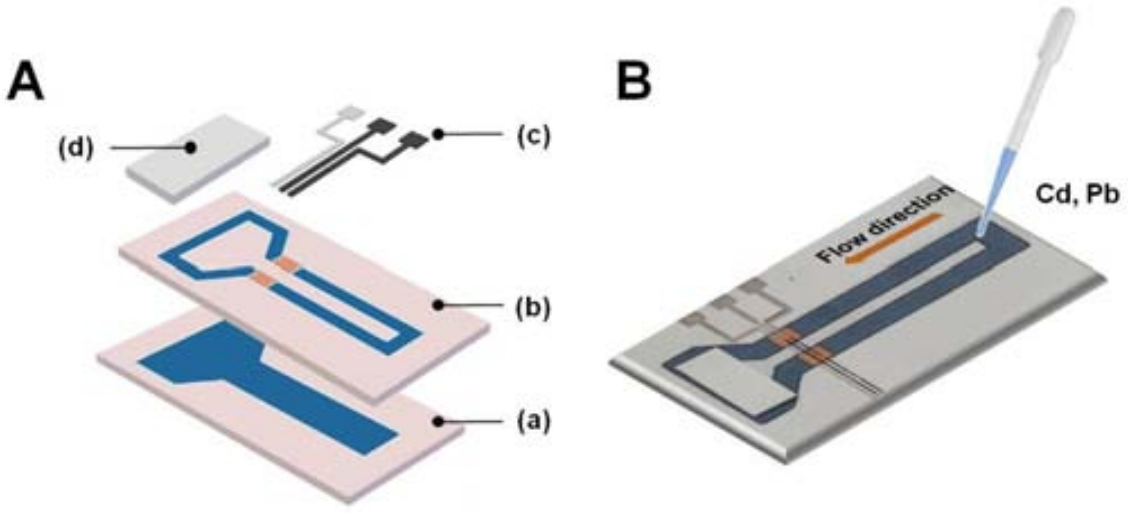

Figure AII .4 Schematic of a *lab-on-paper* device. (A) Different components of the chip: a) bottom layer, b) channel layer, c) RE (grey color), WE (in center) and CE and d) absorbent pad. (B) Picture of the fabricated device.

AII .1.4 References

(1) Alarcón, G.; Guix, M.; Ambrosi, A.; Ramirez Silva, M. T.; Palomar Pardave, M. E.; Merkoçi, A. *Nanotechnology* **2010**, *21*, 245502.

(2) Aragay, G.; Pons, J.; Merkoçi, A. *J. Mater. Chem.* **2011**, *21*, 4326.

(3) De la Escosura-Muñiz, A.; Chunglok, W.; Surareungchai, W.; Merkoçi, A. *Biosens. Bioelectron.* **2013**, *40*, 24–31.

(4) Medina-Sánchez, M.; Miserere, S.; Merkoçi, A. *Lab Chip* **2012**, *12*, 1932–1943.

(5) Medina-Sánchez, M.; Miserere, S.; Morales-Narváez, E.; Merkoçi, A. *Biosens. Bioelectron.* **2014**, *54*, 279–284.

(6) Dossi, N.; Toniolo, R.; Pizzariello, A.; Impellizzieri, F.; Piccin, E.; Bontempelli, G. *Electrophoresis* **2013**, *34*, 2085–2091.

(7) Su, S.; Ali, M. M.; Filipe, C. D. M.; Li, Y.; Pelton, R. *Biomacromolecules* **2008**, *9*, 935–941.

(8) Carrilho, E.; Martinez, A. W.; Whitesides, G. M. *Anal. Chem.* **2009**, *81*, 7091–7095.

(9) Savolainen, A.; Zhang, Y.; Rochefort, D.; Holopainen, U.; Erho, T.; Virtanen, J.; Smolander, M. *Biomacromolecules* **2011**, *12*, 2008–2015.

(10) Martinez, A. W.; Phillips, S. T.; Whitesides, G. M.; Carrilho, E. *Anal. Chem.* **2010**, *82*, 3–10.

ANNEX III: GLOSSARY OF TERMS,

ACRONYMS AND ABBREVIATIONS

In this thesis some acronyms and a bbreviations have been used; in this annex there are listed the more relevant for the better understanding of the reader.

Bismuth nanopartilces	BiNPs
Counter electrode	CE
Gluteraldehide	Glu
Laterl flow analysis	LFA
Limit of detection	LOD
Limit of quantification	LOQ
Magentic nanoparticles	MNPs
Microparticles	MPs
Nanoparticles	NPS
Phosphate saline buffer	PBS
Phosphate saline buffer (Tween 20)	PBST
Polycarbonate	PC
Polydimethylsiloxane	PDMS
Polyvinyl pyrrolidone	PVP
Reference electrode	RE

revolutuions per minute	rpm
Scanning electron microscopy	SEM
Screen Pinted Carbon electrodes	SPCE
Silver / silver chloride	Ag/AgCl
Square wave anodic stripping voltammetry	SW-ASV
Transmision electron microscopy	TEM
Tyrossinasse	Tyr
Working electrode	WE
X-Ray difraction	XRD

ANNEX IV: ACKNOWLEDGEMENTS

AGRAÏMENTS

En aquesta part voldria agrair a tothom qui ha fet possible que el que va començar fa anys a dia d'avui pugui ser una realitat. Però abans de començar m'agradaria dedicar questa tesis al professor Joan Sola, que ens va deixar; ell havia de formar part d'aquesta història i em va animar a tirar-la endavant quan encara havia de començar.

En primer lloc m'agradaria agrair la possibilitat de fer una tesi doctoral amb els professors Arben Merkoçi i Josep Ros, el primer per animar-me a començar aquesta aventura i el segon per suplir la baixa del Joan. A tots dos us agraeixo molt la paciència que heu tingut i els esforços que heu fet per atendre'm sempre que ha sigut possible. Al llarg d'aquest anys he après molt del món de la investigació i he pogut conèixer molts altres investigadors a qui també els dec molt.